University of Nottingham

School of Mathematical Sciences

Mirror Symmetry for Orbifold del Pezzo Surfaces

Daniel Cavey

A thesis submitted to the University of Nottingham for the degree of

Doctor of Philosophy

August 2019

This thesis is dedicated to
Gran and Grandpa Mark.

Acknowledgements

Firstly I would like to thank my supervisor Alexander Kasprzyk for introducing me to the topic of this thesis, for his enthusiasm throughout his invaluable teachings, and for his encouragement and patience. It has been a pleasure to learn and work alongside him.

I extend my thanks to all the mathematicians I have been fortunate enough to work alongside over the course of this PhD. In particular to Akihiro Higashitani, Edwin Kutas and Thomas Prince all of whom have co-authored articles or publications based on work appearing in this thesis.

My family have encouraged and supported me unwaveringly throughout all these years. In particular my parents have offered guidance and wise advice to me without which I do not believe this thesis would have become a reality.

Throughout my education including my time at Belfast High School, University of Warwick and University of Nottingham, I am happy to have met a great many friends who have made day-to-day work life such fun (though admittedly often acting as a distraction from work). I have many fond memories from all these years.

Finally, a special thank you to my girlfriend Gigi who has been by my side making me laugh and smile throughout it all.

Abstract

Mirror symmetry evokes a correspondence between deformation equivalence classes of toric varieties and mutation equivalence classes of the corresponding Fano varieties. This thesis discusses many computations and examples of this ilk, in the case when the varieties are 2-dimensional and permitted to possess cyclic quotient singularities.

The mutation graph of weighted projective planes has been well studied by Akhtar–Kasprzyk. We similarly analyse the mutation graph of $\mathbb{P}^1 \times \mathbb{P}^1$ which involves looking at quivers and Plücker coordinates.

An algorithm is presented to classify mutation equivalence classes of Fano polygons where the corresponding surfaces have fixed singularities. These surfaces are subsequently studied using Laurent inversion and found to lie in a cascade structure introduced by Reid–Suzuki.

By studying the combinatorics of Fano polygons, which involves matrix calculations, continued fractions and r-modular sequences, we provide results regarding combinations of cyclic quotient singularities that do not occur for a del Pezzo surface admitting a toric degeneration.

CONTENTS

1

TORIC GEOMETRY

1.1 FANS AND POLYTOPES

Toric geometry, the study of particular algebraic varieties known as toric varieties, can be studied from Cox–Little–Schenck [30], Ewald [33] and Fulton [36].

Definition 1.1.1 ([30, Definition 3.1.1])**.** A *toric variety* of dimension n is a normal variety X that contains the torus $T \cong (\mathbb{C}^*)^n$ as a Zariski open subset, together with an algebraic action $T \times X \to X$ of T on X that extends the natural action of T on itself.

Here by algebraic action, we mean that $T \times X \to X$ is a morphism.

Often toric geometry has a combinatorial flavour in exploiting the underlying structure of these varieties.

Consider an n-dimensional lattice $N \cong \mathbb{Z}^n$. The dual lattice is $M := \mathrm{Hom}(N, \mathbb{Z})$, and is equip with the natural pairing $\langle \cdot, \cdot \rangle : N \times M \to \mathbb{Z}$. By tensoring the lattice N with $\mathbb{R}$, obtain the vector space $N_{\mathbb{R}} = N \otimes \mathbb{R}$. Similarly use $M_{\mathbb{R}}$ to denote $M \otimes \mathbb{R}$.

Definition 1.1.2 ([30, Definition 1.2.1])**.** A *rational polyhedral cone* $\sigma \in N_{\mathbb{R}}$ is a set of the form:

$$\sigma := \left\{ \sum_{u \in S} \lambda_u u : \lambda_u \geq 0 \right\} \subseteq N_{\mathbb{R}},$$

where S is a finite set of rational points in $N_{\mathbb{R}}$. The rational polyhedral cone is *strongly convex* if $\sigma \cap (-\sigma) = \{\mathbf{0}\}$.

By an abuse of notation we often say 'cone' to mean 'strongly convex rational polyhedral cone'.

Definition 1.1.3 ([30, Definition 1.2.5])**.** A *face* of a cone is given by:

$$\tau := \left\{ u \in N_{\mathbb{R}} : \langle u, m \rangle = 0 \right\} \cap \sigma,$$

for some $m \in \sigma^{\vee} = \{m \in M_{\mathbb{R}} : \langle u, m \rangle \geq 0, \forall u \in \sigma\}$. This is denoted $\tau \preceq \sigma$.

Definition 1.1.4 ([30, Definition 3.1.2])**.** A *fan* $\Sigma \subset N_{\mathbb{R}}$ is a finite collection of cones such that:

- If $\sigma \in \Sigma$ and $\tau \preceq \sigma$, then $\tau \in \Sigma$;
- If $\sigma, \sigma' \in \Sigma$, then $\sigma \cap \sigma' \in \Sigma$.

From a fan Σ, we construct a unique toric variety X_{Σ} as follows: Let $\sigma \in \Sigma$, and $\sigma^{\vee} \subset M_{\mathbb{R}}$ be the *dual cone*, that is $\sigma^{\vee} := \{m \in M_{\mathbb{R}} : \langle u, m \rangle \geq 0, \forall u \in \sigma\}$. Define the semigroup $S_{\sigma} := \sigma^{\vee} \cap M$.

Lemma 1.1.5 (Gordan's Lemma, [30, Proposition 1.2.17])**.** If σ is a cone, then the semigroup S_{σ} is finitely generated.

It follows that $\mathbb{C}[S_{\sigma}]$ is an affine ring, and so $U_{\sigma} := \operatorname{Spec}(\mathbb{C}[S_{\sigma}])$ is an affine variety. For a fan Σ, the toric variety X_{Σ} is constructed by glueing the disjoint union of the affine toric varieties U_{σ} together along the common faces of any two cones in the fan using the following lemma:

Lemma 1.1.6 ([30, Section 3.1])**.** If $\tau \preceq \sigma$, then there exists a map $U_{\tau} \to U_{\sigma}$ which embeds U_{τ} as a principal open subset of U_{σ}.

For $\sigma, \sigma' \in \Sigma$, let $\tau = \sigma \cap \sigma' \in \Sigma$ be the common face. Then there are embeddings $U_\tau \to U_\sigma$ and $U_\tau \to U_{\sigma'}$ and so we can glue U_σ and $U_{\sigma'}$ along U_τ. Glueing together all cones of Σ in this fashion gives the toric variety X_Σ.

Example 1.1.7. Consider the fan Σ containing a single 2-dimensional cone σ generated by the rays with primitive vertices $(0,1)$ and $(2,-1)$ in $N \cong \mathbb{Z}^2$ represented by e_2 and $e_1^2 e_2^{-1}$ repectively.

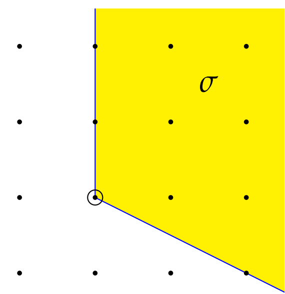

The dual cone has rays generated by e_1^* and $e_1^* e_2^{*2}$.

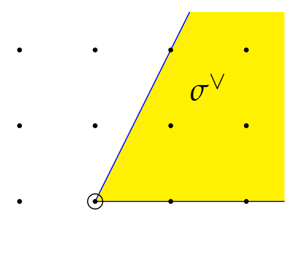

Therefore the semigroup S_σ is generated by the monomials $X = e_1^*$, $XY = e_1^* e_2^*$ and $XY^2 = e_1^* e_2^{*2}$, and so it follows that:

$$X_\Sigma = U_\sigma = \operatorname{Spec}\left(\mathbb{C}[S_\sigma]\right) = \operatorname{Spec}\left(\mathbb{C}[X, XY, XY^2]\right) \cong \operatorname{Spec}\left(\mathbb{C}[U,V,W]/(V^2 - UW)\right),$$

which is the quadric cone $\{V^2 - UW\} \subset \mathbb{C}^3_{U,V,W}$.

Example 1.1.8. Consider the fan Σ with three full-dimensional cones:

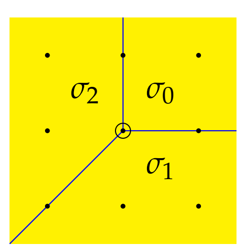

Calculating the dual for each cone obtain:

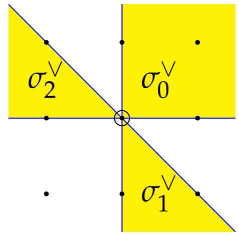

As before, it follows that the toric variety is covered by the affine open patches:

$$U_{\sigma_0} = \mathrm{Spec}\left(\mathbb{C}[S_{\sigma_0}]\right) = \mathrm{Spec}\left(\mathbb{C}[X,Y]\right) = \mathbb{C}^2_{X,Y},$$
$$U_{\sigma_1} = \mathrm{Spec}\left(\mathbb{C}[S_{\sigma_1}]\right) = \mathrm{Spec}\left(\mathbb{C}\left[\frac{1}{X},\frac{Y}{X}\right]\right) = \mathbb{C}^2_{\frac{1}{X},\frac{Y}{X}},$$
$$U_{\sigma_2} = \mathrm{Spec}\left(\mathbb{C}[S_{\sigma_2}]\right) = \mathrm{Spec}\left(\mathbb{C}\left[\frac{X}{Y},\frac{1}{Y}\right]\right) = \mathbb{C}^2_{\frac{X}{Y},\frac{1}{Y}},$$

where the subscripts on $\mathbb{C}^2$ denote the coordinates. It is routine to check that these three patches glue together in an identical fashion to how the three standard affine patches of $\mathbb{P}^2_{T_0:T_1:T_2}$ glue together, via the substitution $X = \frac{T_1}{T_0}$ and $Y = \frac{T_2}{T_0}$. Therefore $X_\Sigma = \mathbb{P}^2$.

Although stated, it has not yet been formally verified that the variety X_Σ obtained from a fan Σ is indeed toric as per Definition 1.1.1.

Lemma 1.1.9 ([30, Theorem 3.1.5])**.** The variety X_Σ obtained from a fan $\Sigma \subset N_\mathbb{R}$ via the above construction is indeed a toric variety.

Proof. Note that every cone $\sigma \in \Sigma$ has by definition, a 0-dimensional cone $\{\mathbf{0}\}$ as a face. By Lemma 1.1.6, $U_{\{\mathbf{0}\}}$ lies inside $U_\sigma \subset X_\Sigma$. In calculating $U_{\{\mathbf{0}\}}$, find that $S_{\{\mathbf{0}\}} = M$ which has $2n$ generators, namely $X_i^{\pm 1} = \pm e_i^*$ for $1 \leq i \leq n$. Therefore:

$$U_{\{\mathbf{0}\}} = \mathrm{Spec}\left(\mathbb{C}[X_1, X_1^{-1}, \cdots, X_n, X_n^{-1}]\right) = (\mathbb{C}^*)^n \subset X_\Sigma.$$

$\square$

Alternatively given a toric variety X, we would like to recover a fan Σ. Start by considering a torus $T \cong (\mathbb{C}^*)^n$.

Definition 1.1.10 ([30, Section 1.1]). A *character* of T is a group homomorphism $\chi : T \to \mathbb{C}^*$. The *character group* of T is the group $M := \mathrm{Hom}(T, \mathbb{C}^*)$.

Let $a = (a_1, \ldots, a_n) \in \mathbb{Z}^n$. There is a corresponding character defined by:

$$\chi^a(t_1, \ldots, t_n) = t_1^{a_1} t_2^{a_2} \ldots t_n^{a_n}.$$

Indeed all the characters of T arise in this way, and so $M \cong \mathbb{Z}^n$.

Definition 1.1.11 ([30, Section 1.1]). A *one-parameter subgroup* of T is a morphism $\lambda : \mathbb{C}^* \to T$ that is also a group homomorphism. The *lattice of one-parameter subgroups* of T is $N := \mathrm{Hom}(\mathbb{C}^*, T)$.

Let $b = (b_1, \ldots, b_n) \in \mathbb{Z}^n$. There is a one-parameter subgroup:

$$\lambda^b(t) = (t^{b_1}, \ldots, t^{b_n}).$$

Again all the one-parameter subgroups arise in this way, and so $N \cong \mathbb{Z}^n$.

The choice of notation here for the character group and lattice of one-parameter subgroups is not accidental.

For $a \in \mathbb{Z}^n \cong M$ and $b \in \mathbb{Z}^n \cong N$, we obtain the composition $\chi^a \circ \lambda^b : \mathbb{C}^* \to \mathbb{C}^*$. Since this is also a homomorphism it is of the form $t \mapsto t^l$ for some $l \in \mathbb{Z}$. Define a natural pairing $\langle \cdot, \cdot \rangle : M \times N \to \mathbb{Z}$ by $\langle a, b \rangle = l$. This identifies N with $\mathrm{Hom}(M, \mathbb{Z})$, and M with $\mathrm{Hom}(N, \mathbb{Z})$.

Let X be a toric variety with torus $T \cong (\mathbb{C}^*)^n$. The fan for X can be reconstructed in the lattice of one-parameter subgroups. Let $\lambda^b \in N$. Define the map $\widetilde{\lambda^b} : \mathbb{C}^* \to X$ as given by the torus action of $\widetilde{\lambda^b}(t)$ on X, namely:

$$\widetilde{\lambda^b}(t) := \lambda^b(t) \cdot 1,$$

where 1 is the identity element of T. Since the closure of the torus $T \subset X$ is X itself, it follows that $x_0^b := \lim_{t \to 0} \widetilde{\lambda^b}(t) \in X$. This point is known as the *distinguished point*. Define an equivalence relation on the set of points in N by $b \sim b'$ if and only if $x_0^b = x_0^{b'}$. This equivalence class can be extended to $N_\mathbb{R}$. The set of points of $N_\mathbb{R}$ belonging to an equivalence class is equal to the interior of a cone σ. The collection of such cones give a fan $\Sigma \subseteq N_R$ as desired. It follows that there is a one to one correspondence between toric varieties and fans considered up to a change of basis on N.

Although thus far we have used the language of fans, in this thesis we are more accustomed to working with *polytopes*. To get from a fan to the corresponding polytope is routine: take the convex hull of the unique *primitive* (a lattice point whose coordinates are coprime) generators of each ray in the fan.

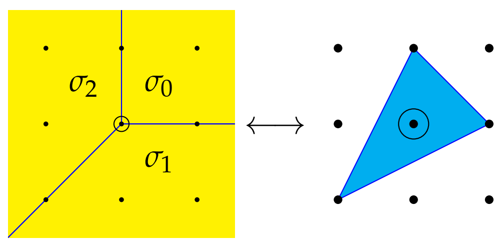

Definition 1.1.12. A *Fano polytope P* is a full dimensional convex polytope such that:

- for all vertices $v \in \mathcal{V}(P) \subset N$, then v is primitive;
- the origin lies in the strict interior of P.

These conditions on the polytope to be Fano are exactly the conditions required for the corresponding toric variety to be Fano. This thesis focuses on the case where N is a rank 2 lattice. In rank 2, Fano polytopes are referred to as *Fano polygons*. A polytope being Fano is the combinatorial interpretation of a geometric property of X_P, namely that the anticanonical divisor $-K_{X_P}$ is ample.

1.2 TORIC MORPHISMS

Consider toric varieties X_1 and X_2, whose tori are given respectively by T_1 and T_2.

Definition 1.2.1 ([30, Definition 3.3.3])**.** A morphism of varieties $\phi : X_1 \to X_2$ is a *toric morphism* if $\phi(T_1) \subseteq T_2$, and $\phi \mid_{T_1}$ is a group homomorphism.

As is typical in toric geometry, this definition of a toric morphism has a combinatorial interpretation in terms of the fans $\Sigma_1 \subset (N_1)_{\mathbb{R}}$ and $\Sigma_2 \subset (N_2)_{\mathbb{R}}$ of X_1 and X_2 respectively.

Definition 1.2.2 ([30, Definition 3.3.1])**.** Consider a lattice homomorphism $\psi : N_1 \to N_2$ which induces a linear map $\psi : (N_1)_{\mathbb{R}} \to (N_2)_{\mathbb{R}}$. We say ψ is *compatible* with (Σ_1, Σ_2) if for every cone $\sigma_1 \in \Sigma_1$, then there exists $\sigma_2 \in \Sigma_2$ such that $\psi(\sigma_1) \subseteq \sigma_2$.

Theorem 1.2.3 ([30, Theorem 3.3.4])**.** A linear map $\psi : (N_1)_{\mathbb{R}} \to (N_2)_{\mathbb{R}}$ compatible with (Σ_1, Σ_2), corresponds to a toric morphism $\phi : X_1 \to X_2$, and vice-versa.

It is worth noting that the proof of Theorem 1.2.3 is constructive. In particular given a compatible map $\psi : \Sigma_1 \to \Sigma_2$ it is easy to find the corresponding toric morphism:

$$\begin{aligned}
& \psi(\sigma_1) \subseteq \sigma_2, \\
\Longrightarrow \quad & \psi^{\vee}(\sigma_2^{\vee}) \subseteq \sigma_1^{\vee}, \\
\Longrightarrow \quad & \psi^{\vee}(S_{\sigma_2}) \subseteq S_{\sigma_1}, \\
\Longrightarrow \quad & \exists\, \phi \text{ such that } \phi(\mathrm{Spec}(S_{\sigma_1})) \subseteq \mathrm{Spec}(S_{\sigma_2}), \\
\Longrightarrow \quad & \phi(U_{\sigma_1}) \subseteq U_{\sigma_2},
\end{aligned}$$

and so this map is an affine toric morphism. Furthermore since ψ is the same linear map on all of Σ_1, the affine maps ϕ acting on U_σ for all $\sigma \in \Sigma_1$, glue together to give a toric morphism $\phi : X_1 \to X_2$.

Example 1.2.4. Consider the following fans both lying in the vector space $N_{\mathbb{R}}$ where N is a rank two lattice:

$\Sigma_1 =$ 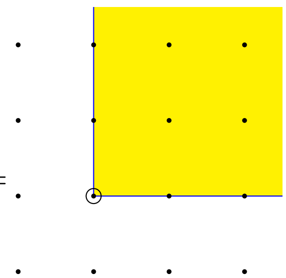

$\Sigma_2 =$ 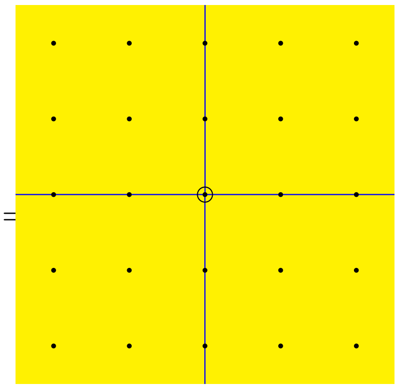

The fans correspond to the toric varieties $X_{\Sigma_1} = \mathbb{C}^2$ and $X_{\Sigma_2} = \mathbb{P}^1 \times \mathbb{P}^1$ respectively. Consider the linear map $\psi_1 : N \to N$ defined by

$$(a, b) \mapsto (a, b).$$

The map ψ_1 is compatible with (Σ_1, Σ_2), and corresponds to a toric morphism ϕ_1 which embeds $\mathbb{C}^2$ into $\mathbb{P}^1 \times \mathbb{P}^1$. Indeed it is possible to find other compatible linear maps and therefore other toric morphisms which give different embeddings of $\mathbb{C}^2$ into $\mathbb{P}^1 \times \mathbb{P}^1$.

Example 1.2.5. For a rank n lattice N, let $\Sigma_1 \subset N_{\mathbb{R}}$ be a fan with a single maximal cone whose rays are generated by the standard basis $e_1, \ldots, e_n$ of N. Set $e_0 = e_1 + \ldots + e_n$, and define Σ_2 as the fan with cones defined by primitive ray generators forming a set S satisfying $\{e_1, \ldots, e_n\} \not\subseteq S \subset \{e_0, e_1, \ldots, e_n\}$. Note that the identity map $\psi : N \to N$ is linear and compatible with (Σ_2, Σ_1), and so there is a corresponding toric morphism $\phi : X_{\Sigma_2} \to X_{\Sigma_1} = \mathbb{C}^n$.

The maximal cones of Σ_2 are given by $\sigma_i = \mathrm{span}_{\mathbb{R}_{\geq 0}}(e_0, e_1, \ldots, e_{i-1}, e_{i+1}, \ldots e_n)$, for $1 \leq i \leq n$. By calculating $\sigma_i^\vee$, note that S_{σ_i} is generated by the monomials $e_i^\star, e_1^\star - e_i^\star, \ldots, e_n^\star - e_i^\star$, and so it follows that:

$$U_{\sigma_i} = \mathrm{Spec}\left(\mathbb{C}[X_i, X_1 X_i^{-1}, \ldots, X_n X_i^{-1}]\right).$$

The glueing between the patches U_{σ_i} is identical to the glueing between the patches of the blow up of $\mathbb{C}^n$ at the origin, that is the complete intersection of the equations $X_i T_j = X_j T_i$ in $\mathbb{C}^n_{X_1,\dots,X_n} \times \mathbb{P}^{n-1}_{T_1,\dots,T_n}$. Therefore the toric variety X_{Σ_2} is the blow up of $X_{\Sigma_1} = \mathbb{C}^n$ at the origin.

This second example can be easily generalised to an arbitrary cone whose primitive ray generators $v_1, \dots, v_n$ form a basis of the lattice N. Adding the ray generated by $v_0 = v_1 + \dots + v_n$ to a fan is equivalent to the blow-up of the corresponding toric variety in a smooth point.

1.3 ORBIT-CONE CORRESPONDENCE

The aim of this section is to study the orbits of the action of T on the toric variety X_Σ.

It is known that ring homomorphisms $A \to B$ are in correspondence with morphisms of varieties $\mathrm{Spec}(B) \to \mathrm{Spec}(A)$. In particular setting $B = \mathbb{C}$, it follows that $\mathrm{Spec}(B)$ is a point and that the image of this point, that is a closed point of $\mathrm{Spec}(A)$, corresponds to a ring homomorphism from A to $\mathbb{C}$. Setting $A = \mathbb{C}[S_\sigma]$, then points of $U_\sigma = \mathrm{Spec}(\mathbb{C}[S_\sigma])$ are in bijective correspondence to semigroup homomorphisms $\phi : S_\sigma \to \mathbb{C}$.

Definition 1.3.1 ([30, Section 3.2])**.** For a cone σ, there is a point of U_σ defined by the homomorphism $S_\sigma \to \mathbb{C}$:

$$m \mapsto \begin{cases} 1, & \text{if } m \in \sigma^\perp \cap M\,, \\ 0, & \text{otherwise,} \end{cases}$$

where $\sigma^\perp = \{m \in M_\mathbb{R} : \langle u, m\rangle = 0, \forall u \in \sigma\}$. We denote this point γ_σ and call it the *distinguished point* corresponding to σ.

Note that the distinguished point is well-defined: $\sigma^\vee \cap \sigma^\perp$ is a face of $\sigma^\vee$, so if $m, m' \in S_\sigma$ such that $m + m' \in S_\sigma \cap \sigma^\perp$ then $m, m' \in S_\sigma \cap \sigma^\perp$ hence the homomorphism of Definition 1.3.1 is well-defined.

Example 1.3.2. Consider the fan $\Sigma_{\mathbb{P}^2} \subset N_\mathbb{R}$:

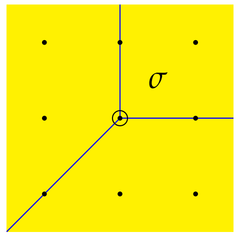

Let σ be the cone with rays generated by $(1,0)$ and $(0,1)$. Consider, as above, the morphism $\phi : \mathbb{C}[S_\sigma] \cong \mathbb{C}[X, Y] \to \mathbb{C}$ described by:

$$X^i Y^j \mapsto \begin{cases} 1, & \text{if } (i,j) = (0,0) \\ 0, & \text{otherwise.} \end{cases}$$

Note $\mathrm{Spec}(\mathbb{C}) = \{(0)\} = \{\text{point}\}$. Then:

$$\phi^{-1}((0)) = \mathbb{C} \cdot \left\{ X^i Y^j : (i,j) \neq (0,0)) \right\} = \langle X, Y \rangle$$

which is a prime ideal, and the distinguished point is $\gamma_\sigma = (0 : 0 : 1) \in \mathbb{P}^2$.

In general this calculation to find the distinguished point of a cone is cumbersome. Fortunately there is an easier method.

Let $a = (a_1, \cdots, a_n) \in N$ where $\mathrm{rank}(N) = n$. Consider the one-parameter subgroup $\lambda^a : (\mathbb{C}^*) \to (\mathbb{C}^*)^n$ defined by:

$$\lambda^a(t) := (t^{a_1}, \cdots, t^{a_n}).$$

Indeed we have seen that all one-parameter subgroups arise in this way.

Proposition 1.3.3 ([30, Proposition 3.2.2])**.** Let $u \in N$, and $\sigma \subseteq N_\mathbb{R}$ be a cone. Then $u \in \sigma$ if and only if $\lim_{t \to 0} \lambda^u(t)$ exists in U_σ. Furthermore if u belongs to the relative interior of σ, then $\lim_{t \to 0} \lambda^u(t) = \gamma_\sigma$.

Each cone $\sigma \in \Sigma$ has an associated distinguished point γ_σ and so an associated torus orbit given by $O(\sigma) := T \cdot \gamma_\sigma \subseteq X_\Sigma$. Properties of these orbits are studied by the Orbit-Cone Correspondence:

Theorem 1.3.4 (Orbit-Cone Correspondence, [30, Theorem 3.2.6])**.** Let X_Σ be the toric variety, with torus T, of the fan $\Sigma \subset N_\mathbb{R}$. Then:

(i) There is a bijective correspondence between cones $\sigma \in \Sigma$ and T-orbits of X_Σ given by:

$$\sigma \longleftrightarrow O(\sigma);$$

(ii) Let $n = \dim N_\mathbb{R}$. Then $\dim (O(\sigma)) = n - \dim(\sigma)$, $\forall$ cones $\sigma \in \Sigma$;

(iii) For a cone $\sigma \in \Sigma$, the affine patch $U_\sigma = \bigcup_{\tau \preceq \sigma} O(\tau)$;

(iv) Let $\sigma, \tau \in \Sigma$ be cones. Then $\tau \preceq \sigma$ if and only if $O(\sigma) \subseteq \overline{O(\tau)}$. Furthermore $\overline{O(\tau)} = \bigcup_{\tau \preceq \sigma} O(\sigma)$.

Example 1.3.5. Consider the fan $\Sigma_{\mathbb{P}^1 \times \mathbb{P}^1}$:

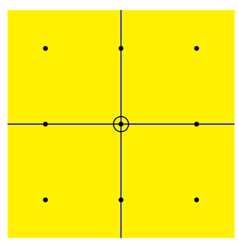

This fan has four two-dimensional cones, four one-dimensional cones and a single zero-dimensional cone. Therefore the Orbit-Cone correspondence tells us that $\mathbb{P}^1 \times \mathbb{P}^1$ has nine T-orbits, of which four are fixed points, four are one-dimensional and one is two dimensional. This is easily verified.

1.4 DIVISORS ON TORIC VARIETIES

For a fan Σ, we introduce the notation $\Sigma(r)$ for the set of r-dimensional cones in Σ. For a toric variety X_Σ, the Orbit-Cone Correspondence, see Theorem 1.3.4, tells us that a ray $\rho \in \Sigma(1)$ corresponds to a codimension one orbit $O(\rho)$ under the action of T. Hence $D_\rho = \overline{O(\rho)}$ is a T-invariant prime divisor on X_Σ. Indeed the Weil divisors of X_Σ that are invariant under the action of T, are exactly those of the form $\sum\limits_{\rho\in\Sigma(1)} a_\rho D_\rho$. Denote this set by $\mathrm{div}_T(X_\Sigma)$.

Recall that for each $m \in M$, there is a corresponding character $\chi^m : T \to \mathbb{C}^*$. Since T is a dense subvariety of X_Σ, it follows that χ^m can be extended to a rational function on X_Σ. The divisor of this rational function is given by $\mathrm{div}(\chi^m) := \sum\limits_{\rho\in\Sigma(1)} \langle m, u_\rho\rangle D_\rho$, where u_ρ is the primitive generator of ρ.

Theorem 1.4.1 ([30, Theorem 4.1.3])**.** There is an exact sequence:

$$M \xrightarrow{f} \mathrm{div}_T(X_\Sigma) \xrightarrow{g} \mathrm{Cl}(X_\Sigma) \longrightarrow 0,$$

where $f(m) = \mathrm{div}(\chi^m)$ and $g(D) = [D]$. Furthermore the sequence is short exact if and only if $\{u_\rho : \rho \in \Sigma(1)\}$ span $N_\mathbb{R}$.

Corollary 1.4.2. $\mathrm{Cl}(X_\Sigma)$ is a finitely generated group.

Indeed we can calculate $\mathrm{Cl}(X_\Sigma)$ by finding all the relations among $[D_\rho]$.

Example 1.4.3. Consider the fan $\Sigma_{\mathbb{C}^2}$ from Example 1.2.4. The fan has two rays which we call ρ_1 and ρ_2 with primitive generators $(1,0)$ and $(0,1)$ respectively. Hence $\mathrm{Cl}(\mathbb{C}^2)$ is generated by the classes $[D_{\rho_1}]$ and $[D_{\rho_2}]$. However:

$$\mathrm{div}\left(\chi^{(1,0)}\right) = \langle(1,0),(1,0)\rangle D_{\rho_1} + \langle(1,0),(0,1)\rangle D_{\rho_2} = D_{\rho_1},$$
$$\mathrm{div}\left(\chi^{(0,1)}\right) = \langle(0,1),(1,0)\rangle D_{\rho_1} + \langle(0,1),(0,1)\rangle D_{\rho_2} = D_{\rho_2}.$$

Since $[\mathrm{div}(\chi^m)] \sim 0, \forall m \in M$, it follows that $\mathrm{Cl}(\mathbb{C}^2) = 0$.

Example 1.4.4. Consider the fan $\Sigma_{\mathrm{Bl}_\mathbf{0}(\mathbb{C}^2)}$ described in Example 1.2.5, of the blow up of $\mathbb{C}^2$ at the origin. The three rays ρ_0, ρ_1 and ρ_2 have primitive generators

$(1,1)$, $(1,0)$ and $(0,1)$ respectively. As before we look for relations between the classes $[D_{\rho_i}]$:

$$\operatorname{div}\left(\chi^{(1,0)}\right) = D_{\rho_1} + D_{\rho_2} \sim 0,$$
$$\operatorname{div}\left(\chi^{(0,1)}\right) = D_{\rho_1} + D_{\rho_3} \sim 0.$$

Therefore $\mathrm{Cl}\left(\mathrm{Bl}_{\mathbf{0}}(\mathbb{C}^2)\right) = \mathbb{Z}$, and is generated by any of the classes $[D_{\rho_i}]$.

Having looked at Weil divisors, what about Cartier divisors? Since all Cartier divisors are Weil, they will also be of the form $D = \sum_{\rho \in \Sigma(1)} a_\rho D_\rho$. Denote the set of the T-invariant Cartier divisors by $\mathrm{Cdiv}_T\left(X_\Sigma\right)$.

Let $m \in M$. Since χ^m is a rational function on X_Σ, the divisor $\operatorname{div}(\chi^m)$ is Cartier. We obtain a short exact sequence similar to that for Weil divisors.

Theorem 1.4.5 ([30, Theorem 4.2.1])**.** There is an exact sequence:

$$M \longrightarrow \mathrm{Cdiv}_T(X_\Sigma) \longrightarrow \mathrm{Pic}(X_\Sigma) \longrightarrow 0.$$

The sequence is short exact if and only if $\{u_\rho : \rho \in \Sigma(1)\}$ span $N_\mathbb{R}$. Furthermore the exact sequence for Weil divisors maps into this sequence by inclusion.

Theorem 1.4.5 shows that $\mathrm{Pic}(X_\Sigma) = 0$ if and only if every T-invariant Cartier divisor on X_Σ is the divisor of a character χ^m.

Proposition 1.4.6. A toric variety X_Σ is smooth if and only if $\mathrm{Cl}(X_\Sigma) = \mathrm{Pic}(X_\Sigma)$.

This combined with Examples 1.4.3 and 1.4.4 together show that the blow-up of a smooth toric variety at the origin increases the Picard rank by one. Indeed the blow-up of any toric variety in a smooth point has this effect.

Usually a Cartier divisor D on a variety X is described by *local data*, that is a set of pairs $(U_i, f_i)_{i\in I}$, where $\{U_i\}_{i\in I}$ is an open cover of X and $D\big|_{U_i} = \operatorname{div}(f_i)$ for all $i \in I$. The local data has a combinatorial description:

Theorem 1.4.7 ([30, Theorem 4.2.8])**.** Let $D = \sum_{\rho \in \Sigma(1)} a_\rho D_\rho$ be a divisor on a toric variety X_Σ. Then D is Cartier if and only if $\forall \sigma \in \Sigma_{\max}$, there exists m_σ such that

$$\langle m_\sigma, u_\rho \rangle = -a_\rho, \qquad \forall \rho \in \sigma(1).$$

Namely D is principal on every affine patch $U_\sigma \subset X_\Sigma$ and given by

$$D\big|_{U_\sigma} = \operatorname{div}(\chi^{-m_\sigma})\big|_{U_\sigma}.$$

The content of Theorem 1.4.7 is that the set $\{m_\sigma\}_{\sigma \in \Sigma}$ describes local data of the Cartier divisor D.

The discussion of Cartier divisors on toric varieties has an interpretation in terms of support functions. The *support* of Σ is $|\Sigma| := \bigcup_{\sigma \in \Sigma} \sigma \subseteq N_{\mathbb{R}}$.

Definition 1.4.8 ([30, Definition 4.2.8])**.** A *support function* on Σ is a function $\phi : |\Sigma| \to \mathbb{R}$ which is linear of every cone $\sigma \in \Sigma$. The support function ϕ is *integral* on N if $\phi(|\Sigma| \cap N) \subseteq \mathbb{Z}$.

Denote the set of integral support functions by $\mathrm{SF}(\Sigma, N)$.

Proposition 1.4.9 ([30, Theorem 4.2.12])**.** Consider the map $\mathrm{CDiv}_T(X_\Sigma) \to \mathrm{SF}(\Sigma, N)$ which sends the Cartier divisor D given by local data $\{m_\sigma\}_{\sigma \in \Sigma}$ to the function $\phi_D : |\Sigma| \to \mathbb{R}$ where:

$$\phi_D(u) = \langle m_\sigma, u \rangle, \qquad \text{for } u \in \sigma.$$

This map is an isomorphism between the set of Cartier divisors on X_Σ and integral support functions on Σ.

The final thing we associate to a T-invariant divisor is the polyhedron of sections:

Definition 1.4.10 ([30, Section 4.3])**.** The *polyhedron of sections* of a divisor $D = \sum_{\rho \in \Sigma(1)} a_\rho D_\rho$ is given by:

$$P_D := \left\{ m \in M_{\mathbb{R}} : \langle m, u_\rho \rangle \geq -a_\rho, \forall \rho \in \Sigma(1) \right\}.$$

Consider the sheaf $\mathcal{O}_{X_\Sigma}(D)$ on X_Σ defined by:

$$\mathcal{O}_{X_\Sigma}(D)(U) := \{f \in \mathbb{C}(X_\Sigma)^* : (\mathrm{div}(f) + D)\,|_U \geq 0\} \cup \{0\}\,.$$

The significance of the polyhedron of sections is that it governs the global sections of the sheaf $\mathcal{O}_{X_\Sigma}(D)$, namely:

$$\Gamma\left(X_\Sigma, \mathcal{O}_{X_\Sigma}(D)\right) = \bigoplus_{m \in P_D \cap M} \mathbb{C} \cdot \chi^m.$$

Definition 1.4.11 ([30, Definition 6.3.2])**.** Consider a divisor $D = \sum_i a_i p_i$ on an irreducible smooth complete curve C. The degree of D is:

$$\deg(D) := \sum_i a_i \in \mathbb{Z}.$$

The degree definition can be used to define an intersection degree between a Cartier divisor D and an irreducible curve C on a normal variety X. The sheaf $\mathcal{O}_X(D)$ can restricted to C as $\mathcal{O}_C(D) := \iota^*\left(\mathcal{O}_X(D)\right)$ where $\iota : C \hookrightarrow X$ is the inclusion map.

Definition 1.4.12 ([30, Definition 6.3.6])**.** The *intersection number* of D and C is given by:

$$D \cdot C := \deg\left(\phi^* \mathcal{O}_C(D)\right).$$

Definition 1.4.13 ([30, Definition 6.3.10])**.** Let X be a normal variety. Then a Cartier divisor D on X is *nef* if $D \cdot C \geq 0$, for every irreducible complete curve $C \subseteq X$.

On a toric variety X_Σ such that $|\Sigma| = N_\mathbb{R}$, a Cartier divisor D is nef if and only if $\mathcal{O}_{X_\Sigma}(D)$ is generated by global sections.

1.5 CLASSIFICATION OF FANO POLYGONS BOUNDED BY INDEX

The toric variety of a Fano polygon is a toric log *del Pezzo surface*. These surfaces have been studied extensively and many classification results exist. We recall an algorithm of Kasprzyk–Kreuzer–Nill [50] which exploits the combinatorics of Fano polygons.

Definition 1.5.1 ([50])**.** Let P be a Fano polygon, and E be an edge of P. Denote the inward pointing normal of E by n_E. Define the *order* of P by:

$$o_P := \min\left\{k \in \mathbb{Z}_{>0} : (P/k)^\circ \cap N = \{\mathbf{0}\}\right\},$$

where $P/k = \{p/k : p \in P\} \subset N_\mathbb{R}$. The *local index* of E is given by $l_E = |\langle E, n_E\rangle|$ and the *maximal local index* of P is defined by:

$$m_P := \max\{l_E : E \text{ is an edge of } P\}.$$

Define the *index* of P by:

$$l_P := \operatorname{lcm}\{l_E : E \text{ is an edge of } P\}.$$

The choice of terminology here is not coincidental: the index of P is equal to the index of X_P, that is the smallest positive integer l such that $-lK_{X_P}$ is very ample

Proposition 1.5.2 ([50, Proposition 4.1])**.** Let P be a Fano polygon. Then for an edge E of P, we have that:

$$|E \cap N| \leq 2o_P(l_E + 1) + 1.$$

Proof. By a change of basis assume without loss of general that E has vertices (a, l_E) and (b, l_E). Set $c = |E \cap N| - 1$. Note $(\pm o_P, 0) \notin P^\circ$, since otherwise $(\pm 1, 0) \in (P/o_P)^\circ$ which contradicts o_P being the order of P. Therefore for $|E \cap N| > 2o_P$, P is bounded by the lines $L1, L2$ and $L3$, where $L1$ is the line through (a, l_E) and (b, l_E), $L2$ is the line through (a, l_E) and $(-o_P, 0)$, and $L3$ is the line through (b, l_E) and $(o_P, 0)$.

The lines $L2$ and $L3$ intersect at a point (x, y) where $y = \frac{2o_P l_E}{2o_P - c}$. Since $\mathbf{0} \in P^\circ$, necessarily:

$$y = \frac{2o_P l_E}{2o_P - c} \leq -1,$$
$$2o_P(l_E + 1) \geq c = |E \cap N| - 1,$$

which is the desired identity. □

Definition 1.5.3 ([57, Definition 3.1])**.** Let $P \subset N_\mathbb{R}$ be a Fano polygon. An edge E of P is a *special facet* if:

$$\sum_{v \in \mathcal{V}(P)} v \in \mathbb{R}_{\geq 0} E.$$

Example 1.5.4. Consider $P = \operatorname{conv}\Big\{(0,1), (1,0), (-5,-1)\Big\}$, and calculate that:

$$\sum_{v \in \mathcal{V}(P)} v = (0,1) + (1,0) + (-5,-1) = (-4,0).$$

So P has a unique special facet given by $F = \operatorname{conv}\Big\{(0,1), (-5,-1)\Big\}$.

By the definition of Fano polygon, $\mathbf{0} \in P^\circ$. Therefore the union of all cones obtained from a Fano polygon P is equal to $N_\mathbb{R}$, so P has at least one special facet. We use a result from [50] which is derived from a proof in [32].

Lemma 1.5.5 ([50, Lemma 6.1])**.** Let P be a Fano polygon. Let F be a special facet of P of local index l_F and with inward pointing normal $n_F \in M$. Then:

$$P \subset \big\{(a,b) \in N_\mathbb{R} : -l_F(l_F + 1) \leq \langle (a,b), n_F \rangle \leq l_F \big\}.$$

Proof. For each vertex $v \in \mathcal{V}(P)$, there exists $k \in \mathbb{Z}$ such that $\langle v, n_F \rangle = k$. Clearly $k \leq l_F$. Indeed for a given $k \in \mathbb{Z}_{\leq l_F}$, there are at most two vertices satisfying $\langle n_F, v\rangle = k$. Therefore, using initially that F is a special facet, we have:

$$\begin{aligned}
0 &\leq \langle \sum_{v\in\mathcal{V}} v, n_F\rangle \\
&= \sum_{v:\langle v,n_F\rangle<0} \langle v, n_F\rangle + \sum_{v:\langle v,n_F\rangle\geq 0} \langle v, n_F\rangle \\
&\leq \sum_{v:\langle v,n_F\rangle<0} \langle v, n_F\rangle + 2\sum_{i=0}^{l_F} i \\
&= \sum_{v:\langle v,n_F\rangle<0} \langle v, n_F\rangle + l_F(l_F+1)
\end{aligned}$$

which implies that:

$$\sum_{v:\langle v,n_F\rangle<0} \langle v, n_F\rangle \geq -l_F(l_F+1).$$

So for any given vertex $v \in \mathcal{V}(P)$ necessarily $\langle v, n_F\rangle \geq -l_F(l_F+1)$, and the result follows. □

Corollary 1.5.6. Let P be a Fano polygon with index l_P, and E be an edge given by $\operatorname{conv}\{(a, l_E), (b, l_E)\}$ where $-l_E < a \leq 0 < b$. Then:

$$P \subset \left\{ (x,y) \in N_{\mathbb{R}} : \begin{array}{c} -l_E x + (l_P + a)y \leq l_E l_P \\ l_E x + (l_P - b)y \leq l_E l_P \end{array} \right\}.$$

Proof. This follows from Proposition 1.5.2. □

Lemma 1.5.5 and Corollary 1.5.6 are used to create the following algorithm which, by running for all choices of special facet $F = \operatorname{conv}\{(a, l_F), (b, l_F)\}$, classifies all Fano polygons with index given by a fixed number $l \in \mathbb{Z}_{>0}$. Note that there is indeed a finite number of choices for F since $l_F \leq l$, and we can assume $-l_F < a \leq 0 < b$ where $b - a \leq 2l(l_F - 1)$ by Proposition 1.5.2.

Algorithm 1 Classification of Fano Polygons with index l

1: **Input:** Special facet $F = \text{conv}((a, l_F), (b, l_F))$, index l.
2: $L1 := \{(x, y) \in N_{\mathbb{R}} : -l_F x + (l_P + a)y \leq l_F l_P\}$.
3: $L2 := \{(x, y) \in N_{\mathbb{R}} : l_F x + (l_P - b)y \leq l_F l_P\}$.
4: $L := \{(x, y) \in N_{\mathbb{R}} : y = -l_F(l_F + 1)\}$.
5: $T :=$ region bounded by $F, L, L1$ and $L2$.
6: PossiblePoints := {primitive points $v \in N$ contained in T}.
7: ActiveConstructions := $\{v_0 = (a, l_F), v_1 = (b, l_F)\}$, an ordered set.
8: CompleteConstructions := $\varnothing$.
9: **for** $P = \{v_0, \dots v_i\} \in$ ActiveConstructions, **do**
10:     **for** $v \in$ PossiblePoints that respect convexity, and the special facet F, **do**
11:         **if** $v \neq (a, l_F)$ and the edge E from v_i to v satisfies $l_E \mid l$, **then**
12:             ActiveConstructions $\leftarrow$ (ActiveConstructions$\setminus\{P\}) \cup \{P \cup v\}$.
13:         **if** $v = (a, l_F)$ and the edge E from adding v_i to v_0 satisfies $l_E \mid l$, **then**
14:             ActiveConstructions $\leftarrow$ ActiveConstructions$\setminus\{P\}$.
15:             **if** $l_P = l$, **then**
16:                 CompleteConstructions $\leftarrow$ CompleteConstructions $\cup \{P\}$.
17: **if** ActiveConstructions $\neq \varnothing$, **then**
18:     **go to** 9.
19: **Output:** CompleteConstructions.

The authors of [50] have implemented the algorithm through computer code to classify all Fano polygons with index up to and including 16:

l	# Fano polygons with index l
1	16
2	30
3	99
4	91
5	250
6	379
7	429
8	307
9	690
10	916
11	939
12	1279
13	1142
14	1545
15	4312
16	1030

Note that the algorithm recovers the classification of the sixteen reflexive polygons since reflexive polygons are exactly those with index $l = 1$.

2

MIRROR SYMMETRY

2.1 10 SMOOTH DEL PEZZO SURFACES

One of the most famous examples in algebraic geometry is that of the famous 10 smooth del Pezzo surfaces. We follow a derivation of this classification by Manin [54]. Recall the formal definition of a del Pezzo surface.

A line bundle L on a surface (a 2-dimensional variety) V is said to be *ample* if there exists $n \in \mathbb{Z}_{\geq 1}$, and a closed embedding $i : V \mapsto \mathbb{P}^N$ defined by the global sections of $L^n = L^{\otimes n}$, such that:

$$L^n \cong i^* \left(\mathcal{O}_{\mathbb{P}^N}(1)\right).$$

In the case $n = 1$, we say L is *very ample*.

Definition 2.1.1 ([54, Definition 24.2])**.** A smooth birationally trivial surface V on which the anticanonical sheaf, denoted Ω_V^{-1}, is ample is called a *del Pezzo surface*.

Consider a projective variety $V \subset \mathbb{P}^N$, and a general linear subspace $L \subset \mathbb{P}^N$ such that $\dim(L) = \operatorname{codim}(V)$. Then recall that the *projective degree* of V is given by:

$$\deg(V) := \#(V \cap L).$$

If $\operatorname{codim}(V) = 1$, that is V is a hypersurface, then the projective degree is given by the degree of the homogeneous polynomial defining V. Now given a del Pezzo surface V, the self-intersection number $d = \Omega_V \cdot \Omega_V$ defined using Definition 1.4.12, is called the *degree* of the del Pezzo surface and agrees with the projective degree of the image $i(V) \subset \mathbb{P}^N$.

Lemma 2.1.2 ([54, Lemma 24.3.1])**.** Let V be a smooth projective surface which is birationally trivial. Then the group $\operatorname{Pic}(V)$ is free with a finite number of generators, and furthermore:

$$\operatorname{rank}(\operatorname{Pic}(V)) + \Omega_V \cdot \Omega_V = 10.$$

Proof. Consider the blow-up of a smooth point $f : V' \to V$. It is known:

- From Section 1.4 that, $\operatorname{Pic}(V') = f^*(\operatorname{Pic}(V)) \oplus \mathbb{Z}D$, where D is orthogonal to $f^*(\operatorname{Pic}(V))$.
- $\Omega_{V'} = f^*(\Omega_V) + D$.

So:

$$\begin{aligned}
&\operatorname{rank}\left(\operatorname{Pic}(V')\right) + \Omega_{V'} \cdot \Omega_{V'} \\
=&\operatorname{rank}(\operatorname{Pic}(V)) + 1 + f^*(\Omega_V) \cdot f^*(\Omega_V) + 2f^*(\Omega_V) \cdot D + D \cdot D \\
=&\operatorname{rank}(\operatorname{Pic}(V)) + 1 + \Omega_V \cdot \Omega_V + 2(0) - 1 \\
=&\operatorname{rank}(\operatorname{Pic}(V)) + \Omega_V \cdot \Omega_V.
\end{aligned}$$

Therefore the statement holds for V if and only if it holds for V'. Since every birational morphism is a composition of blow-ups in a smooth point, it is enough to show the statement holds for a single arbitrary surface. Consider the surface $\mathbb{P}^2$. Then $\Omega_{\mathbb{P}^2} \cong \mathcal{O}_{\mathbb{P}^2}(-3)$, which has self-intersection 9, and $\operatorname{rank}\left(\operatorname{Pic}(\mathbb{P}^2)\right) = \operatorname{rank}(\mathbb{Z}) = 1$. ☐

Theorem 2.1.3 ([54, Theorem 24.3])**.** Let V be a del Pezzo surface of degree d. Then:

(i) $1 \leq d \leq 9$;

(ii) Every irreducible curve with a negative self-intersection number on V is exceptional;

(iii) If V has no exceptional curves, then either $d = 9$ and V is isomorphic to $\mathbb{P}^2$, or $d = 8$ and V is isomorphic to $\mathbb{P}^1 \times \mathbb{P}^1$.

Proof. '(i)' Since Ω_V^{-1} is ample it follows by the Nakai-Moishezon criteria, see for example [39], that $\Omega_V \cdot \Omega_V \geq 1$. Also necessarily rank $(\mathrm{Pic}(V)) \geq 1$. Therefore the bounds follow from Lemma 2.1.2.

'(ii)' Let $D \subset V$ be a curve with negative self-intersection. By the Nakai-Moishezon criteria $D \cdot \Omega_V^{-1} > 0$, since Ω_V^{-1} is ample. By the Riemann-Roch theorem for surfaces:

$$2\rho_a(D) - 2 = D \cdot D - D \cdot \Omega_V^{-1}. \tag{1}$$

Since D is irreducible, $\rho_a(D) \geq 0$. This implies that the only possible values satisying equation (1) are:

$$D \cdot D = -1, \qquad \text{and} \qquad \rho_a(D) = 0.$$

Now $\rho_a(D) = 0$ implies that $D \cong \mathbb{P}^1$. Therefore D is exceptional.

'(iii)' Since there are no exceptional curves, V is minimal, and additionally by part (ii) contains no curves of negative self intersection. The only surfaces with these properties are known to be $\mathbb{P}^2$ and $\mathbb{P}^1 \times \mathbb{P}^1$. It is routine to check that both of these surfaces are del Pezzo. □

A collection of at most 8 points are said to be in *general position* if:

- No 3 points lie on a line;
- No 6 points lie on a conic;

- Any cubic passes through at most 7 points with at most 1 double point;
- Any quartic passes through at most 8 points with at most 3 of them a double point;
- Any quintic that passes through the 8 points has at most 6 of them double points;
- Any sextic that passes through the 8 points has at most 1 triple point.

Theorem 2.1.4 ([54, Theorem 24.4])**.** Let V be a del Pezzo surface of degree d. Then:

- If $d = 9$, then V is isomorphic to $\mathbb{P}^2$;
- If $d = 8$, then V is isomorphic either to $\mathbb{P}^1 \times \mathbb{P}^1$ or to the blow-up of $\mathbb{P}^2$ in a point;
- If $1 \leq d \leq 7$, then V is isomorphic to the blow-up of $\mathbb{P}^2$ in $9 - d$ points in general position.

Proof. The minimal del Pezzo surfaces have been classified as $\mathbb{P}^2$ and $\mathbb{P}^1 \times \mathbb{P}^1$ in Theorem 2.1.3. Hence suppose V is a non-minimal del Pezzo surface. Then there exists a birational morphism $f : V \to W$, where W is a minimal rational surface.

Suppose W is a non-trivial ruled surface. It is known then that there is an irreducible curve D on W with self-intersection -2. It follows that:

$$f^{-1}(D) \cdot f^{-1}(D) \leq -2.$$

This is in contradiction with Theorem 2.1.3. So W is not a non-trivial ruled surface, and is therefore either $\mathbb{P}^2$ or $\mathbb{P}^1 \times \mathbb{P}^1$.

Suppose $W = \mathbb{P}^1 \times \mathbb{P}^1$. Let $x = (x_0, x_1) \in \mathbb{P}^1 \times \mathbb{P}^1$ be a point at which f^{-1} is not defined. The morphism f can be split up into separate morphisms:

$$V \xrightarrow{g} W' \xrightarrow{h} \mathbb{P}^1 \times \mathbb{P}^1,$$

where $h : W' \to \mathbb{P}^1 \times \mathbb{P}^1$ is the blow up at x. By contracting both the curves $h^{-1}\left(\mathbb{P}^1 \times \{x_1\}\right)$ and $h^{-1}\left(\{x_0\} \times \mathbb{P}^1\right)$, obtain a morphism $h' : W' \to \mathbb{P}^2$. So there is also a composition of morphisms giving a birational morphism from V to $\mathbb{P}^2$:

$$V \xrightarrow{f} W' \xrightarrow{h'} \mathbb{P}^2.$$

Hence we can assume $W = \mathbb{P}^2$ and there is a morphism $f : V \to \mathbb{P}^2$. Recall that a blow-up at a point causes the rank of the Picard group to increase by 1. Therefore

$$\operatorname{rank}\left(\operatorname{Pic}(V)\right) = 10 - d$$

where f splits into $r = 9 - d$ blow-ups.

Label the set of points where f^{-1} is not defined by $x_1, \cdots, x_s \in \mathbb{P}^2$. By the definition of a blow-up, necessarily $s \leq r$. Suppose $s < r$. Then one of the points that gets blown up would lie on the exceptional divisor D of the blow-up of some point x_i. It follows that

$$f^{-1}(D) \cdot f^{-1}(D) \leq -2$$

which contradicts Theorem 2.1.3. Hence $s = r$.

Suppose that 3 of the x_i lie on a line D. Then after blowing up these 3 points, the inverse image of D will have self-intersection number less than or equal -2 which again contradicts Theorem 2.1.3. Similar statements hold for each of the other requirements to show $x_1, \cdots, x_r$ lie in general position. □

The converse is also true: all surfaces described in Theorem 2.1.4 are del Pezzo surfaces though the proof is omitted from this thesis. This completes the classification of the 10 smooth del Pezzo surfaces and their structure, that is, every surface is obtained via a blow-up of $\mathbb{P}^2$ with the exception of $\mathbb{P}^1 \times \mathbb{P}^1$ which is obtained via blowing up $\mathbb{P}^2$ in two distinct points and contracting the strict transform of the unique line through these two points. This structure is referred to as a *cascade*; a terminology coined by Reid–Suzuki [65].

$$\begin{tikzcd}
\mathbb{P}^2 & dP_8 \arrow[l] & dP_7 \arrow[l] \arrow[d] & dP_6 \arrow[l] & \cdots \arrow[l] & dP_1 \arrow[l] \\
& & \mathbb{P}^1 \times \mathbb{P}^1 & & &
\end{tikzcd}$$

This cascade structure appears again in Chapter 4 when we consider del Pezzo surfaces with cyclic quotient singularities.

2.2 CYCLIC QUOTIENT SINGULARITIES

A *quotient singularity* $\frac{1}{R}(a,b)$ is given by the action of the cyclic group of order R, denoted μ_R, on $\mathbb{C}^2_{x,y}$ by:

$$\epsilon \cdot (x,y) = (\epsilon^a x, \epsilon^b y),$$

where ϵ is an R^{th} root of unity, and considering $Z = \operatorname{Spec}(\mathbb{C}[x,y]^{\mu_R})$. The germ of the origin is the singularity.

For example consider a $\frac{1}{2}(1,1)$ singularity. Let $G = \mathbb{Z}/2\mathbb{Z}$ and $\epsilon = -1$. The action of G on $\mathbb{C}^2$ is described by:

$$-1 \cdot (x,y) = (-x,-y).$$

Then:

$$\begin{aligned}
Z &= \operatorname{Spec}\left(\mathbb{C}[x,y]^{\mathbb{Z}/2\mathbb{Z}}\right) \\
&= \operatorname{Spec}\left(\mathbb{C}[x^2,xy,y^2]\right) \\
&\cong \operatorname{Spec}\left(\mathbb{C}[u,v,w]/(uw-v^2)\right) \\
&= \mathbb{V}(uw-v^2) \subset \mathbb{C}^3.
\end{aligned}$$

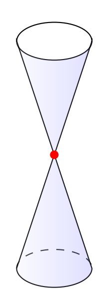

A quotient singularity $\frac{1}{R}(a,b)$ is *cyclic* if:

$$\gcd(R,a) = \gcd(R,b) = 1.$$

In this case, set:

$$k = \gcd(a+b,R).$$

So:

$$a+b = kc, \qquad \text{and} \qquad R = kr.$$

It follows that the cyclic quotient singularity can be written as $\frac{1}{kr}(1,kc-1)$. Three types of cyclic quotient singularities are defined by Kollar–Shepherd-Barron [52]:

- A cyclic quotient singularity $\frac{1}{kr}(1,kc-1)$ is a *T-singularity* if $r \mid k$;
  - A T-singularity admits a qG-smoothing (which will be defined in Section 2.4) ;
- A T-singularity $\frac{1}{kr}(1,kc-1)$ is *primitive* if $r = k$;
- A cyclic quotient singularity $\frac{1}{kr}(1,kc-1)$ is an *R-singularity* if $k < r$;
  - An R-singularity is rigid under qG-deformation.

Consider an arbitrary cyclic quotient singularity $\sigma = \frac{1}{kr}(1,kc-1)$ not necessarily satisfying either $r \mid k$ or $k < r$. There exists unique non-negative integers n and k_0 such that $k_0 < r$ and $k = nr + k_0$. If $k_0 > 0$, then σ is qG-deformation equivalent to a $\frac{1}{k_0 r}(1,k_0 c-1)$ cyclic quotient singularity. Informally the n copies of r correspond to *primitive T-parts* of σ and can be smoothed away. The *residue* of σ is given by

$$\operatorname{res}(\sigma) := \begin{cases} \varnothing, & \text{if } k_0 = 0, \\ \frac{1}{k_0 r}(1,k_0 c-1), & \text{otherwise.} \end{cases}$$

Definition 2.2.1 ([5, Definition 2.4])**.** The *singularity content* of σ is given by the pair:

$$\mathrm{SC}(\sigma) := (n, \mathrm{res}(\sigma))\,.$$

2.3 CYCLIC QUOTIENT SINGULARITIES ON A TORIC VARIETY

Many properties of X_P, the Fano toric variety corresponding to a Fano polygon P, have combinatorial analogues that can be observed in P: examples include the singularities of X_P and the anticanonical degree $(-K_{X_P})^2$. In particular the cyclic quotient singularities of Section 2.2 can be observed at the level of Fano polygons.

Proposition 2.3.1 ([36])**.** An affine toric variety U_σ is nonsingular if and only if σ is generated by part of a basis for the lattice N, in which case:

$$U_\sigma \cong \mathbb{C}^k \times (\mathbb{C}^*)^{n-k},$$

where $k = \dim(\sigma)$.

Consider a cone $\sigma \subset N_{\mathbb{R}}$ whose rays are generated by $(0,1)$ and $(k,-1)$ for $k \geq 2$ (the case $k = 2$ is seen in Example 1.1.7):

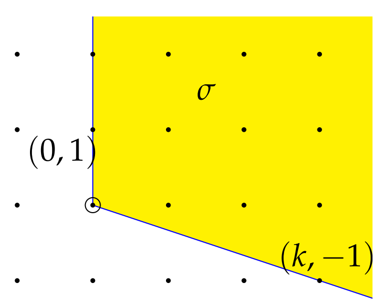

Note these points do not form a basis of N, and so U_σ will be singular. The dual cone is given by:

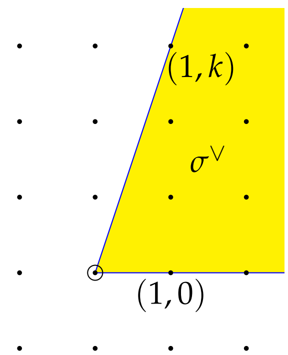

It follows that:

$$\mathbb{C}[S_\sigma] = \mathbb{C}[X, XY, XY^2, \cdots, XY^k].$$

Substituting $X = U^k, Y = \frac{V}{U}$:

$$\mathbb{C}[S_\sigma] = \mathbb{C}[U^k, U^{k-1}V, U^{k-2}V^2, \cdots, V^k].$$

Note the inclusion $\mathbb{C}[S_\sigma] \subset \mathbb{C}^2_{U,V}$. Consider the action of $G = \mathbb{Z}/k\mathbb{Z}$ on $\mathbb{C}^2$ via:

$$\zeta \cdot (U, V) \mapsto (\zeta U, \zeta V).$$

It is routine to check that $\mathrm{Spec}\,(\mathbb{C}[S_\sigma]) = U_\sigma = \mathbb{C}^2/G = \mathrm{Spec}\,(\mathbb{C}[U,V])/G$. That is, following the definition from Section 2.2, U_σ contains a $\frac{1}{k}(1,1)$ cyclic quotient singularity.

We have not covered all possible cones up to $GL(N)$-equivalence: to do so one would need to consider a cone $\sigma \subset N_\mathbb{R}$ generated by e_2 and $ke_1 - me_2$ where $0 < m < k$, which leads to a $\frac{1}{k}(1,m)$ cyclic quotient singularity, via a similar argument to the $m = 1$ case.

Consider a cone σ defined by an edge E of a Fano polygon $P \subset N_\mathbb{R}$. This edge corresponds to a (possibly trivial) cyclic quotient singularity on X_P. The decomposition of an arbitrary cyclic quotient singularity into primitive T-parts and a residual singularity seen in Section 2.2, has an analogous description in the combinatorics of E:

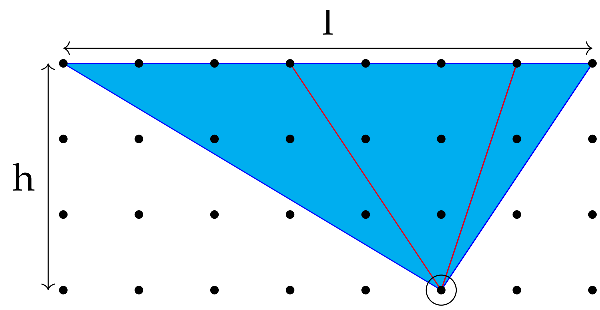

The *lattice length* l of $E \subset N_{\mathbb{R}}$ is given by the value $|E \cap N| - 1$. The *lattice height* h of E is given by the lattice distance from the origin: that is, given the unique primitive inward pointing normal n_E of E belonging to M, the height is given by $|\langle v, n_E \rangle|$, for any $v \in E$.

There exists unique non-negative integers n, r such that $r < h$ and $l = hn + r$. Divide C into separate sub-cones $C_0, \cdots, C_n$ where $C_1, \cdots, C_n$ (known as T-cones) have lattice length h, and C_0 has lattice length r and is known as an R-cone. The T-cones correspond to primitive T-singularities on X_P and the R-cone to an R-singularity. The choice of subdivision of C is not important. This is known as a *partial crepant resolution*.

We are able to generalise the definition of singularity content to a Fano polygon P.

Definition 2.3.2 ([5, Definition 3.1])**.** Let $P \subset N_{\mathbb{R}}$ be a polygon. Label the edges of P in clockwise order $E_1, \cdots E_k$. Each edge E_i corresponds to a cyclic quotient singularity σ_i. Let:

$$\mathrm{SC}(\sigma_i) = (n_i, \mathrm{res}(\sigma_i)) .$$

Define the *singularity content* of P to be:

$$\mathrm{SC}(P) := \left(\sum_{i=1}^{k} n_i, \mathcal{B} \right),$$

where $\mathcal{B} := \{\mathrm{res}(\sigma_1), \cdots, \mathrm{res}(\sigma_k)\}$ is a cyclically ordered set.

The singularity content of P, a combinatorial property, describes the singularities on X_P, a geometrical property.

2.4 DEFORMATION THEORY

Deformation theory can be studied from many sources such as Hartshorne [40], and has been specialised to the toric case by Mavlyutov [56] and Altmann [9, 10, 11, 12, 13] amongst others.

Definition 2.4.1. A *deformation* of an affine algebraic variety X_0 is a flat map $\pi : \chi \to S$ over a ring S, such that:

- $\pi^{-1}(0) = X_0$;
- There is a commutative diagram:

$$\begin{tikzcd} X_0 \arrow[r, hook] \arrow[d] & \chi \arrow[d, "\pi"] \\ 0 \arrow[r, hook] & S \end{tikzcd}$$

Recall that informally flatness means that the fibres vary continuously. We have the following terminology:

- χ is the *total space*;
- S is the *base space* of the deformation.

The simplest example of a deformation is the trivial deformation over a set S which is given by $\chi = X_0 \times S$ and the usual projection $X_0 \times S \to S$.

Definition 2.4.2. Consider two deformations of X_0 given by $\pi : \chi \to S$ and $\pi' : \chi' \to S$. The deformations are *isomorphic* if there exists a map $\phi : \chi \to \chi'$ over S inducing the identity on X_0.

Definition 2.4.3. An *Artin ring* is a ring satisfying the descending chain condition.

Artin rings over $\mathbb{C}$ are exactly those that are finite-dimensional vector spaces.

Definition 2.4.4. Let S be the spectrum of an Artin ring and X_0 be an affine algebraic variety. Define $\mathrm{Def}_{X_0}(S)$ to be the *set of deformations* of X_0 over S modulo isomorphism.

Recall that the dual numbers are given by $\mathbb{C}[x]/(x^2)$. The variety $\mathrm{Spec}\left(\mathbb{C}[x]/(x^2)\right)$ is an infinitesimally short line segment, that is, a point together with a tangent direction. Hence giving a map $\mathrm{Spec}\left(\mathbb{C}[x]/(x^2)\right) \to X$ is the same as giving a point $x \in X$ together with a tangent vector in $T_x X$.

Definition 2.4.5. A deformation $\pi : \chi \to S$ is called a *first order deformation* of X_0 if $S = \mathrm{Spec}\left(\mathbb{C}[x]/(x^2)\right)$. Set $T^1_{X_0} = \mathrm{Def}_{X_0}(\mathrm{Spec}\left(\mathbb{C}[x]/(x^2)\right))$.

Definition 2.4.6. A variety X_0 is called *rigid* if $T^1_{X_0} = 0$, that is, every first order deformation is isomorphic to the trivial deformation.

Example 2.4.7. Let $X \hookrightarrow \mathbb{A}^n$ be a complete intersection given by:

$$(f_1 = \ldots = f_r = 0) \subset \mathbb{A}^n.$$

Specifically X is the variety $\mathrm{Spec}\left(\mathbb{C}[x_1,\ldots,x_n]/\langle f_1,\ldots,f_r\rangle\right)$. Consider the ideal given by $I = \langle f_1 + g_1 x, \ldots, f_r + g_r x\rangle \subset \left(\mathbb{C}[x]/(x^2)\right)[x_1,\ldots,x_n]$, where $g_i \in \mathbb{C}[x_1,\ldots,x_n]$ are arbitrary. We can check that $\chi = \mathrm{Spec}\left(\left(\mathbb{C}[x]/(x^2)\right)[x_1,\ldots,x_n]/I\right)$ is flat over $\mathrm{Spec}\left(\mathbb{C}[x]/(x^2)\right)$. Also the fiber over $t = 0$ recovers X. Therefore this is a first order deformation.

For the purpose of this thesis, we are primarily concerned with $\mathbb{Q}$-Gorenstein (qG-)deformations. Recall that for a del Pezzo surface X, the Gorenstein index is the smallest possible integer $r \in \mathbb{Z}_{>0}$ such that rK_X is Cartier.

Definition 2.4.8 ([52, 53])**.** Let S be the spectrum of a local Artin ring, and consider a deformation $\pi : \chi \to S$. Consider the *relative canonical divisor* $K_{\chi/S} = K_\chi - \pi^*(K_S)$, where π^* is the pullback map of divisors. Then π is a *qG-deformation* if $rK_{\chi/S}$ is a Cartier divisor for some $r \in \mathbb{Z}_{>0}$.

It follows that K_X^2 is constant on fibers over S.

Example 2.4.9. Consider the primitive T-singularity $\frac{1}{k^2}(1, kc-1)$ given by the action of μ_{k^2} on $\mathbb{C}^2_{x,y}$. We have an identification:

$$\frac{1}{k^2}(1, kc-1) \cong (uv = w^k) \subset \frac{1}{k}(1, k-1, c) = \mathbb{C}^3_{u,v,w}/\mu_k,$$

where $u = x^k, v = y^k$ and $w = xy$. A smoothing via a qG-Gorenstein deformation is given by:

$$(uv = w^k + t) \subset \frac{1}{k}(1, k-1, c) \times \mathbb{C}^1_t.$$

2.5 MIRROR SYMMETRY

Mirror symmetry, introduced by Coates–Corti–Kasprzyk et al. [3, 22], has provided a new approach to classifying del Pezzo surfaces in recent years. Mirror symmetry associates to a n-dimensional Fano variety X, a Laurent polynomial $f \in \mathbb{C}[x_1^{\pm 1}, \cdots, x_n^{\pm 1}]$, known as the *mirror dual*. The condition for this correspondence is that the regularised quantum period $\widehat{G}_X$ of X, a property of X studied in Gromov-Witten invariant theory and discussed below, should coincide with the classical period π_f of f given by:

$$\begin{aligned}\pi_f(t) &:= \left(\frac{1}{2\pi i}\right)^n \int\limits_{|x_1|=\cdots=|x_n|=1} \frac{1}{1 - tf(x_1, \cdots, x_n)} \frac{dx_1}{x_1} \cdots \frac{dx_n}{x_n} \\ &= \sum_{k \geq 0} \mathrm{coeff}_1(f^k) t^k.\end{aligned}$$

To a Laurent polynomial, we associate a Newton polytope:

Definition 2.5.1. Given a Laurent polynomial $f = \sum\limits_{\omega \in \mathbb{Z}^n} a_\omega \mathbf{x}^\omega$, define the *Newton polytope* by:

$$\mathrm{Newt}(f) = \mathrm{conv}\{\omega \in \mathbb{Z}^n : a_\omega \neq 0\}.$$

Example 2.5.2. Consider the Laurent polynomial $x + y + \frac{1}{xy} \in \mathbb{C}[x^{\pm 1}, y^{\pm 1}]$. The corresponding Newton polytope is:

$$\mathrm{Newt}\left(x + y + \tfrac{1}{xy}\right) = \mathrm{conv}\left\{(1,0),(0,1),(-1,-1)\right\} =$$ 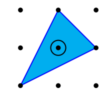

The Newton polytope P associated to a mirror dual f is itself Fano, and will correspond to a toric Fano variety X_P. To bring us round full circle, it is expected that that X_P admits a qG-deformation to the original variety X.

$$\begin{tikzcd}
\text{Smooth Fano variety} \arrow[r, leftrightarrow, "\text{Mirror Symmetry}"] \arrow[d, leftrightarrow, "\text{deformation}"'] & \text{Laurent polynomial} \arrow[d, "\mathrm{Newt}(f)"] \\
\text{Toric Fano variety} \arrow[r, leftrightarrow, "\text{Toric Geometry}"'] & \text{Fano polytope}
\end{tikzcd}$$

The cost here is that we have introduced singularities at the level of toric varieties.

So what exactly is the regularised quantum period $\widehat{G}_X$ of a Fano variety X? Informally the regularised quantum period counts curves of a certain degree on X up to some equivalence. The formal definition is omitted from this thesis but can be studied in [22]. Fortunately Givental [37] gives a simple method to calculate the *quantum period* $G_X := \sum a_n t^n$ in the case of X being a toric Fano manifold. From here the regularised quantum period is given by $\widehat{G}_X := \sum (n!) a_n t^n$.

The method makes use of the GIT quotient construction for a toric variety X_Σ which presents the variety in the form $X = \mathbb{C}^n \backslash Z(\Sigma) /\!\!/ (\mathbb{C}^*)^r$ where $(\mathbb{C}^*)^r$ acts on $\mathbb{C}^n$ via an action described by a group homomorphism $\rho : (\mathbb{C}^*)^n \to (\mathbb{C}^*)^r$ whose dual matrix is given by:

$$D = (D_1, \ldots, D_n) \,.$$

It can be deduced that $-K_X = \sum_{i=1}^{n} D_i$. The model also specifies a set of points $Z(\Sigma)$ which are removed from $\mathbb{C}^n$ to guarantee the quotient $(\mathbb{C}^n \backslash Z(\Sigma)) \,/\, (\mathbb{C}^*)^r$ is well-behaved.

Theorem 2.5.3 ([37])**.** Let X be a toric Fano manifold. Then:

$$G_X(t) = \sum_{k \in \mathbb{Z}^r \cap \mathrm{NE}(X)} t^{-K_X \cdot k} \frac{1}{(D_1 \cdot k)! \cdots (D_n \cdot k)!},$$

where $\mathrm{NE}(X)$ is the cone in the Picard lattice generated by classes of algebraic curves on X.

Example 2.5.4. Consider the del Pezzo surface $\mathbb{P}^2$ whose GIT quotient construction is rather well-known, namely $\mathbb{P}^2 = \left(\mathbb{C}^3 \backslash \{0\}\right) / (\mathbb{C}^*)$, where $\lambda \in \mathbb{C}^*$ acts linearly on each component of $\mathbb{C}^3 \backslash \{0\}$. In the above notation, the matrix D is given by $(1, 1, 1)$. Hence $-K_X = 3$, as is already known, and we can calculate that $\mathrm{NE}(X)$ is the cone $\mathbb{R}_{\geq 0}$. Therefore:

$$G_X(t) = \sum_{k \in \mathbb{N}} \frac{1}{(k!)^3} t^{3k}, \qquad \text{and so} \qquad \widehat{G}_X(t) = \sum_{k \in \mathbb{N}} \frac{(3k)!}{(k!)^3} t^{3k}.$$

Indeed this result has been generalised by Coates–Givental [22, 24] to smooth Fano complete intersections on toric Fano manifolds.

Theorem 2.5.5 ([22])**.** Let Y be a Fano toric manifold defined by the weight matrix D. Consider general sections $f_1, \ldots, f_c$ of the nef line bundles $L_1, \ldots, L_c$ such that X defined by $(f_1 = \ldots = f_c = 0) \subset Y$ is smooth, Fano and of codimension c. Noting that $-K_X = -K_Y - \sum_{i=1}^{c} L_i$, consider the polynomial:

$$F(t) := \sum_{k \in \mathbb{Z}^r \cap \mathrm{NE}(Y)} t^{-K_X \cdot k} \frac{(L_1 \cdot k)! \cdots (L_c \cdot k)!}{(D_1 \cdot k)! \cdots (D_n \cdot k)!}.$$

Define a_1 as the coefficient of t in $F(t)$. Then:

$$G_X(t) = e^{-a_1 t} F(t).$$

Example 2.5.6. Consider the zero locus X of a general section $f \in \mathcal{O}(2)$ on $Y = \mathbb{P}(1,1,1,1)$, that is the well-known Segre embedding of $\mathbb{P}^1 \times \mathbb{P}^1$ into $\mathbb{P}^3$. This is a toric Fano complete intersection. In the above notation:

$$D_0 = D_1 = D_2 = D_3 = 1, \qquad L = 2, \qquad -K_Y = 4, \qquad -K_X = 2.$$

It follows that:

$$F(t) = \sum_{k \in \mathbb{N}} \frac{(2k)!}{(k!)^4} t^{2k}.$$

Since $\mathrm{coeff}_t(F(t)) = 0$, it follows that $G_X(t) = F(t)$, and therefore the regularised quantum period of X is given by:

$$\begin{aligned}\widehat{G}_X(t) &= \sum_{k \in \mathbb{N}} \frac{(2k)!^2}{(k!)^4} t^{2k} \\ &= 1 + 4t^2 + 36t^4 + 400t^6 + \dots\end{aligned}$$

Alternatively how do we find a mirror dual Laurent polynomial who classical period is equal to this regularised quantum period? Hori-Vafa [42] provide a construction for the mirror dual in the case of a toric Fano complete intersection. Fix a Fano toric complete intersection X described by the notation established in Theorem 2.5.3, with the additional information that the weight matrix is given by $D = (D_{i,j})_{i \in \{0,\dots n\}, j \in \{1,\dots,r\}}$. The Hori-Vafa construction is as follows:

Choose some $S_k \subseteq \{1, \dots, n\}, \forall k \in \{1, \dots, c\}$ such that:

- $S_k \cap S_l = \varnothing$,
- $L_k = \sum_{i \in S_k} D_i$.

Define the set:

$$W := \left\{ (x_0, \dots, x_n) : \begin{array}{ll} \prod_{i=0}^{n} x_i^{D_{i,j}} = 1, & \text{for } j \in \{1, \dots, r\} \\ \sum_{i \in S_k} x_i = 1, & \text{for } k \in \{1, \dots, c\} \end{array} \right\} \subseteq (\mathbb{C}^*)^n.$$

The Hori-Vafa mirror is given by the function :

$$\omega := \sum_{i \notin \bigcup_{k=1}^{c} S_k} x_i : W \to \mathbb{C}.$$

which has the property that $\widehat{G}_X(t) = \pi_\omega(t)$, and so ω is indeed a mirror dual to X.

Example 2.5.7. Consider the zero locus X of a general section $f \in \mathcal{O}(2)$ in $Y = \mathbb{P}^3$. In the above notation, we have seen that:

$$D_0 = D_1 = D_2 = D_3 = 1, \qquad L = 2.$$

Choosing $S = \{2, 3\}$, then the Hori-Vafa construction defines:

$$\begin{aligned} W &= \left\{ (x_0, x_1, x_2, x_3) : \begin{array}{c} x_0 x_1 x_2 x_3 = 1 \\ x_2 + x_3 = 1 \end{array} \right\} \\ &\cong \{(x_1, x_2, x_3) : x_2 + x_3 = 1\} \\ &\cong (\mathbb{C}^*)^2_{x,y}, \end{aligned}$$

where:

$$x_1 = x, \qquad x_2 = \frac{1}{1+y}, \qquad x_3 = \frac{y}{1+y}.$$

So:

$$x_0 = \frac{1}{x_1 x_2 x_3} = \frac{1}{x\left(\frac{1}{1+y}\right)\left(\frac{y}{1+y}\right)} = \frac{(1+y)^2}{xy}.$$

Therefore by the Hori-Vafa construction the mirror dual $\omega : (\mathbb{C}^*)^2 \to \mathbb{C}$ to the Fano variety X is given by:

$$\omega = x_0 + x_1 = \frac{(1+y)^2}{xy} + x.$$

It is easy to check that the classical period of ω is:

$$\begin{aligned} \pi_\omega(t) &= \sum_{k \geq 0} \mathrm{coeff}_1(\omega^k) t^k \\ &= 1 + 4t^2 + 36t^4 + 400t^6 + \dots \end{aligned}$$

which agrees with the regularised quantum period from Example 2.5.6. Therefore ω is indeed a mirror dual of $\mathbb{P}^1 \times \mathbb{P}^1$.

There is the additional complication to this application of Mirror symmetry; the choice of mirror dual of a Fano variety X is not unique. How does a different choice of Laurent polynomial get pulled though the Mirror symmetry diagram? This is explored by Akhtar–Coates–Galkin–Kasprzyk [4].

Definition 2.5.8 ([4, Definition 2])**.** A *mutation* of a Laurent polynomial in 3 variables is a birational transformation given as the composition of:

1. a $GL_3(\mathbb{Z})$ transformation, that is a transformation of the form:
$$(x,y,z) \mapsto (x^a y^b z^c, x^d y^e z^f, x^g y^h z^j),$$
where $\begin{pmatrix} a & b & c \\ d & e & f \\ g & h & i \end{pmatrix} \in GL_3(\mathbb{Z})$;
2. a birational transformation of the form:
$$(x,y,z) \mapsto (x,y,A(x,y)z)\,,$$
where the input Laurent polynomial is of the form $f = \sum_{i=k}^{l} C_i(x,y)z^i$ with $k < 0 < l$, and A^{-i} divides C_i for $i \in \{k, k+1, \cdots, -1\}$;
3. A second $GL_3(\mathbb{Z})$ transformation.

This definition easily generalises to n variables.

Lemma 2.5.9 ([4, Lemma 1])**.** If the Laurent polynomials f and g are related by a mutation, then the periods of f and g coincide. In particular f is mirror dual to a Fano variety X if and only if g is mirror dual to X.

Example 2.5.10. Consider the del Pezzo surface $\mathbb{P}^2$ and the Laurent polynomial given by $f = x + y + \frac{1}{xy} \in \mathbb{C}[x^{\pm 1}, y^{\pm 1}]$. The classical period of f is given by:

$$\begin{aligned} \pi_f(t) &= \sum_{k \geq 0} \operatorname{coeff}_1(f^k) t^k \\ &= \sum_{k \geq 0} \frac{(3k)!}{(k!)^3} t^{3k} \\ &= 1 + 6t^3 + 90t^6 + \dots \end{aligned}$$

Note the classical period agrees with the regularised quantum period in Example 2.5.4 and so f is a mirror dual of $\mathbb{P}^2$. Consider a mutation of f described by the composition of the following three maps as per Definition 2.5.8:

1. The $GL_2(\mathbb{Z})$ transformation:
$$(x, y) \longmapsto \left(\frac{1}{y}, xy^2\right);$$

2. The birational transformation:
$$(x, y) \longmapsto (x, (1 + x)y);$$

3. The $GL_2(\mathbb{Z})$ transformation:
$$(x, y) \longmapsto \left(x^2 y, \frac{1}{x}\right).$$

Under this mutation:

$$f \longmapsto g = \frac{1}{xy} + y + 2x^2 y + x^4 y^3.$$

We can check that $\pi_g(t) = \pi_f(t)$. The Newton polytopes of f and g are given respectively by:

$$\operatorname{Newt}(f) =$$ 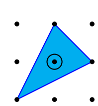

$\mathrm{Newt}(g) =$ 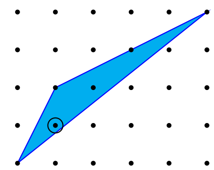

Motivated by Example 2.5.10, this notion of mutation of Laurent polynomials can be pulled through taking Newton polytopes and is captured at the level of Fano polytopes. This is outlined in [4, 48]. We define a mutation of a Fano polygon:

Recall the definition of the Minkowski sum of lattice polygons.

Definition 2.5.11. Let $P, Q \subset N_{\mathbb{R}}$ be two lattice polytopes. Define the *Minkowski sum* of P and Q by:

$$P + Q := \{p + q : p \in P, q \in Q\}.$$

By convention $P + \varnothing = \varnothing$.

Let $P \subset N_{\mathbb{R}}$ be a Fano polygon, and E be an edge of P. Consider the primitive inward pointing normal $n_E \in M$ of this edge. This vector acts as a grading function on the polygon P. For $h \in \mathbb{Z}$, define:

$$\omega_h(P) := \mathrm{conv}\{v \in N \cap P : \langle v, n_E \rangle = h\}.$$

Note that $\omega_h(P)$ may be empty (indeed it will be for infinitely many values of h) and that $\omega_{-h_E}(P) = E$, where h_E is the height of E. Choose v_E to be a primitive vector of the lattice N such that $\langle v_E, n_E \rangle = 0$. Note in two dimensions, v_E is uniquely determined up to sign. Set $F = \mathrm{conv}\{\mathbf{0}, v_E\}$; a line of lattice length 1 and height 0, that is parallel to E. The following definition of a mutation uses the convention that $kF = \{kp : p \in F\}$, where $k \in \mathbb{Z}_{>0}$.

Definition 2.5.12 ([48, Definition 2.1])**.** For all $h < 0$, suppose that there exists $G_h \subset N_{\mathbb{R}}$ such that:

$$\left\{v \in \mathcal{V}(P) : n_E(v) = h\right\} \subseteq G_h + |h|F \subseteq \omega_h(P).$$

In the case $\omega_h(P) = \varnothing$ the inclusion trivially holds by taking $G_h = \varnothing$. Define the *mutation* of P with respect to n_E, F and G_h to be:

$$\mathrm{mut}_{(n_E,F)}(P) := \mathrm{conv}\left(\bigcup_{h<0} G_h \cup \bigcup_{h\geq 0}(\omega_h(P) + hF)\right) \subset N_{\mathbb{R}}.$$

Example 2.5.13. Consider the polygon $P = \mathrm{conv}\{(1,0),(0,1),(-5,-1)\}$ corresponding to the weighted projective space $\mathbb{P}(1,1,5)$. Mutate P with respect to the edge $E = \mathrm{conv}\{(1,0),(0,1)\}$. The primitive inner pointing normal of E is given by $n_E = (-1,-1) \in M$. This describes a grading on the points of N.

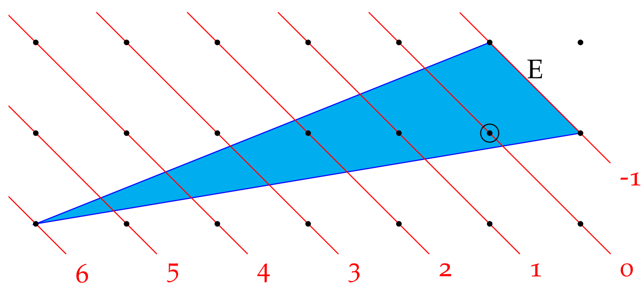

Choose $v_E = (1,-1)$, and so $F = \mathrm{conv}\{\mathbf{0},(1,-1)\}$ which is a primitive slice at height 0. Choose $G_{-1} = \{(0,1)\}$ which satisfies the required inclusion:

$$\{(0,1),(1,0)\} \subseteq G_{-1} + F \subseteq \mathrm{conv}\{(0,1),(1,0)\}.$$

For $h < -1$, $\omega_h(P) = \varnothing$, so trivially choose $G_h = \varnothing$. Calculating the mutation of P with respect to the primitive inner point normal n_E, the factor F and the polygon G_{-1} obtain:

$$\begin{aligned} Q &= \mathrm{mut}_{(n_E,F)}(P) \\ &= \mathrm{conv}\Big\{\ (G_{-1}) \cup (\omega_0(P)) \cup (\omega_1(P) + F) \cup \cdots \cup (\omega_6(P) + 6F)\ \Big\} \\ &= \mathrm{conv}\Big\{(0,1),(-5,-1),(1,-7)\Big\}. \end{aligned}$$

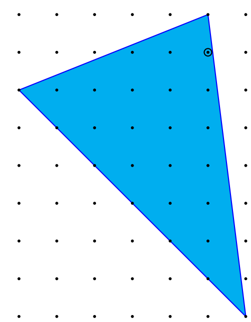

Q corresponds to the toric variety $\mathbb{P}(1,5,36)$. Informally this mutation subtracts one copy of F from P along the edge E, and adds six copies of F at the opposite vertex $(-5,-1)$ of P (which is of height 6 with respect to the grading defined by n_E). This can be seen in the above pictures.

Note $\mathrm{mut}_{(n_E,F)}(P)$ is independent of the choice for G_h. Alternatively if there is no possible choice of G_h, then the mutation with respect to n_E does not exist.

Lemma 2.5.14 ([48, Lemma 2.3])**.** Let E be an edge of a Fano polygon P with primitive inner normal vector $n_E \in M$. Then P admits a mutation with respect to n_E if and only if:

$$|E \cap N| - 1 \geq h_E.$$

Considering the polygon P from Example 2.5.13, then Lemma 2.5.14 tells us the edge $\mathrm{conv}\{(0,1),(-5,-1)\}$ does not admit a mutation since the edge has lattice length 1 and lattice height 5.

There are a number of additional properties of mutations:

- The choice of v_E is unimportant: By a $GL(N)$-equivalence $\mathrm{mut}_{(n_E,F)}(P)$ is isomorphic to $\mathrm{mut}_{(n_E,-F)}(P)$;
- Mutation is invertible: If $Q = \mathrm{mut}_{(n_E,F)}(P)$, then $P = \mathrm{mut}_{(-n_E,F)}(Q)$;
- [4, Proposition 2] P is a Fano polytope if and only if $\mathrm{mut}_{(n_E,F)}(P)$ is a Fano polytope.

Most important is the following theorem regarding mutations:

Theorem 2.5.15 ([44, Theorem 1.3]). Let P and Q be Fano polygons related by a mutation. Then there exists a flat family $\pi : \chi \to \mathbb{P}^1$ such that $\pi^{-1}(0) \cong X_P$ and $\pi^{-1}(\infty) \cong X_Q$.

Theorem 2.5.15 is saying that this application of mirror symmetry and the study of mutations is really a study of toric degenerations.

Mirror Symmetry has been used in [23] to recover the classification of Mori–Mukai of the smooth Fano threefolds. The quantum period, and hence the regularised quantum period, for each of the 105 Fano threefolds in the Mori–Mukai classification is calculated. In [47], mutations are implemented to help construct toric degenerations for each of the smooth Fano threefolds to Gorenstein toric Fano varieties.

Definition 2.5.16 ([48, Section 2]). Let $P, Q \subset N_{\mathbb{R}}$ be two Fano polygons. Then P and Q are *mutation-equivalent* if there exists a finite sequence of polygons $P_0, P_1, \cdots, P_n$ such that $P_0 \cong P$, $P_n \cong Q$ and, $P_{i+1} = \mathrm{mut}_{(n_i,F_i)}(P_i)$ for some appropriate choice of n_i and F_i, for all $i \in \{0, \cdots, n-1\}$.

Mutation-equivalence defines an equivalence relation.

Importantly singularity content defined in Section 2.3 is an invariant under mutation. This invariance is particularly useful in Chapter 3 when considered in conjuction with the famous Conjecture A, stated in [3].

Conjecture A: There exists a bijective correspondence between the set of mutation-equivalence classes of Fano polygons and the set of qG-deformation equivalence classes of class TG del Pezzo surfaces with cyclic quotient singularities that are strictly R-singularities.

Since the singularity content of a Fano polygon describes the cyclic quotient singularities on the corresponding del Pezzo surface, Conjecture A could be strengthened to comment on the connection between the two properties: the singularity content of the mutation equivalence classes of Fano polygons and the singular locus of the corresponding del Pezzo surfaces. Recent results from Corti–Heuberger [27] and Kasprzyk–Nill–Prince [48] certainly support this.

Theorem 2.5.17 ([48, Theorem 1.2])**.** There are precisely ten mutation-equivalence classes of Fano polygons such that the toric del Pezzo surface X_P has only T-singularities. They are in bijective correspondence with the ten families of smooth del Pezzo surfaces.

Theorem 2.5.18 ([27, 48])**.** There are precisely 29 qG-deformation families of del Pezzo surfaces with $m \geq 1$ singular points of type $\frac{1}{3}(1,1)$ and precisely 26 of these admit a toric degeneration. These 26 del Pezzo surfaces are in bijective correspondence with 26 mutation-equivalence classes of Fano polygons with singularity content $\left(n, \{m \times \frac{1}{3}(1,1)\}\right)$, where $m \geq 1$.

3

CLASSIFICATION OF POLYGONS BY SINGULARITY CONTENT

The aim of this chapter is to describe an efficient algorithm to classify mutation equivalence classes of Fano polygons with a given singularity content. This would allow us to build on the classifications of Theorem 2.5.17 and 2.5.18. In the event of Conjecture A being proven, this algorithm is equivalent to providing a classification of del Pezzo surfaces that admit a toric degeneration and have the cyclic quotient singularities described by the prescribed singularity content. As a corollary to the algorithm the following classifications (derived in Section 3.3) have been completed:

Theorem 3.0.1. There are precisely 14 mutation-equivalence classes of Fano polygons with singularity content $\left(n, \{m_1 \times \frac{1}{3}(1,1), m_2 \times \frac{1}{6}(1,1)\}\right)$ where $m_1 \geq 0$, $m_2 > 0$.

Theorem 3.0.2. There are precisely 12 mutation-equivalence classes of Fano polygons with singularity content $\left(n, \{m \times \frac{1}{5}(1,1)\}\right)$ where $m > 0$.

The material of this chapter is joint work with Edwin Kutas [20].

3.1 PRELIMINARIES

Before stating the algorithm we require some preliminaries on Hirzeburch–Jung continued fractions, and our choice of representative of a mutation equivalence class of Fano polygons.

There is information about the del Pezzo surface X_P corresponding to a polygon P written into the singularity content $SC(P) = (n, \mathcal{B})$; X_P is qG-deformation equivalent to a del Pezzo surface X such that the topological Euler number $\chi\,(X\backslash \mathrm{Sing}(X)) = n$ and the set of singular points is given by $\mathrm{Sing}(X) = \mathcal{B}$. Furthermore the anticanonical degree and Hilbert series of X_P are totally determined by the singularity content, see [3, 5].

Definition 3.1.1. Let $p, q \in \mathbb{Z}_{>0}$ be coprime. Then the *Hirzebruch–Jung continued fraction* of $\frac{p}{q}$ is the continued fraction of the form:

$$\frac{p}{q} = a_1 - \cfrac{1}{a_2 - \cfrac{1}{a_3 - \cfrac{1}{\ddots}}} := [a_1, \cdots, a_k].$$

Given a cyclic quotient singularity $\sigma = \frac{1}{R}(1, a)$, consider the associated variety $Z = \mathrm{Spec}(\mathbb{C}[x, y]^{\mu_R})$. Information about a minimal resolution of Z can be calculated from the Hirzebruch–Jung continued fraction of $\frac{R}{a}$. Consider the minimal resolution $\pi : Y \to Z$ with:

$$K_Y = \pi^*\left(K_Z\right) + \sum_{i=1}^{k_\sigma} d_i E_i. \tag{2}$$

Let the Hirzebruch–Jung continued fraction of $\frac{R}{a}$ be given by $[a_1, \cdots, a_{k_\sigma}]$. The values $-a_i$ are the self-intersection numbers of the exceptional divisors E_i appearing in equation (2). Furthermore set:

$$\alpha_1 = \beta_{k_\sigma} = 1,$$

$$\frac{\alpha_i}{\alpha_{i-1}} = [a_{i-1}, \cdots, a_1], \qquad \text{for } i \in \{2, \cdots, k_\sigma\},$$
$$\frac{\beta_i}{\beta_{i+1}} = [a_{i+1}, \cdots, a_{k_\sigma}], \qquad \text{for } i \in \{1, \cdots, k_\sigma - 1\}.$$

The discrepancy of E_i is given by $d_i = -1 + \frac{\alpha_i+\beta_i}{R}$. For further reading on minimal resolutions, see Reid [63].

Proposition 3.1.2 ([5, Proposition 3.3, Corollary 3.5])**.** Let P be a Fano polygon, and let X_P be the corresponding toric surface. Suppose P has singularity content $(n, \mathcal{B})$. Then:

$$(-K_{X_P})^2 = 12 - n - \sum_{\sigma\in\mathcal{B}} A_\sigma,$$

where $A_\sigma = k_\sigma + 1 - \sum_{i=1}^{k_\sigma} d_i^2 a_i + 2 \sum_{i=1}^{k_\sigma - 1} d_i d_{i+1}$. Furthermore the Hilbert series of X_P admits a decomposition:

$$\mathrm{Hilb}(X_P, -K_{X_P}) = \frac{1 + \left((-K_{X_P})^2 - 2\right) t + t^2}{(1-t)^3} + \sum_{\sigma\in\mathcal{B}} Q_\sigma(t),$$

where $Q_{\frac{1}{R}(1,a)}(t) = \frac{1}{1-t^R} \sum_{i=1}^{R-1} (\delta_{(a+1)i} - \delta_0) t^{i-1}$ is the Riemann-Roch contribution coming from the singularity $\frac{1}{R}(1, a)$, where $\delta_j = \frac{1}{R} \sum_{\epsilon\in\mu_R, \epsilon\neq 1} \frac{\epsilon^j}{(1-\epsilon)(1-\epsilon^a)}$ are the Dedekind sums.

Example 3.1.3. The Fano polygon $P = \mathrm{conv}\{(0, 1), (1, 0), (-5, -1)\}$ of Example 2.5.13 has singularity content $\left(2, \{\frac{1}{5}(1, 1)\}\right)$. The Hirzebruch–Jung continued fraction of the cyclic quotient singularity $\frac{1}{5}(1, 1)$ is simply $[5]$, so it follows that $d_1 = -\frac{3}{5}$ and $A_{\frac{1}{5}(1,1)} = \frac{1}{5}$. Furthermore $Q_{\frac{1}{5}(1,1)} = \frac{t-2t^2+t^3}{5(1-t^5)}$. Therefore the anticanonical degree and Hilbert series of $\mathbb{P}(1, 1, 5)$ are given by:

$$(-K_{\mathbb{P}(1,1,5)})^2 = 12 - 2 - \frac{1}{5} = \frac{49}{5},$$
$$\mathrm{Hilb}\left(\mathbb{P}(1, 1, 5), -K_{\mathbb{P}(1,1,5)}\right) = \frac{1 + \frac{39}{5} t + t^2}{(1-t)^3} + \frac{t - 2t^2 + t^3}{5(1-t^5)}$$
$$= \frac{1 + 8t + 2t^3 - 2t^4 - 8t^6 - t^7}{(1-t^5)(1-t)^3}.$$

More generally for a polygon P with n primitive T-singularities and basket of singularities $\mathcal{B} = \{m \times \frac{1}{5}(1,1)\}$, we have:

$$(-K_{X_P})^2 = 12 - n - \frac{1}{5}m,$$

and:

$$\begin{aligned}&\mathrm{Hilb}(X_P, -K_{X_P})\\ &\quad = \frac{-t^7 + (n-10)t^6 + (m-1)t^5 - 2mt^4 + 2mt^3 + (1-m)t^2 + (10-n)t + 1}{(1-t)^3(1-t^5)}.\end{aligned}$$

Hirzebruch–Jung fractions can be further studied in [36, 62].

Studying mutation-equivalence classes raises a question about the choice of representative when considering a mutation-equivalence class of Fano polygons. This leads to the definition of a minimal polygon from [48]. For a polygon P, the notation ∂P denotes the boundary of P.

Definition 3.1.4 ([48, Definition 4.1])**.** Let $P \subset N_{\mathbb{R}}$ be a Fano polygon. The polygon P is *minimal* if:

$$|\partial P \cap N| \leq |\partial Q \cap N|, \qquad \forall Q = \mathrm{mut}_{(n,F)}(P).$$

For an edge E of P, let $n_E \in M$ be the primitive inward pointing normal of E. Define $h^E_{\min} = \min\{\langle v, n_E\rangle : v \in P\}$ and $h^E_{\max} = \max\{\langle v, n_E\rangle : v \in P\}$. Then [48, Corollary 4.5] states that P is minimal if and only if for every edge E satisfying $|E \cap N| - 1 \geq |h^E_{\min}|$, then $|h^E_{\min}| \leq h^E_{\max}$.

Given a Fano polygon P, we can find a minimal representative of the mutation-equivalence class by calculating all possible mutations of P. If none of the Fano polygons obtained via these mutations have fewer boundary points, then P is minimal. Otherwise choose one of the mutations of P that have fewer boundary points as our new representative. Repeat this inductively, until we obtain a minimal representative. The process must terminate since the number of boundary points of a Fano polygon is finite and non-negative.

A minimal representative of a mutation-equivalence class is not necessarily unique. We will always choose the representative of any equivalence class of Fano polygons to be minimal.

Example 3.1.5. In Example 2.5.13, $|\partial P \cap N| = 3$ and $|\partial Q \cap N| = 8$ and we have also seen by Lemma 2.5.14 that the edge $\operatorname{conv}\{(0,1),(-5,-1)\}$ does not admit a mutation. We know there is only one other existing mutation of P. It is routine to check that this remaining mutation does not have fewer boundary points that P. Therefore P is minimal.

3.2 ALGORITHM

Recall from Definition 1.5.1 that the maximal local index of a Fano polygon P is:

$$\begin{aligned} m_P &= \max\{l_E : E \text{ is a face of } P\} \\ &= \max\{\text{height}(E) : E \text{ is a face of } P\}. \end{aligned}$$

Similarly define $m_{\mathcal{B}}$ to be the maximum height among the cones representing the R-singularities of P.

The classification of Fano polygons with a given basket of singularities $\mathcal{B}$ up to mutation-equivalence is split into two cases:

- Case (i): $m_P = m_{\mathcal{B}}$;
- Case (ii): $m_P > m_{\mathcal{B}}$.

A proof in [48] efficiently tackles case (ii), although the polygons this proof outputs are not necessarily minimal. It remains for us to deal with case (i). An algorithm to compute this classification has been completed in [50]. However it is inefficient when tackling classifications beyond the simple cases of polygons with only T-singularities and $\frac{1}{3}(1,1)$ R-singularities.

The main result of this chapter is an efficient algorithm to calculate the polygons arising through case (i). The basic idea is to start with only a single edge F described by endpoints (a, l_F) and (b, l_F), where $0 < l_F < m_{\mathcal{B}}$ and $a < b$, and inductively add appropriate edges. The edge F will eventually be a special facet (recall Definition 1.5.3) of a Fano polygon P. By convexity we require that P lies below the line $\{(x, y) \in N_{\mathbb{R}} : y = l_F\}$ formed by extending F. Consider the line $L1$ through (a, l_F) and $(-m_{\mathcal{B}}, 0)$. This line provides a bound on the gradient for the second edge of P with endpoint (a, l_F); any edge with gradient less than that of $L1$ will be of height greater than $m_{\mathcal{B}}$ contradicting the assumption $m_P = m_{\mathcal{B}}$. Similarly the line $L2$ through the points (b, l_F) and $(m_{\mathcal{B}}, 0)$ bounds P. Finally by Lemma 1.5.5, all vertices of P must lie above the line $L = \{(x, y) \in N_{\mathbb{R}} : y = -l_F(l_F + 1)\}$. These bounds define a region $T \subset N_{\mathbb{R}}$, shown in Figure 1, such that $P \subseteq T$. We inductively construct all possible minimal polygons by adding in edges contained within T in a clockwise fashion so that the edges contribute T-singularities or appropriate R-singularities to P. The full algorithm is described formally below. The notation E_{v_1,v_2} is used to denote the line segment between the lattice points v_1 and v_2.

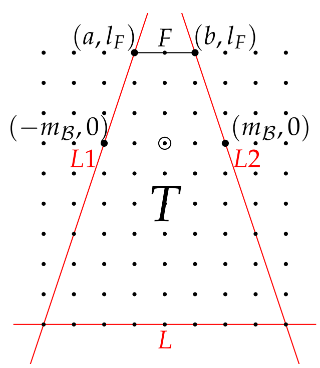

Figure 1: Region of Possible Points.

Algorithm 2 Classification of Minimal Fano Polygons with given basket of singularities with $m_P = m_{\mathcal{B}}$

1: **Input:** $F = \{v_1, v_2\} = \{(a, l_F), (b, l_F)\}$, Basket of singularities $\mathcal{B}$.
2: $L1 :=$ line through (a, l_F) and $(-m_{\mathcal{B}}, 0)$.
3: $L2 :=$ line through (b, l_F) and $(m_{\mathcal{B}}, 0)$.
4: $L := \{(x, y) \in N : y = l_F(l_F + 1)\}$.
5: $T :=$ region bounded by $F, L, L1$ and $L2$.
6: PossiblePoints $:= \{$primitive points $v \in N$ contained in $T\}$.
7: ActiveConstructions $:= \{F\}$, and CompleteConstructions $:= \varnothing$.
8: **for** $\{v_1, \dots, v_k\} \in$ ActiveConstructions **do**,
9: $\quad S^h := \{v_{k+1} : v_{k+1} - v_k$ primitive, height$(E_{v_k, v_{k+1}}) = h\}$, for $h > 0$.
10: $\quad L^{(h)} :=$ line through the points of S^h, for $h > 0$.
11: $\quad L^{(v,h)} :=$ line through v_k and v for some $v \in L^{(h)}$.
12: $\quad$ **for** $v \in L^{(v,h)} \cap T$, where $0 \leq h \leq m_{\mathcal{B}}$ **do**,
13: $\quad\quad$ **if** $v \neq (a, l_F)$ and adding v to $\{v_1, \dots, v_k\}$ satisfies convexity, and conv$\{v_k, v\}$ describes a T-singularity or a singularity in $\mathcal{B}$ **then**,
14: $\quad\quad\quad$ ActiveConstructions $\leftarrow$ (ActiveConstructions$\setminus\{v_1, \dots v_k\}) \cup \{v_1, \dots, v_k, v\}$.
15: $\quad\quad$ **if** $v = (a, l_F)$ and adding v to $\{v_1, \dots, v_k\}$ satisfies convexity **then**,
16: $\quad\quad\quad$ ActiveConstructions $\leftarrow$ ActiveConstructions$\setminus\{v_1, \dots v_k\}$.
17: $\quad\quad\quad$ CompleteConstructions $\leftarrow$ CompleteConstructions $\cup \{v_1, \dots, v_k, v\}$.
18: **if** ActiveConstructions $\neq \varnothing$ **then**,
19: $\quad$ **go to** 8.
20: **for** $\{v_1, \dots, v_k\} \in$ CompleteConstructions **do**,
21: $\quad$ **if** $P :=$ conv $\{v_1, \dots, v_k\}$ not minimal or F not a special facet of P or $\{$R-singularities of $P\} \neq \mathcal{B}$ **then**,
22: $\quad\quad$ CompleteConstructions $\leftarrow$ CompleteConstructions $\setminus\{v_1 \dots, v_k\}$.
23: Check CompleteConstructions for mutation equivalence.
24: **Output:** CompleteConstructions.

Theorem 3.2.1. The algorithm gives a complete classification for Fano polygons with a specific basket of singularities $\mathcal{B}$.

Proof. Firstly we prove that there are only finitely many choices for the input special facet F, since the algorithm will be run for all possible choices. Since $m_P = m_{\mathcal{B}}$, and the height of F is l_F, it follows that $l_F \in \{1, \cdots, m_{\mathcal{B}}\}$. Translate the edge F horizontally using a $GL(N)$-transformation of the form $\begin{pmatrix} 1 & kl_F \\ 0 & 1 \end{pmatrix}$ for some $k \in \mathbb{Z}$, to assume that $-l_F < a \leq 0$. It remains to show that for a fixed value of l_F and a that there are only finitely many choices for b. Suppose $b \geq a + l_F$. By minimality the region T contains a point (x, y) with $y \leq -l_F$. It is easy to see that if b gets too big then the point of intersection of $L1$ and $L2$ will bound T so as not to include such a point. Therefore there are only finitely many choices of special facet. Note it is only necessary to consider a and b such that (a, l_F) and (b, l_F) are primitive and the singularity contributed by F is either a T-singularity and/or an R-singularity contained in $\mathcal{B}$.

Secondly note that the set of points belonging to $S^{(h)}$ in step 10, do indeed belong to a line. Namely suppose if $v_k = (x, y)$, and $(a, b) \in S^{(h)}$, then necessarily $\gcd(a - x, b - y) = 1$ and so the height condition on the edge $E_{(x,y),(a,b)} = \operatorname{conv}\{(x, y), (a, b)\}$ becomes:

$$\begin{aligned} -h &= \left\langle (x, y), n_{E_{(x,y),(a,b)}} \right\rangle \\ -h &= \langle (x, y), (a - x, b - y) \rangle \\ b &= \left(-\frac{x}{y}\right) a + \left(\frac{-h + x^2 + y^2}{y}\right) \end{aligned} \tag{3}$$

where equation (3) gives the equation of the straight line $L^{(h)}$.

Finally it is easy to see that at step 13 of the algorithm, there are only finitely many choices for v since T is a bounded region. $\square$

By Proposition 3.1.2:

$$(-K_{X_P})^2 = 12 - n - \sum_{\sigma \in \mathcal{B}} A_\sigma.$$

Since P is Fano, $(-K_{X_P})^2 > 0$. Additionally our chosen basket $\mathcal{B}$ consists of finitely many R-singularities, so $\sum_{\sigma \in \mathcal{B}} A_\sigma$ is finite and therefore there exists a bound on n, the number of T-cones contained in P.

When checking for mutation-equivalence in the algorithm, two polygons can be shown to be mutation-equivalent by explicitly calculating a sequence of mutations between them. Conversely a polygon P has corresponding to it a mirror dual Laurent polynomial $f \in \mathbb{C}[x_1^{\pm 1}, \cdots, x_n^{\pm 1}]$, as discussed in Section 2.5. The classical period of f, given by:

$$\begin{aligned} \pi_f(t) &= \left(\frac{1}{2\pi i}\right)^n \int_{|x_1| = \cdots = |x_n| = 1} \frac{1}{1 - tf(x_1, \cdots, x_n)} \frac{dx_1}{x_1} \cdots \frac{dx_n}{x_n} \\ &= \sum_{k \geq 0} \mathrm{coeff}_1(f^k) t^k, \end{aligned}$$

is an invariant under mutation. Hence two polygons with different periods cannot be mutation-equivalent.

We have successfully written computer code in Sage that efficiently implements the algorithm.

It is important to compare the LDP-algorithm [50], described in Section 1.5, used to calculate the $\frac{1}{3}(1,1)$ classification of Fano polygons in Theorem 2.5.18 with this new algorithm. The LDP-algorithm takes as input a desired value for the *index* $l_P = \mathrm{lcm}\{\mathrm{height}(E) : E \text{ is an edge of } P\}$, and returns all Fano polygons P with this index. Hence when used to calculate the case $m_P = m_{\mathcal{B}}$ in the $\frac{1}{3}(1,1)$ classification, edges of height $1, 2$ and 3 are permitted, and so the LDP-algorithm needs to be run for $l_P \in \{3, 6\}$. In the $\frac{1}{5}(1,1)$ classification of Theorem 3.0.2 the value of l_P can be up to 60. All polygons P satisfying $l_P \leq 16$ have been classified using the LDP-algorithm but this took approximately three days to obtain and the run time will increase at least quadratically with l_P.

A classification of Fano polygons with singularity content $\left(n, \{m \times \frac{1}{r}(1,1)\}\right)$, where $r \geq 7$ would be extremely costly to calculate using the LDP-algorithm (l_P would be bounded above by 420 in the $r = 7$ case).

In comparison we had the following run times to calculate the classifications of Theorems 3.0.1 and 3.0.2 using our algorithm:

Basket in classification	Run Time
$\left(n, \{m_1 \times \frac{1}{3}(1,1), m_2 \times \frac{1}{6}(1,1)\}\right)$	40 seconds
$\left(n, \{m \times \frac{1}{5}(1,1)\}\right)$	8 minutes

Furthermore a classification of Fano polygons whose basket of singularities only contains $\frac{1}{7}(1,1)$ R-singularities has been informally completed. The main reasons for the difference in speed between the algorithms are:

- We only look for minimal representatives for each mutation equivalence class. This is not the case in the LDP algorithm;
- The LDP-algorithm is not designed to look for polygons based on the singularity content. For example, in the $\frac{1}{3}(1,1)$ classification running the LDP-algorithm for $l_P \in \{3,6\}$ will output many polygons that do not have singularity content $\left(n, \{m \times \frac{1}{3}(1,1)\}\right)$.

3.3 CLASSIFICATIONS

We first apply Algorithm 2 to classify all Fano polygons whose basket of residual singularities contains only $\frac{1}{3}(1,1)$ and $\frac{1}{6}(1,1)$ cyclic quotient singularities. Set $\mathcal{B} = \left\{m_1 \times \frac{1}{3}(1,1), m_2 \times \frac{1}{6}(1,1)\right\}$, where $m_1 \in \mathbb{Z}_{\geq 0}$ and $m_2 \in \mathbb{Z}_{>0}$. Here m_2 is non-zero since a classification for Fano polygons with only $\frac{1}{3}(1,1)$ R-singularities has been completed in Theorem 2.5.18. Upper bounds on m_1 and

m_2 are required, to prove that the algorithm only needs to be run a finite number of times in order to get a complete classification.

In the $\frac{1}{3}(1,1)$ classifiation of Theorem 2.5.18 a bound on the number of R-singularities is found by substituting the degree contribution $A_{\frac{1}{3}(1,1)} > 0$ into the expression for the anticanonical degree of the corresponding toric Fano variety from Proposition 3.1.2. However the degree contribution $A_{\frac{1}{6}(1,1)}$ is negative and a similar argument does not yield a bound. We appeal to a combinatorial argument instead.

Lemma 3.3.1. There exist no minimal Fano polygons $P \subset N_{\mathbb{R}}$, with $m_P = 3$ and residual basket given by $\mathcal{B} = \left\{m \times \frac{1}{6}(1,1)\right\}$, where $m \geq 3$.

Proof. The result for $m > 3$ follows from the argument for the base case $m = 3$.

Let P be a polygon with $\mathcal{B} = \{3 \times \frac{1}{6}(1,1)\}$. By a $GL(N)$-transformation, assume that one of the R-singularities is given by $E_1 = \operatorname{conv}\{(-1,3),(1,3)\}$. By mutating with respect to any T-singularity lying between E_1 and a second R-singularity, assume this second R-singulary is adjacent to E_1, given by an edge E_2 with endpoints $(1,3)$ and (a,b). The primitive inner pointing normal of E_2 is given by:

$$n_{E_2} = \left(\frac{b-3}{g}, \frac{1-a}{g}\right) \in M$$

where $g = \gcd(b-3, 1-a)$. The height of E_2 is:

$$h = -\langle (1,3), n_{E_2} \rangle = \frac{3a-b}{g}.$$

Since E_2 represents a $\frac{1}{6}(1,1)$ singularity, set $h = 3$:

$$\frac{3a-b}{g} = 3,$$
$$b = 3a - 3\gcd(b-3, 1-a).$$

By convexity $b < 3$. The only remaining integer solution with $a \geq 0$, is given by $(0,-3)$. However this point is not primitive so it can not be chosen as a vertex of a Fano polygon. Hence $a < 0$.

Suppose the second edge from $(-1,3)$, denoted E_3, is vertical. By convexity $a = -1$ and (a,b) is a vertex of E_3. But then E_3 is of height 1 so cannot represent the final $\frac{1}{6}(1,1)$ singularity and $m < 3$. Suppose E_3 is not vertical. Again convexity demands that the second endpoint of E_3 has first coordinate less than -1. Then height$(E_3) > 3$ which contradicts $m_P = 3$.

Therefore there can be no minimal Fano polygon with residual basket given by $\mathcal{B} = \{3 \times \frac{1}{6}(1,1)\}$ with $m_P = 3$. $\square$

A similar argument to the proof of Lemma 3.3.1 shows the more general statement that for a basket of residual singularities $\mathcal{B} = \left\{m_1 \times \frac{1}{3}(1,1), m_2 \times \frac{1}{6}(1,1)\right\}$ of a Fano polygon, then $m_1 + m_2 < 3$. Therefore the algorithm can be run a finite number of times to get the desired classification.

Examples in this particular classification demonstrate a notion known as shattering introduced by Wormleighton [67]. Consider two cones in $N_{\mathbb{R}}$ given by $C_1 = \text{span}_{\mathbb{R}_{\geq 0}}(u,v)$ and $C_2 = \text{span}_{\mathbb{R}_{\geq 0}}(v,w)$ such that the vectors $v - u$ and $w - v$ have the same unit direction vector. Then define the hyperplane sum of C_1 and C_2 to be given by $C_1 * C_2 = \text{span}_{\mathbb{R}_{\geq 0}}(u,w)$.

Corollary 3.3.2 ([67] Corollary 2.2)**.** Let $\sigma_1 * \sigma_2 * \cdots * \sigma_n = \tau$ be a T-singularity. Then the Riemann-Roch contributions Q_{σ_i} and the degree contributions A_{σ_i} satisfy:

$$Q_{\sigma_1} + \cdots + Q_{\sigma_n} = 0,$$
$$A_{\sigma_1} + \cdots + A_{\sigma_n} = A_\tau = \frac{\text{lattice length}(\tau)}{\text{lattice height}(\tau)}.$$

Consider a T-cone at lattice height 3 which without loss of generality is given by $C = \text{cone}\{(-2,3),(1,3)\}$. By adding an additional ray generated by the primitive lattice point $(-1,3)$, decompose C into two sub-cones C_1 and C_2 representing a $\frac{1}{3}(1,1)$ and a $\frac{1}{6}(1,1)$ R-singularity respectively. By Corollary 3.3.2:

$$Q_{\frac{1}{3}(1,1)} + Q_{\frac{1}{6}(1,1)} = 0,$$

$$A_{\frac{1}{3}(1,1)} + A_{\frac{1}{6}(1,1)} = 1.$$

Knowing $A_{\frac{1}{3}(1,1)} = \frac{5}{3}$ and $Q_{\frac{1}{3}(1,1)} = -\frac{t}{3(1-t^3)}$, derive:

$$A_{\frac{1}{6}(1,1)} = -\frac{2}{3},$$

$$Q_{\frac{1}{6}(1,1)} = \frac{t}{3(1-t^3)}.$$

By Proposition 3.1.2, calculate $(-K_{X_P})^2 = 12 - n - \frac{5}{3}m_1 + \frac{2}{3}m_2$. Since we are interested in Fano polygons, $(-K_{X_P})^2 > 0$, and so $n \leq 13$.

The table of results for the classification of Fano polygons with singularity content of the form $\left(n, \{m_1 \times \frac{1}{3}(1,1), m_2 \times \frac{1}{6}(1,1)\}\right)$ with $m_2 \neq 0$, up to mutation-equivalence is given. All the polygons listed arose in the case $m_{\mathcal{B}} = m_P$ with the exception of polygon 1.12 for which $m_P > m_{\mathcal{B}}$.

#	Vertices of Polygon P	n	m_1	m_2	$(-K_X)^2$
1.1	(-1,3), (1,3), (0,-1)	2	0	1	$\frac{32}{3}$
1.2	(-1,3), (1,3), (1,2), (0,-1)	3	0	1	$\frac{29}{3}$
1.3	(-1,3), (1,3), (1,1), (0,-1)	4	0	1	$\frac{26}{3}$
1.4	(-1,3), (1,3), (1,0), (0,-1)	5	0	1	$\frac{23}{3}$
1.5	(-1,3), (1,3), (1,2), (0,-1), (-1,0)	6	0	1	$\frac{20}{3}$
1.6	(-1,3), (1,3), (1,2), (0,-1), (-1,-1)	7	0	1	$\frac{17}{3}$
1.7	(-1,3), (1,3), (1,0), (0,-1), (-1,0)	8	0	1	$\frac{14}{3}$
1.8	(-1,3), (1,3), (1,0), (-1,-1)	8	0	1	$\frac{14}{3}$
1.9	(-1,3), (1,3), (1,0), (0,-1), (-1,-1)	9	0	1	$\frac{11}{3}$
1.10	(-1,3), (1,3), (1,2), (-1,-4)	10	0	1	$\frac{8}{3}$
1.11	(-1,3), (1,3), (1,-1), (-1,-3)	11	0	1	$\frac{5}{3}$
1.12	(-1,3), (1,3), (5,-1), (-5,-1)	12	0	1	$\frac{2}{3}$
1.13	(-1,1), (1,1), (5,-1), (-5,-1)	12	0	2	$\frac{4}{3}$
1.14	(-1,3), (1,3), (1,-1), (-1,-2)	9	1	1	2

These polygons are illustrated in Figure 2.

Recall from Section 2.5 that associated to a toric variety X_P is the mirror dual Laurent polynomial. This is a Laurent polynomial f such that $\mathrm{Newt}(f) = P$, and whose classical period is a mutation invariant. The mirror duals of polygons 1.7 and 1.8 are given respectively by a polynomial of the form:

$$
\begin{aligned}
f &= xy^3 + 3xy^2 + ay^3 + 3xy + by^2 + x^{-1}y^3 \\
&\qquad + x + cy + 3x^{-1}y^2 + 3x^{-1}y + y^{-1} + x^{-1}, \\
g &= xy^3 + 3xy^2 + dy^3 + 3xy + ey^2 + x^{-1}y^3 \\
&\qquad + x + fy + 4x^{-1}y^2 + 6x^{-1}y + 4x^{-1} + x^{-1}y^{-1}.
\end{aligned}
$$

Calculating the corresponding periods of f and g obtain:

$$
\pi_f = 1 + (2a+2)x^2 + (3b+36)x^3 + (6a^2+24a+4c+186)x^4
$$

$$
+(20ab+360a+60b+760)x^5 + \cdots,
$$

$$
\pi_g = 1 + 14x^2 + 6ax^3 + 546x^4 + (420a+30b)x^5 + \cdots.
$$

It is easy to see that these periods are not equal and hence the polygons cannot be mutation-equivalent. All other Fano polygons in this classification have pairwise distinct singularity contents, hence are not mutation equivalent.

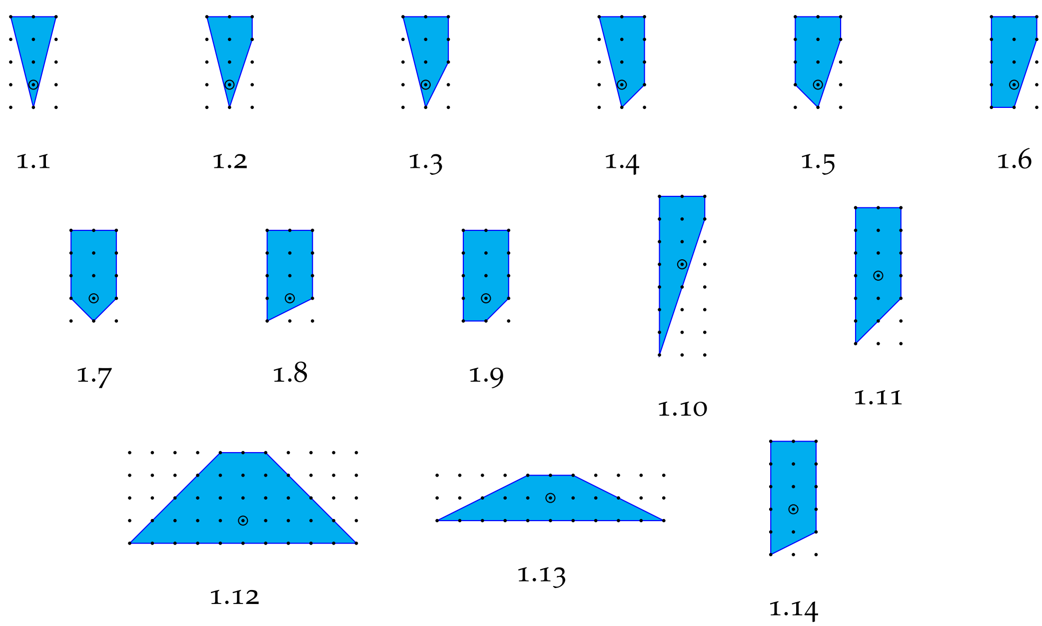

Figure 2: Minimal Representatives of Mutation-Equivalence Classes of Fano Polygons with Singularity Content $\left(n, \{m_1 \times \frac{1}{3}(1,1), m_2 \times \frac{1}{6}(1,1)\}\right)$ where $m_1 \geq 0, m_2 > 0$.

Similarly we find all Fano polygons with singularity content $\left(n, \{m \times \frac{1}{5}(1,1)\}\right)$ with $m > 0$. As before a bound on m is required to ensure a complete classification.

Lemma 3.3.3. There exist no minimal Fano polygons $P \subset N_{\mathbb{R}}$, with $m_P = 5$ and residual basket given by $\mathcal{B} = \left\{m \times \frac{1}{5}(1,1)\right\}$, where $m \geq 3$.

Proof. Similar to the proof of Lemma 3.3.1. □

By Example 3.1.2 and Proposition 3.1.3 the anticanonical degree of the toric variety corresponding to a Fano polygon whose only R-singularities are of type $\frac{1}{5}(1,1)$ is given by:

$$(-K_{X_P})^2 = 12 - n - \frac{1}{5}m > 0.$$

Therefore $n < 12$. We apply the algorithm finitely many times to complete the classification.

The table of results for the classification of Fano polygons with singuarity content of the form $\left(n, \{m \times \frac{1}{5}(1,1)\}\right)$ with $m > 0$ is given. All the polygons satisfy $m_{\mathcal{B}} = m_P$.

#	Vertices of Polygon P	n	m	$(-K_X)^2$
2.1	(-3,5), (-2,5), (1,-2)	2	1	$\frac{49}{5}$
2.2	(-3,5), (-2,5), (-1,3), (1,-2)	3	1	$\frac{44}{5}$
2.3	(-3,5), (-2,5), (-1,3), (1,-2), (-2,3)	4	1	$\frac{39}{5}$
2.4	(-3,5), (-2,5), (-1,3), (1,-2), (-1,1)	5	1	$\frac{34}{5}$
2.5	(-3,5), (-2,5), (0,1), (1,-2), (-1,1)	6	1	$\frac{29}{5}$
2.6	(-3,5), (-2,5), (0,1), (1,-2), (0,-1)	7	1	$\frac{24}{5}$
2.7	(-3,5), (-2,5), (1,-1), (0,-1)	7	1	$\frac{24}{5}$
2.8	(-3,5), (-2,5), (1,-1), (1,-2), (0,-1)	8	1	$\frac{19}{5}$
2.9	(-3,5), (-2,5), (1,-1), (1,-3)	9	1	$\frac{14}{5}$
2.10	(-3,5), (-2,5), (2,-3), (2,-5)	10	1	$\frac{9}{5}$
2.11	(-3,5), (-2,5), (4,-1), (-3,-1)	11	1	$\frac{4}{5}$
2.12	(-3,5), (-2,5), (3,-5), (2,-5)	10	2	$\frac{8}{5}$

These polygons are illustrated in Figure 3.

Similarly to the previous classification note that polygons 2.6 and 2.7 are not mutation equivalent by looking at the periods π_f, π_g of their respective mirror duals f and g:

$$\pi_f = 1 + 12x^2 + 6ax^3 + 396x^4 + (360a + 30b)x^5 + \cdots,$$

$$\pi_g = 1 + (2c + 12)x^2 + (6c + 3d + 90)x^3 + (6c^2 + 24d + 144c + 636)x^4$$
$$+ (20cd + 60c^2 + 390d + 1260c + 6900)x^5 + \cdots.$$

All other Fano polygons in the classification have pairwise distinct singularity content and therefore belong to different mutation equivalence classes.

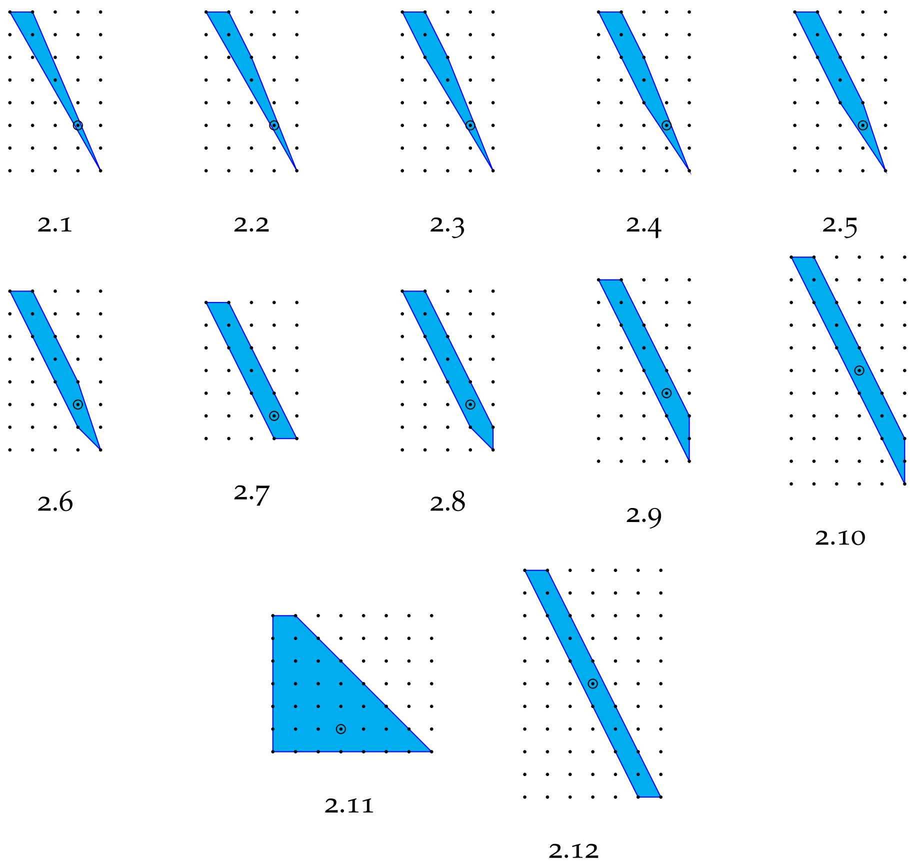

Figure 3: Minimal Representatives of Mutation-Equivalence Classes of Fano Polygons with Singularity Content $\left(n, \{m \times \frac{1}{5}(1,1)\}\right)$ where $m > 0$.

4

DEL PEZZO SURFACES WITH A SINGLE $\frac{1}{k}(1,1)$ SINGULARITY

Given the classifications of Theorem 3.0.1 and Theorem 3.0.2, the next problem is to study and understand them. This involves calculating the corresponding del Pezzo surfaces, and the distinct qG-deformation families that they belong to. The material of this chapter was completed as joint work with Thomas Prince [21].

The crucial observation follows from recalling the construction of the blow-up of a toric fan from Chapter 1, that is, given a cone $\sigma \in \Sigma \subset N_{\mathbb{R}}$ with primitive ray generators u_1, u_2, set $u_0 = u_1 + u_2$ and replace σ by $\sigma_1 = \mathrm{span}_{\mathbb{R}_{\geq 0}}(e_1, e_0)$, $\sigma_2 = \mathrm{span}_{\mathbb{R}_{\geq 0}}(e_0, e_2)$ and $\sigma_1 \cap \sigma_2$ to define a fan Σ'. Then $X_{\Sigma'}$ is the blow of X_Σ in a smooth point of U_σ.

Focussing on the classification of Theorem 3.0.1, observe that polygon 1.2 arises from polygon 1.1 by a toric blow-up in the cone $\mathrm{span}_{\mathbb{R}_{\geq 0}}((1,3),(0,-1))$. Hence the toric variety of polygon 1.2 arises from the toric variety of polygon 1.1 via a blow-up. Similarly polygon 1.3 arises from polygon 1.2 by a toric blow-up, and indeed this continues through the classification with a few exceptions:

- Polygons 1.13 and 1.14 do not fit into the sequence of toric blow-ups. Both of these surfaces have two R-singularities.

- Polygon 1.8 does not arise from a toric blow-up of polygon 1.7, however both 1.7 and 1.8 can be blown up to give polygon 1.9.

Considering only the Fano polygons with a single $\frac{1}{6}(1,1)$ R-singularity, note that these surfaces fall into a similar cascade structure to that of the ten smooth del Pezzo surfaces. The classification of the polygons with a single $\frac{1}{5}(1,1)$ R-singularity of Theorem 3.0.2, has this same cascade structure.

We generalise this to constructing an analogous cascade of qG-deformation families of del Pezzo surfaces with a single $\frac{1}{k}(1,1)$ R-singularity. For each entry of the cascade, we construct models and toric degenerations of the deformation family which is embedded in a toric variety in codimension ≤ 2 using Laurent inversion. The cascades are shown to be a classification of the qG-deformation families of del Pezzo surfaces with a single $\frac{1}{k}(1,1)$ singularity by the minimal model program.

4.1 LAURENT INVERSION

In this section we recall the method of *Laurent inversion* [25], which is used to construct models for the surfaces in these cascades.

Broadly speaking Laurent inversion takes a polytope $P \subset N_{\mathbb{R}}$ together with a certain decoration of P (called a *scaffolding*) as input and returns a torus invariant embedding of the toric variety associated to P into a second toric variety.

A scaffolding of a Fano polytope $P \subset N_{\mathbb{R}}$ is a presentation of P as the convex hull of a collection of polyhedra of sections (see Definition 1.4.10) of nef divisors on a (fixed) toric variety. As usual, we restrict our interest to the case of N being a rank two lattice.

Definition 4.1.1 ([25, Definition 13])**.** Fix the following data:

(i) a lattice $N \cong \mathbb{Z}^2$ with a decomposition $N = \bar{N} \oplus N_U$. Denote the dual lattice by M and the dual decomposition $M = \bar{M} \oplus M_U$;

(ii) a Fano polygon $P \subset N_{\mathbb{R}}$;

(iii) a projective toric variety Z, known as the *shape*, given by a fan in $\bar{M}_{\mathbb{R}}$ whose primitive ray generators span $\bar{M}$.

A *scaffolding* of P is a set S of pairs (D, χ), known as *struts*, where D is a nef divisor on Z and χ is an element of N_U such that:

$$P = \operatorname{conv}\{P_D + \chi : (D, \chi) \in S\},$$

where P_D is the polyhedron of sections of the torus invariant divisor D.

Although not required by the definition, impose two additional assumptions to simplify the Laurent inversion algorithm:

(i) every vertex of P is met by precisely one strut;

(ii) there is a basis $\{e_i : 1 \leq i \leq \dim N_U\}$ of N_U such that the pair $(\mathcal{O}, e_i) \in S$ for all values of i. We say, following [25], that these struts correspond to *uneliminated variables*.

Example 4.1.2. First fix the data (i)–(iii) appearing in Definition 4.1.1. Let N be a rank two lattice with $N_U = \{0\}$. Thus $M \cong \mathbb{Z}^2$ and $M_U = \{0\}$. Consider the Fano polygon P with vertices $(0,1), (1,0), (1,-1), (0,-1), (-1,0), (-1,1)$, and choose $Z = \mathbb{P}^2$. The fan Σ_Z corresponding to Z is:

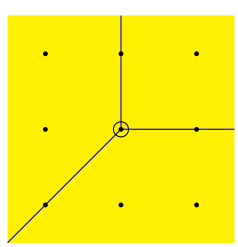

Let $\Sigma_Z(1) = \{\rho_1, \rho_2, \rho_3\}$ and denote the generator of the ray ρ_i by u_i. Define a piecewise-linear function $\phi_i, \forall i \in |\Sigma_Z(1)|$ by:

$$\phi_i(u_j) := \begin{cases} 1, & \text{if } i = j, \\ 0, & \text{otherwise.} \end{cases}$$

By Theorem 1.4.9, these piecewise linear functions correspond to divisors, denoted D_i, on Z. Consider the scaffold given by the three struts $(D_1, 0)$, $(D_2, 0)$ and $(D_3, 0)$. Computing the polyhedra P_{D_i} obtain:

$$P_{D_1} = \left\{ (x,y) \in N_{\mathbb{R}} : \begin{array}{r} \langle (x,y), (1,0) \rangle \geq -1 \\ \langle (x,y), (0,1) \rangle \geq 0 \\ \langle (x,y), (-1,-1) \rangle \geq 0 \end{array} \right\} = \left\{ (x,y) \in N_{\mathbb{R}} : \begin{array}{r} x \geq -1 \\ y \geq 0 \\ x + y \leq 0 \end{array} \right\},$$

$$P_{D_2} = \left\{ (x,y) \in N_{\mathbb{R}} : \begin{array}{r} x \geq 0 \\ y \geq -1 \\ x + y \leq 0 \end{array} \right\},$$

$$P_{D_3} = \left\{ (x,y) \in N_{\mathbb{R}} : \begin{array}{r} x \geq 0 \\ y \geq 0 \\ x + y \leq 1 \end{array} \right\},$$

which then satisfy the condition $P = \operatorname{conv}\left\{P_{D_1}, P_{D_2}, P_{D_3}\right\}$ as illustrated:

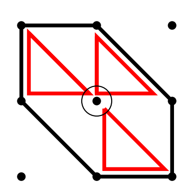

With the exception of the scaffolding appearing in Figure 7 we will only use three types of scaffolding:

(i) $N = \mathbb{Z}^2$, $N_U = \mathbb{Z}$, $Z = \mathbb{P}^1$;

(ii) $N = \mathbb{Z}^2$, $N_U = \{0\}$, $Z = \mathbb{P}^1 \times \mathbb{P}^1$;

(iii) $N = \mathbb{Z}^2$, $N_U = \{0\}$, $Z = \mathbb{P}^2$.

Examples for each of these types of scaffolding can be found in Section 4.2.

Laurent inversion is an algorithm to pass from a scaffolding S of a Fano polytope P to an embedding of the corresponding Fano toric variety X_P in an ambient toric variety Y_S. The form of the algorithm presented applies to a scaffolding with shape Z isomorphic to a product of projective spaces; this is true of all three cases enumerated above.

The algorithm of [25] for Laurent inversion is as follows: Let S be a scaffolding of a Fano polytope P with shape Z. Let $u = \dim(N_U)$ and let $r = |S| - u$, so that S contains u struts that correspond to uneliminated variables and r struts that do not correspond to uneliminated variables. Let R be the sum of $|S|$ and the number of rays of Z. We determine an $r \times R$ matrix $\mathcal{M}$, which will act as the weight matrix for a toric variety Y_S, as follows. Let $m_{i,j}$ denote the $(i,j)^{th}$ entry of $\mathcal{M}$. Fix an identification of the rows of $\mathcal{M}$ with the r elements (D_i, χ_i) of S which do not correspond to uneliminated variables, and an ordering $\Delta_{\rho_1}, \ldots, \Delta_{\rho_{R-|S|}}$ of the toric divisors corresponding to the rays of the fan of Z. Let $e_1, \ldots, e_u$ be the basis of N_U given by the uneliminated variables.

(i) For $1 \leq j \leq r$ and any i, let $m_{i,j} = \delta_{i,j}$;

(ii) For $1 \leq j \leq u$ and any i, let $m_{i,r+j}$ be determined by the expansion:

$$\chi_i = \sum_{j=1}^{u} m_{i,r+j} e_j;$$

(iii) For $1 \leq j \leq z$, let $m_{i,|S|+j}$ be determined by the expansion:

$$D_i = \sum_{j=1}^{R-|S|} m_{i,|S|+j} \Delta_j.$$

The weight matrix $\mathcal{M}$ alone does not determine a unique toric variety – a stability condition ω also needs to be specified. Unless otherwise stated, assume

ω to be the sum of the first $|S|$ columns in $\mathcal{M}$. Let Y_S denote the toric variety determined by the GIT data $(\mathcal{M}, \omega)$.

After choosing bases of N_U and $\mathrm{Div}_{T_{\bar{M}}}(Z)$ the fan of the toric variety Y_S is contained in $(N_U \oplus \mathrm{Div}_{T_{\bar{M}}}(Z)) \otimes \mathbb{R}$.

Theorem 4.1.3 ([25, Theorem 20])**.** Given a scaffolding S of a Fano polytope P, the GIT data $(\mathcal{M}, \omega)$ defines a toric variety Y_S with $\mathrm{Cl}(Y_S) \cong \mathbb{Z}^r$. Furthermore, there is a canonical embedding $X_P \hookrightarrow Y_S$. If Z is isomorphic to a product of k projective spaces, X_P is the intersection of k divisors, each of which is defined by a single equation in Cox co-ordinates, on Y_S, and:

$$\omega = -K_X - \sum_i L_i,$$

where the linear systems L_i define X_P.

Of course, if Y_S is smooth, this defines a complete intersection. In general smoothness needs to verified on a case-by-case basis. There are many ways of embedding a toric variety into another toric variety, but Theorem 4.1.3 allows us to unify a large number of classical constructions of Fano varieties into a simple format.

Definition 4.1.4 ([25, Proposition 27])**.** Fix a Fano polygon P and let Z be the minimal resolution of the toric variety determined by the normal fan of P. The *anti-canonical scaffolding* of P is the scaffolding S with shape Z consisting of the single nef divisor D on Z such that the polyhedron of sections of D is equal to P.

The Laurent inversion algorithm applied to the anti-canonical scaffold determines an embedding of X_P into a weighted projective space $\mathbb{P}(1, a_1, \ldots, a_N)$. By construction this is the map into weighted projective space defined by the elements of $-K_{X_P}$; that is, the usual anti-canonical embedding. Combining this with Theorem 4.1.3 gives the following proposition:

Proposition 4.1.5. Given a Fano polygon P isomorphic to the polyhedron of sections of a nef divisor on $\mathbb{P}^2$ or $\mathbb{P}^1 \times \mathbb{P}^1$, or isomorphic to the cone over the polyhedron of sections of a nef divisor on $\mathbb{P}^1$, then X_P is anti-canonically embedded as complete intersection in a weighted projective space.

Any low codimension model obtained via the anti-canonical scaffolding of a polygon can also be obtained by studying the Hilbert series of the corresponding toric variety; by using the anti-canonical scaffolding we only obtain models already accessible by well known methods. Several examples of such models appear in 4.2, and so we recall the work of Reid–Suzuki [65].

We want to study the Hilbert series of the blow-up of $\mathbb{P}(1,1,k)$ in $l \in \{k+2, k+3, k+4\}$ general smooth points. Namely following [65], consider the Hilbert series of $\mathbb{P}(1,1,k)$ polarised by the anti-canonical divisor $-K_{\mathbb{P}(1,1,k)} = \mathcal{O}(k+2)$. This can be calculated by taking the Hilbert series of $\mathbb{P}(1,1,k)$ polarised by $\mathcal{O}(1)$, which is:

$$\frac{1}{(1-s)^2(1-s^k)},$$

multiplying through by $(1-s^{k+2})^2(1-s^{k(k+2)})$, truncating to the polynomial consisting only of terms divisible by t^{k+2}, and making the substitution $s^{k+2} = t$. The calculation splits into two cases:

(i) Suppose k is even. Setting $k = 2m$, obtain:

$$H_{\mathbb{P}(1,1,k)} = \frac{P_{\mathbb{P}(1,1,k)}(t)}{(1-t)^2(1-t^k)},$$

where:

$$P_{\mathbb{P}(1,1,k)}(t) = 1 + \sum_{i=1}^{m-1}(k+4)t^i + (k+5)t^m + (k+5)t^{m+1} + \sum_{i=m+2}^{k}(k+4)t^i + t^{k+1}.$$

(ii) k is odd. In this case, letting $k = 2m - 1$, obtain:

$$H_{\mathbb{P}(1,1,k)} = \frac{P_{\mathbb{P}(1,1,k)}(t)}{(1-t)^2(1-t^k)},$$

where:

$$P_{\mathbb{P}(1,1,k)}(t) = 1 + \sum_{i=1}^{m-1}(k+4)t^i + (k+6)t^m + \sum_{i=m+1}^{k}(k+4)t^i + t^{k+1}.$$

A smooth blow-up has a Hilbert contribution:

$$Q = -\frac{t}{(1-t)^3} = -\frac{t(1-t^k)}{(1-t)^3(1-t^k)} = -\frac{t+t^2+t^3+t^4+\ldots+t^k}{(1-t)^2(1-t^k)},$$

and hence the Hilbert series of the blow up of $\mathbb{P}(1,1,k)$ in l general points is $H_{\mathbb{P}(1,1,k)} + l \times Q$. Calculating the Hilbert series for $l \in \{k+2, k+3, k+4\}$ suggests a low codimension model for the surface in each case. When these models occur in codimension ≤ 2 they coincide with models for these varieties obtained by Laurent inversion in Section 4.2. When the Hilbert series models occur in codimension three or four we present a different model in Section 4.2. First consider the case $k = 2m$ for some $m \in \mathbb{Z}_{\geq 1}$:

l	Hilbert Series	Suggested Model
$k+4$	$\frac{1-t^{k+2}}{(1-t)^2(1-t^m)(1-t^{m+1})}$	$X_{k+2} \subset \mathbb{P}(1,1,m,m+1)$
$k+3$	$\frac{1-t^{m+2}}{(1-t)^3(1-t^m)}$	$X_{m+2} \subset \mathbb{P}(1,1,1,m)$
$k+2$	$\frac{(1-t^2)(1-t^{m+1})}{(1-t)^4(1-t^m)}$	$X_{2,m+1} \subset \mathbb{P}(1,1,1,1,m)$

Consider the case $k = 2m - 1$ for some $m \in \mathbb{Z}_{\geq 1}$:

l	Hilbert Series	Suggested Model
$k+4$	$\frac{(1-t^{k+1})^2}{(1-t)^2(1-t^m)^2(1-t^k)}$	$X_{k+1,k+1} \subset \mathbb{P}(1,1,m,m,k)$
$k+3$	$\frac{1-2t^{m+1}-3t^{k+1}+3t^{k+2}+2t^{3m}-t^{2k+3}}{(1-t)^3(1-t^m)^2(1-t^k)}$	$\mathrm{Pf}_{5,5} \subset \mathbb{P}(1,1,1,m,m,k)$
$k+2$	$\frac{1-t^2-4t^{m+1}+4t^{m+2}-4t^{k+1}+8t^{k+2}-4t^{k+3}+4t^{3m}-4t^{m+2}-t^{2k+2}+t^{2k+4}}{(1-t)^4(1-t^m)^2(1-t^k)}$	codim 4

Note that the Hilbert series models obtained when k is odd generally appear in higher codimension. For odd values of k the codimension appearing in the cascade directly generalises the case $k = 1$ (that is, the original ten del Pezzo surfaces). The proto-typical case for even values of k is the case $k = 2$, for which each of the surfaces given as the blow-up of $\mathbb{P}(1,1,2)$ in l points admits a smoothing to the blow-up of $\mathbb{P}^2$ in $l+1$ general points. For example the blow of $\mathbb{P}(1,1,2)$ admits a smoothing to the del Pezzo surfaces dP_4, which is known to have models of codimension ≤ 2 in weighted projective spaces.

In the cases $k = 2$ and $k = 4$ observe that all the constructions tabulated above are well known models of del Pezzo surfaces. This is expected, since the singularity $\frac{1}{k}(1,1)$ is a non-trivial T-singularity precisely when $k = 2$ or $k = 4$.

4.2 LOW CODIMENSION MODELS

Following Iano-Fletcher [43], let us recall the notion of a quasismooth complete intersection in weighted projective space $w\mathbb{P} = \mathbb{P}(a_0, \ldots, a_n)$. Let $X \subset w\mathbb{P}$ be a closed subvariety, and consider the canonical projection of the weighted projective space $\rho : \mathbb{A}^{n+1}\backslash\{0\} \to w\mathbb{P}$. The *punctured affine cone* is $C_X^\circ = \rho^{-1}(X)$, and the *affine cone* C_X over X is the closure of C_X° in $\mathbb{A}^{n+1}$. Note that the action of the group $\mathbb{C}^*$ on $w\mathbb{P}$ can be restricted to C_X°, and $X = C_X^\circ/\mathbb{C}^*$. The variety $X \subset w\mathbb{P}$ is *quasismooth of dimension* n if its affine cone C_X is smooth of dimension $n+1$ outside its vertex $\underline{0}$. When $X \subset w\mathbb{P}$ is quasismooth the singularities of X are due to the $\mathbb{C}^*$-action and hence are cyclic quotient singularities. Knowing that our models are quasismooth will be vital to checking that they have the correct singularities.

Theorem 4.2.1 ([43, Theorem 8.1])**.** The general hypersurface $X_d \subset \mathbb{P}(a_0, \dots, a_n)$, where $n \geq 1$, is quasismooth if and only if one of the following holds:

(i) there exists a coordinate x_i of $\mathbb{P}(a_0, \dots, a_n)$ for some i of weight d; or

(ii) for every non-empty subset $I = \{i_0, \dots, i_{k-1}\} \subset \{0, \dots, n\}$ either:

  (a) there exists a monomial $x_{i_0}^{m_0} \cdots x_{i_{k-1}}^{m_{k-1}}$ of degree d; or

  (b) for $\mu = 1, \dots, k$ there exist monomials $x_{i_0}^{m_{0,\mu}} \cdots x_{i_{k-1}}^{m_{k-1,\mu}} x_{e_\mu}$ of degree d, where each of the e_μ are distinct.

Theorem 4.2.2 ([43, Theorem 8.7])**.** Consider a codimension two weighted complete intersection $X_{d_1,d_2} \subset \mathbb{P}(a_0, \dots, a_n)$, where $n \geq 2$, which is not the intersection of a linear cone with another hypersurface. The variety X_{d_1,d_2} is quasismooth if and only if for each non-empty subset $I = \{i_0, \dots, i_{k-1}\} \subset \{0, \dots, n\}$ one of the following holds:

(i) there exist monomials $x_{i_0}^{m_{1,0}} \cdots x_{i_{k-1}}^{m_{1,k-1}}$ and $x_{i_0}^{m_{2,0}} \cdots x_{i_{k-1}}^{m_{2,k-1}}$ of degree d_1 and d_2, respectively;

(ii) there exists a monomial $x_{i_0}^{m_{1,0}} \cdots x_{i_{k-1}}^{m_{1,k-1}}$ of degree d_1, and for $1 \leq \mu \leq k-1$ there exist monomials $x_{i_0}^{m_{2,0}} \cdots x_{i_{k-1}}^{m_{2,k-1}} x_{e_\mu}$ of degree d_2 where the $\{e_\mu\}$ are all distinct;

(iii) there exists a monomial $x_{i_0}^{m_{2,0}} \cdots x_{i_{k-1}}^{m_{2,k-1}}$ of degree d_2, and for $1 \leq \mu \leq k-1$ there exist monomials $x_{i_0}^{m_{1,0}} \cdots x_{i_{k-1}}^{m_{1,k-1}} x_{e_\mu}$ of degree d_1 where the $\{e_\mu\}$ are all distinct;

(iv) for $1 \leq \mu \leq k-1$, there exists a degree d_1 monomial $x_{i_0}^{m_{1,0}} \cdots x_{i_{k-1}}^{m_{1,k-1}} x_{e_\mu^1}$ and a degree d_2 monomial $x_{i_0}^{m_{2,0}} \cdots x_{i_{k-1}}^{m_{2,k-1}} x_{e_\mu^2}$ such that $\{e_\mu^1\}$ are all distinct, $\{e_\mu^2\}$ are all distinct and $\{e_\mu^1, e_\mu^2\}$ contains at least $k+1$ distinct elements.

For each integer $k = 3$ or $k > 4$ we will study a cascade of surfaces obtained from the weighted projective space $\mathbb{P}(1,1,k)$ by blowing up points in general position and contracting exceptional curves. Note that here and previously in this chapter, we take general position to be stronger than the notion used in Chapter 2. Informally we take it to mean that the points do not fall on a subvarieties of lower degree more than necessary. As mentioned in the introduction, the cascades are particularly simple: all but one surface in each cascade is obtained from $\mathbb{P}(1,1,k)$ via a blow-up in at most $k+4$ general smooth points.

Definition 4.2.3. For a given $k \in \mathbb{Z}_{>0}$, let $X_k := \mathbb{P}(1,1,k)$ and let $X_k^{(l)}$ denote the blow-up of $\mathbb{P}(1,1,k)$ in l general points. Assume that:

$$l < \frac{(k+2)^2}{k}.$$

The degree of $\mathbb{P}(1,1,k)$ is $(k+2)^2/k$ and thus the bound on l in Definition 4.2.3 ensures that $X_k^{(l)}$ is a del Pezzo surface since as a corollary to Lemma 2.1.2, a blow-up in a smooth point reduces the degree by one. The cascade consists of the surfaces $X_k^{(l)}$ for a fixed value of k and all possible values of l, along with an additional surface obtained by contracting a curve on $X_k^{(k+1)}$.

Definition 4.2.4. Fix a positive integer k and $k+1$ points $\{p_i : 1 \leq i \leq k+1\}$ on $\mathbb{P}(1,1,k)$. There is a unique curve C in the linear system $\mathcal{O}(k)$ passing through these $k+1$ points. Blow-up all the points p_i and let C' be the strict transform of the curve C. Let $B_k^{(k)}$ denote the surface obtained by contacting C'.

This is the obvious generalisation of the construction of $\mathbb{P}^1 \times \mathbb{P}^1 \cong B_1^{(1)}$ from the $\mathbb{P}^2$ cascade. In our constructions of low codimension models for the surfaces $X_k^{(l)}$, $B_k^{(k)}$ we make use of alternate descriptions of $X_k^{(k+2)}$, $X_k^{(k+3)}$, and $X_k^{(k+4)}$ which depend on the parity of k.

Example 4.2.5. The cascade of del Pezzo surfaces with a single $\frac{1}{5}(1,1)$ singularity is:

$$\begin{array}{cccccccccccccccccc} \mathbb{P}(1,1,5) & \leftarrow & X_5^{(1)} & \leftarrow & X_5^{(2)} & \leftarrow & X_5^{(3)} & \leftarrow & X_5^{(4)} & \leftarrow & X_5^{(5)} & \leftarrow & X_5^{(6)} & \leftarrow & X_5^{(7)} & \leftarrow & X_5^{(8)} & \leftarrow & X_5^{(9)} \\ & & & & & & & & & & & & \downarrow & & & & & & \\ & & & & & & & & & & & & B_5^{(5)} & & & & & & \end{array}$$

Properties of these surfaces are given in the following table:

Surface	Fano Index	Is toric?
$\mathbb{P}(1,1,5)$	7	Yes
$X_5^{(i)}$, for $i \in \{1,2\}$	1	Yes
$X_5^{(i)}$, for $i \in \{3,4,\ldots,9\}$	1	No
$B_5^{(5)}$	2	No

These properties generalise to any of the cascades constructed in the obvious way. The above table also illustrates how these cascades overlap with the classifications of del Pezzo surfaces with Fano index > 1 by Alexeev–Nikulin [7] and Fujita–Yasutake [35], and the classification of toric del Pezzo surfaces with exactly one singular point by Dais [31].

Definition 4.2.6. Fix a positive integer k and $k+2$ points $\{p_i : 1 \leq i \leq k+2\}$ on the diagonal $\Delta \subset \mathbb{P}^1 \times \mathbb{P}^1$. Let S_k denote the surface obtained by blowing up the points p_i. Letting Δ also denote the strict transform of the diagonal, it follows immediately that $\Delta^2 = -k$.

Lemma 4.2.7. The surface S_k is a minimal resolution of $X_k^{(k+2)}$. The resolution contracts the strict transform of the diagonal in $\mathbb{P}^1 \times \mathbb{P}^1$.

Proof. For $j = 1, 2$, let π_j denote the j^{th} projection $\pi_j : \mathbb{P}^1 \times \mathbb{P}^1 \to \mathbb{P}^1$, and let E_i denote the strict transform of the fibre $\pi_1^{-1}(\pi_1(p_i))$ in $S_k \to \mathbb{P}^1 \times \mathbb{P}^1$. Each morphism π_j induces a morphism $S_k \to \mathbb{P}^1$ with $k+2$ reducible fibres. Each of these fibres contains precisely one of the curves E_i. Thus, by contracting all the curves E_i, obtain a surface $\tilde{S}_k$ together with a morphism $\tilde{S}_k \to \mathbb{P}^1$ such that all its fibres are isomorphic to $\mathbb{P}^1$. That is, $\tilde{S}_k$ is isomorphic to the Hirzebruch surface $\mathbb{F}_k$. Consider the following commuting diagram:

$$\begin{tikzcd}
S_k \arrow[r] \arrow[d] & X_k^{(k+2)} \arrow[d] \\
\tilde{S}_k \arrow[r] & \mathbb{P}(1,1,k)
\end{tikzcd}$$

Thus $S_k \to X_k^{(k+2)}$ is a minimal resolution. □

Definition 4.2.8. Fix a positive integer k and $k+4$ points $\{p_i : 1 \leq i \leq k+4\}$ which lie on a conic in $\mathbb{P}^2$. Let S'_k denote the surface obtained by blowing up the points p_i. If C denotes the strict transform of the conic, it follows immediately that $C^2 = -k$.

Lemma 4.2.9. The surface S'_k is a minimal resolution of $X_k^{(k+3)}$. The resolution contracts the strict transform of the conic in $\mathbb{P}^2$ used to define S'_k.

Proof. Let C be a conic in $\mathbb{P}^2$ and fix $k+4$ points $\{p_i : 1 \leq i \leq k+4\}$ on C. Consider the surface obtained by blowing up only the point p_{k+4} and the strict transform of C. The blow-up is isomorphic to the first Hirzebruch surface $\mathbb{F}_1$. Let $\pi : \mathbb{F}_1 \to \mathbb{P}^1$ be its projection to $\mathbb{P}^1$. Blow-up the points p_i for $1 \leq i \leq k+3$, and contract the strict transforms of the fibres $\pi^{-1}(\pi(p_i))$ of π. In this way obtain a ruled surface with a unique $-k$ curve, i.e. the surface $\mathbb{F}_k$, the minimal resolution of $\mathbb{P}(1,1,k)$. By a similar argument to Lemma 4.2.7, $S'_k \to X_k^{(k+3)}$ is a minimal resolution. □

Consider the anti-canonical degree:

$$\left(-K_{X_k^{(l)}}\right)^2 = k - l + 4 + \frac{4}{k}.$$

When $k > 4$ the value of l is bounded above by $k + 4$. Therefore the cascades grow in length with k: however for large values of k there are no surfaces with geometry as rich as the cubic surface or the lower degree del Pezzo surfaces that occur at the end of the cascade for $k < 4$, when $l > k + 4$. The cases $k = 2, 4$ are closely related to the smooth del Pezzo surfaces (via $\mathbb{Q}$-Gorenstein smoothings) and the case $k = 3$ is considered in detail in [27].

Case $\mathbf{l < k + 2}$:

Every surface $X_k^{(l)}$ in this case may be exhibited as a hypersurface in a toric variety. Let P_k^l denote the Fano polygon obtained as the convex hull of the points:

$$\{(1,0),(0,-1),(-1,k-l),(-1,k)\}.$$

Consider a scaffolding of the polygon P_k^l with shape $\mathbb{P}^1$ consisting of three struts:

(i) the single point $\{(1,0)\}$;

(ii) the segment $\mathrm{conv}\{(0,-1),(0,0)\}$; and

(iii) the segment $\mathrm{conv}\{(-1,k-l),(-1,k)\}$.

The polygon P_4^2, together with its prescribed scaffolding, is shown in Figure 4.

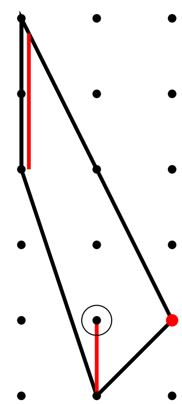

Figure 4: The scaffolding of P_4^2.

The weight matrix obtained via the Laurent inversion algorithm from Section 4.1 for this scaffolding is:

$$\begin{array}{ccccc} y_1 & y_2 & x_1 & x_2 & x_3 \\ \hline 1 & 0 & 0 & 1 & 0 \\ 0 & 1 & 1 & l-k & k \end{array}$$

By Theorem 4.1.3 there is a codimension one embedding of the toric variety $X_{P_k^l}$ into a toric variety $Y_k^{(l)}$.

Lemma 4.2.10. The toric variety defined by this weight matrix and the stability condition $\omega = \begin{pmatrix} 1 \\ 2 \end{pmatrix}$, denoted $Y_k^{(l)}$, is isomorphic to the rational scroll $\mathbb{P}_{\mathbb{P}(1,1,k)}(\mathcal{O} \oplus \mathcal{O}(k-l))$.

The toric variety $X_{P_k^l}$ is a hypersurface given by the vanishing of a section of $\mathcal{O}(1,l)$, namely $y_1 y_2^l = x_2 x_3$, on $Y_k^{(l)}$. We show that the vanishing locus of a general section of $\mathcal{O}(1,l)$ is the blow-up of $\mathbb{P}(1,1,k)$ in l points.

Proposition 4.2.11. Let X be the vanishing locus of a general section of $\mathcal{O}(1,l)$ on Y_k^l. The projection $\pi : Y_k^{(l)} \to \mathbb{P}_{(y_2:x_1:x_3)}(1,1,k)$ maps X onto $\mathbb{P}(1,1,k)$ and contracts l disjoint rational curves.

Proof. The equation defining X has the general form:

$$y_1 f_l(y_2, x_1, x_3) + x_2 g_k(y_2, x_1, x_3) = 0,$$

where f_l, g_k are homogeneous polynomials of bi-degree $(0, l)$ and $(0, k)$ respectively. Therefore X is a section of the projection π except where $f_l = g_k = 0$ in $\mathbb{P}_{(y_2:x_1:x_3)}(1, 1, k)$. The fibre of $\pi|_X$ over a point where these two polynomials vanish, is a $\mathbb{P}^1$ contracted to a point by π. Therefore we only need to count the number of intersection points of the zero locus of f_l and g_k.

First assume that $l < k$. Then no term of f_l contains the variable x_3 and the set $\pi(\{f_l = 0\})$ is a collection of l fibres of the projection $\mathbb{P}(1, 1, k) \to \mathbb{P}^1$ presenting $\mathbb{P}(1, 1, k)$ as the cone over a rational curve of degree k. The vanishing locus of g_k is a section of the standard projection $\mathbb{P}(1, 1, k) \dashrightarrow \mathbb{P}^1$ and thus the two curves meet in precisely l points.

Next consider the case $l = k$. The toric ambient space is $Y_k^l \cong \mathbb{P}(1, 1, k) \times \mathbb{P}^1$. The number of points in the intersection $f_l = g_k$ is the self-intersection number of the toric divisor $(x_3 = 0) \subset \mathbb{P}(1, 1, k)$, that is, l.

Finally consider the case $l = k + 1$. As before the curve $\{g_k = 0\}$ is a section of the projection of $\mathbb{P}(1, 1, k)$ to $\mathbb{P}^1$. The polynomial $f_{k+1} = 0$ can be written as $f_1(x_1, y_2)x_3 + h_{k+1}(x_1, y_2)$, and writing $g_k = x_3 - h_k(x_1, y_2)$, eliminate x_3 and solve $f_1 h_k + h_{k+1} = 0$. Any solution gives a point of intersection, and thus there are $k + 1 = l$ such points of intersection. $\square$

We also need to consider the exceptional case $B_k^{(k)}$. Consider the polygon P_k defined by taking the convex hull of of the points:

$$\{(1, 0), (-1, -1), (-1, k)\}.$$

Consider a scaffolding of the polygon P_k with shape $\mathbb{P}^1$ consisting of two struts:

(i) the single point $\{(1,0)\}$; and

(ii) the segment $\operatorname{conv}\{(-1,-1),(-1,k)\}$.

Applying Laurent inversion to this scaffolding of P_k obtain the toric surface X_{P_k} embedded in $\mathbb{P}(1,1,1,k)$ with co-ordinates x_1, x_2, x_3, y via the homogeneous equation

$$x_1^{k+1} - x_3 y = 0,$$

that is, it is embedded as a section of $\mathcal{O}(k+1)$ in $\mathbb{P}(1,1,1,k)$. Note that in the case $k=1$ this reproduces the Segre embedding $\mathbb{P}^1 \times \mathbb{P}^1 \hookrightarrow \mathbb{P}^3$ cut out via a section of the line bundle $\mathcal{O}(2)$.

Proposition 4.2.12. A general section of $\mathcal{O}(k+1)$ on $\mathbb{P}(1,1,1,k)$ is the surface $B_k^{(k)}$.

Proof. The GIT presentation of $Y_k^{(k+1)}$ (the ambient toric variety in which $X_k^{(k+1)}$ is embedded) immediately shows $Y_k^{(k+1)}$ is a weighted blow-up of $\mathbb{P}(1,1,1,k)$ with centre $\{y_2 = x_1 = x_3 = 0\}$, where the co-ordinates are inherited from those on $Y_k^{(k+1)}$. Thus there are a pair of projections:

$$\begin{tikzcd} Y_k^{(k+1)} \arrow[r, "\pi_2"] \arrow[d, "\pi_1"] & \mathbb{P}(1,1,1,k) \\ \mathbb{P}(1,1,k) & \end{tikzcd}$$

Recall that the hypersurface $X_k^{(k+1)} \subset Y_k^{(k+1)}$ is given by the vanishing of a general section:

$$y_1 f_{k+1}(y_2, x_1, x_3) - x_2 g_k(y_2, x_1, x_3) = 0.$$

The vanishing of this general section intersects the exceptional divisor $\{y_1 = 0\}$ in the curve $C = \{g_k(y_2, x_1, x_3) = 0\}$ (since x_2 is nowhere vanishing on the exceptional divisor). The image of $X_k^{(k+1)}$ under π_2 is the contraction of C. However the image of C under π_1 is a curve in the linear system $\mathcal{O}(k)$ which meets the $k+1$ points blown up by the map $\pi_1 : X_k^{(k+1)} \to \mathbb{P}(1,1,k)$. Finally, observe that the push-forward of the cycle $X_k^{(k+1)}$ is a divisor in the linear system $\mathcal{O}(k+1)$. □

Consider next those cases for which $k+2 \leq l < (k+2)^2/k$. Manipulating the expression $(k+2)^2/k = k+4+4/k$, we see there are precisely three possibilities for l if $k > 3$. Consider each of these three cases in turn, noting that the behaviour of our constructions varies with the parity of k. Our constructions apply for all positive integers k, but note in the cases $k = 2$, and $k = 4$ the general sections of the complete intersections also smooth the $\frac{1}{k}(1,1)$ singularity.

Case $\mathbf{l = k+2}$:

First consider the case $k = 2m$ for some $m \in \mathbb{Z}_{>2}$. Consider the polygon P_k^{k+2} given by the convex hull of the points:

$$\{(-1,-1),(1,-1),(-1,m),(1,m)\}.$$

The case $m = 3$ is shown in Figure 4 equip with its anti-canonical scaffolding.

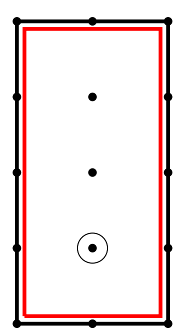

Figure 5: The scaffolding of $P_6^{(8)}$.

Following the Laurent inversion construction (or otherwise) the anti-canonical embedding maps:

$$X_{P_2^{k+2}} \hookrightarrow \mathbb{P}(1,1,1,1,m).$$

This coincides with the model suggested by the Hilbert series appearing in Section 4.1. In particular the image of this embedding is a codimension two complete intersection given by the vanishing of a section of the split bundle $E := \mathcal{O}(2) \oplus \mathcal{O}(m+1)$. In fact, one can show explicitly that the vanishing of a section of E is precisely a surface $X_k^{(k+2)}$.

Proposition 4.2.13. The minimal resolution of the vanishing of any section of E on $Y_k^{(k+2)} := \mathbb{P}(1,1,1,1,m)$ is the blow-up of $\mathbb{P}^1 \times \mathbb{P}^1$ in $k+2$ points.

Proof. Let x_i for $1 \leq i \leq 4$ and y be the co-ordinates on $Y_k^{(k+2)}$ and consider the vanishing locus $V := \{s_2 = 0\}$ of a section of $\mathcal{O}(2)$ on $Y_k^{(k+2)}$. The section s_2 is represented by a homogeneous polynomial with no term containing the variable y. Therefore V is isomorphic to a cone over the Segre embedding of $\mathbb{P}^1 \times \mathbb{P}^1$. The complement of the point $\{x_1 = x_2 = x_3 = x_4 = 0\}$ in V is the total space of $\mathcal{O}(m,m)$ on $\mathbb{P}^1 \times \mathbb{P}^1$.

Let W be the vanishing locus of $\{s_{m+1} = 0\}$, a homogeneous polynomial of degree $m+1$. This has the general form:

$$s_{m+1} = yf_1(x_1, \dots x_4) + f_{m+1}(x_1, \dots x_4).$$

Consider the projection $X := V \cap W \dashrightarrow \mathbb{P}^1 \times \mathbb{P}^1$ which contracts precisely those curves fibering over the points $f_1 = f_{m+1} = 0$. Sections of $\mathcal{O}(a)$ on $\mathbb{P}^3$ for any $a \in \mathbb{N}$, pull back to sections of $\mathcal{O}(a,a)$ on $\mathbb{P}^1 \times \mathbb{P}^1$ under the Segre embedding and thus the locus $f_1 = f_{m+1} = 0$ consists of $2(m+1) = k+2$ points on a curve in the linear system of $\mathcal{O}(1,1)$, and so up to a linear co-ordinate change, consists of $k+2$ points on the diagonal Δ of $\mathbb{P}^1 \times \mathbb{P}^1$.

In fact this projection factors through the blow-up of $Y_k^{(k+2)}$ at the point given by $\{x_1 = \dots = x_4 = 0\}$, resolving the indeterminacy of the projection and resolving the $\frac{1}{k}(1,1)$ singularity of the surface X. This hence exhibits $k+2$ disjoint lines on the minimal resolution of X and contracting these yields the surface $\mathbb{P}^1 \times \mathbb{P}^1$. By Lemma 4.2.7, X is the blow-up of $\mathbb{P}(1,1,k)$ in $k+2$ points.

□

Assume instead that $k = 2m-1$ for some $m \in \mathbb{Z}_{\geq 1}$. This case closely generalises the surface dP_6 in the case $k=1$. The case $k=3$ appears in Reid–Suzuki [65] and has degree $10/3$. There it is observed that the surface $X_3^{(5)}$ naturally embeds in codimension four. However we construct a codimension two embedding into a toric variety via Laurent inversion analogous to the embedding of dP_6 into the fourfold $\mathbb{P}^2 \times \mathbb{P}^2$. Similarly though there is a codimension four Segre type embedding of $Y_k^{(k+2)}$ into $\mathbb{P}(1^4, m^4, k)$ (where superscripts indicate repeated weights).

The case $k=1$ is nothing other than the usual construction of dP_6 as a codimension two complete intersection in $\mathbb{P}^2 \times \mathbb{P}^2$, the *ancestral Tom* of Brown–Reid–Stevens [17]. In the case $k=1$ there is also an embedding into the *ancestral Jerry* ($\mathbb{P}^1 \times \mathbb{P}^1 \times \mathbb{P}^1$). This construction does not appear to generalise to other values of k.

Consider the polygon P_k^{k+2} given as the convex hull of the points:

$$\{(0,-1),(m,-1),(m,m-1),(m-1,m),(-1,m),(-1,0)\},$$

together with the scaffolding shown in Figure 5 with shape $\mathbb{P}^1 \times \mathbb{P}^1$.

This scaffolding induces a toric embedding of $X_{P_k^{k+2}}$ into a toric variety $Y_k^{(k+2)}$ defined by the weight matrix:

x_1	x_2	y_1	y_2	z_1	z_2
1	1	0	0	$m-1$	m
0	0	1	1	m	$m-1$

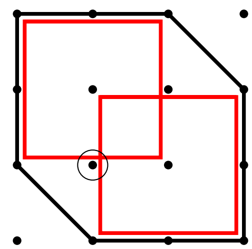

Figure 6: The scaffolding used to construct $X_k^{(k+2)}$ in the case $k = 3$.

together with stability condition $\omega = (1,1)$. The fourfold $Y_k^{(k+2)}$ determined by this data is a $\mathbb{Q}$-factorial Fano variety. The surface $X_{P_k^{k+2}}$ is a codimension two complete intersection defined by the vanishing of the polynomials:

$$x_1^m y_1^m - x_2 z_1, \qquad \text{and} \qquad x_1^m y_1^m - y_2 z_2.$$

In particular $X_{P_k^{k+2}}$ admits a flat deformation to the vanishing locus X of a general section of the split bundle $E := \mathcal{O}(m,m)^{\oplus 2}$.

Proposition 4.2.14. The minimal resolution of the vanishing of any section of E on $Y_k^{(k+2)}$ is the blow-up of $\mathbb{P}^1 \times \mathbb{P}^1$ in $k+2$ points on the diagonal Δ (that is, the surface S_k of Lemma 4.2.7). Moreover this resolution contracts the strict transform of the diagonal of $\mathbb{P}^1 \times \mathbb{P}^1$.

Proof. Any section of the split bundle E is defined by the pair of equations:

$$z_1 f_{1,0}(x_1,x_2) + z_2 g_{0,1}(y_1,y_2) + f_{m,m}(x_1,x_2,y_1,y_2) = 0,$$
$$z_1 h_{1,0}(x_1,x_2) + z_2 k_{0,1}(y_1,y_2) + g_{m,m}(x_1,x_2,y_1,y_2) = 0,$$

where subscripts of polynomials indicate degree in the homogeneous co-ordinate ring of $Y_k^{(k+2)}$. There is an obvious projection:

$$\pi_k : Y_k^{(k+2)} \dashrightarrow \mathbb{P}^1 \times \mathbb{P}^1$$

obtained by projecting out z_1 and z_2. This projection is defined away from the loci $\{x_1 = x_2 = 0\}$ and $\{y_1 = y_2 = 0\}$. These loci meet the vanishing locus of every section of E at the point $x_1 = x_2 = y_1 = y_2 = 0$ (since the loci $\{x_1 = x_2 = z_2 = 0\}$ and $\{y_1 = y_2 = z_1 = 0\}$ are unstable). As in the case of $k \in 2\mathbb{Z}$ the projection π_k contracts a number of curves. These curves are defined by two conditions; first we need the matrix:

$$\begin{pmatrix} f_{1,0} & g_{0,1} \\ h_{1,0} & k_{0,1} \end{pmatrix}$$

to drop rank. This condition defines an equation in $\mathcal{O}(1,1)$ on $\mathbb{P}^1 \times \mathbb{P}^1$. Second we need this locus to intersect the surface $X_k^{(k+2)}$. This occurs when the following matrix also drops rank:

$$\begin{pmatrix} f_{m,m} & f_{1,0} \\ g_{m,m} & h_{1,0} \end{pmatrix}.$$

The first equation determines a section of $\mathcal{O}(1,1)$ which is assumed to be the diagonal Δ in $\mathbb{P}^1 \times \mathbb{P}^1$. The second equation defines an equation in $\mathcal{O}(m+1,m)$ on $\mathbb{P}^1 \times \mathbb{P}^1$. Taking the intersection, note there are $2m+1 = k+2$ points of Δ whose fibre over π_k contains an exceptional curve. Over every point away from Δ, the fibre of π_k consists of a single point. □

Corollary 4.2.15. General sections of E are surfaces in the family $X_k^{(k+2)}$.

Proof. Contracting the strict transform of the diagonal in S_k we obtain a surface in the family $X_k^{(k+2)}$ via Lemma 4.2.7. □

As an interesting aside, we calculate the classical period of the the variety $X_6^{(8)}$. Using binomial coefficients, see [3], a mirror dual of $X_6^{(8)}$ is given by:

$$\begin{aligned} f = \frac{1}{xy} + \frac{4}{x} + \frac{6y}{x} + \frac{4y^2}{x} + \frac{y^3}{x} + \frac{2}{y} + 2y^3 + \frac{x}{y} \\ + 4x + 6xy + 4xy^2 + xy^3 + ay + by^2, \end{aligned}$$

where $a, b \in \mathbb{Z}_{\geq 0}$. Therefore calculate:

$$\pi_f(a,b;t) = 1 + (4a+56)t^2 + (48a+18b+672)t^3 \\ + (36a^2+1344a+384b+14440)t^4 + \dots$$

Case $\mathbf{l = k + 3}$:

Again start by considering the (easier) case of $k = 2m$ for some $m \in \mathbb{Z}_{\geq 1}$. In the case $l = k+2$ and $k \in 2\mathbb{Z}_{\geq 1}$ the anti-canonical embedding of $X_k^{(k+2)}$ is codimension two and there are explicit lines making divisorial contractions to $\mathbb{P}^1 \times \mathbb{P}^1$. It is therefore expected that the $l = k+3$ case will be anti-canonically embedded as a hypersurface in a weighted projective space obtained by a linear projection from $X_k^{(k+2)} \subset \mathbb{P}(1,1,1,1,m)$. We demonstrate this using Laurent inversion.

Consider the polygon P_k^{k+3} with vertices:

$$\{(-1,-1), (-1, m+1), (m+1, -1)\}.$$

Applying Laurent inversion to P_k^{k+3} with the anti-canonical scaffolding with shape $\mathbb{P}^2$, we obtain the ambient variety $Y_k^{(k+3)} := \mathbb{P}(1,1,1,m)$ with homogeneous co-ordinates x_i, $1 \leq i \leq 3$ and y. The toric surface $X_{P_k^{k+3}}$ is given by the vanishing of the section $x_1^{m+2} - x_2x_3y$ of $\mathcal{O}(m+2)$.

The surfaces $X_k^{(k+2)}$ are obtained from these hypersurfaces by the simplest kind of unprojection (unprojections can be studied in [8, 28, 60, 64] among others), from codimension one to codimension two. Explicitly, assume the equation defining a general section of $\mathcal{O}(m+2)$ in $\mathbb{P}(1,1,1,m)$ has the form:

$$Ay - Bx_3 = 0,$$

where A has degree 2 and B has degree $m+1$. Introduce an unprojection variable s and consider the equations:

$$sx_3 = A, \qquad \text{and} \qquad sy = B,$$

in $\mathbb{P}(1,1,1,1,m)$ of degrees 2 and $m+1$ respectively. In particular note that the projection from $X_k^{(k+2)}$ to $X_k^{(k+3)}$ is a blow-up of a single smooth point.

Now suppose $k = 2m-1$ for an integer $m \in \mathbb{Z}_{\geq 1}$. Here the surfaces come anti-canonically embedded in codimension three, as the cases $k = 1$ (dP_5), $k = 3$ (see [65]) and as the Hilbert series calculations suggest. It is therefore reasonable to consider the Pfaffians of a 5×5 matrix. However, following a path suggested by Laurent inversion, we can obtain a hypersurface embedding of $X_k^{(k+3)}$ into a toric variety.

The embedding $X_k^{k+3} \hookrightarrow Y_k^{(k+3)}$ is the most interesting application of Laurent inversion in this thesis. Let P_k^{k+3} be the convex hull of vertices:

$$\{(-1,-1),(-1,m),(m-1,m),(m,m-1),(m,-1)\}\,,$$

and cover P_k^{k+3} by a pair of struts with shape $\mathbb{P}^1 \times \mathbb{P}^1$ as shown in Figure 7.

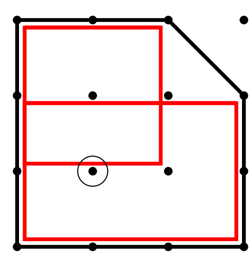

Figure 7: The scaffolding used to construct $X_k^{(k+3)}$ in the case $m = 2$.

This scaffolding determines a toric variety $Y_k^{(k+3)}$ with matrix of weight data:

x_1	x_2	y_1	y_2	z_1	z_2
1	1	0	1	$m-1$	m
0	0	1	1	m	$m-1$

and stability condition $\omega = (1,1)$. The surface $X_{P_k^{k+3}}$ is a codimension two complete intersection defined by the vanishing of the polynomials:

$$x_1^m y_1^m - x_2 z_1, \qquad \text{and} \qquad x_1^{m+1} y_1^m - y_2 z_2.$$

Thus $X_{P_k^{k+3}}$ admits a flat deformation to a general section of the vector bundle $E := \mathcal{O}(m,m) \oplus \mathcal{O}(m+1,m)$. Note that the fourfold $Y_k^{(k+3)}$ is *not* $\mathbb{Q}$-factorial, since $Y_k^{(k+3)}$ contains the point $\{x_1 = x_2 = y_1 = z_1 = z_2 = 0\}$. Also note that the toric subvariety $X_{P_k^{(k+3)}}$ meets this point, although the general section of the split bundle E does not.

Proposition 4.2.16. The minimal resolution of the vanishing of any section of E on $Y_k^{(k+3)}$ is the blow-up of $\mathbb{P}^2$ in $k+4$ points lying on a conic. Moreover the resolution contracts the strict transform of the conic.

Proof. Similarly to the case $l = k+2$ there is an obvious projection:

$$\pi_k : Y_k^{(k+3)} \dashrightarrow \mathbb{F}_1$$

onto the Hirzebruch surface $\mathbb{F}_1$ with homogeneous co-ordinates x_1, x_2, y_1, and y_2. Following the method used in the proof of Proposition 4.2.13 form an expression for a general section of E:

$$\begin{aligned} z_1 f_{1,0} + z_2 f_{0,1} + f_{m,m} &= 0, \\ z_1 f_{2,0} + z_2 f_{1,1} + f_{m+1,m} &= 0, \end{aligned}$$

where $f_{i,j}$ is a polynomial of bidegree (i,j) in the homogeneous co-ordinate ring of $\mathbb{F}_1$. The map π_k is undefined along the loci $\{x_1 = x_2 = 0\}$ and $\{y_1 = y_2 = 0\}$. These loci meet in $Y_k^{(k+3)}$ at $\{x_1 = x_2 = y_1 = y_2 = 0\}$. Restricting the defining equations of $X_{P_k^{k+3}}$ to $\{x_1 = x_2 = 0\}$ obtain:

$$z_2 y_1 + y_2^m = 0, \qquad \text{and} \qquad y_2 z_2 = 0.$$

Noting that the locus $\{x_1 = x_2 = z_2 = y_2 = 0\}$ is empty in $Y_k^{(k+3)}$ (seen by studying the irrelevant ideal of $Y_k^{(k+3)}$), the equations are only satisfied when $y_1 = y_2 = 0$. A similar calculation shows $Y_k^{(k+3)}$ meets the locus $\{y_1 = y_2 = 0\}$ at this point. Next consider the conditions required for a given fibre of π_k to contain a line. There is an equation with bidegree $\mathcal{O}(2,1)$ on $\mathbb{F}_1$ given by the vanishing of the determinant of the matrix:

$$\begin{pmatrix} f_{1,0} & f_{0,1} \\ f_{2,0} & f_{1,1} \end{pmatrix}.$$

There is also an equation of bidegree $\mathcal{O}(m+1,m+1)$ given by the vanishing of the determinant of the matrix:

$$\begin{pmatrix} f_{m,m} & f_{0,1} \\ f_{m+1,m} & f_{1,1} \end{pmatrix}.$$

The intersection form on $\mathbb{F}_1$ in the basis of $\mathrm{Pic}(\mathbb{F}_1)$ determined by the weight matrix defining $Y_k^{(k+3)}$ has matrix:

$$\begin{pmatrix} 0 & 1 \\ 1 & -1 \end{pmatrix}.$$

Thus the intersection product $\langle (m+1,m+1),(2,1)\rangle$ is equal to $2m+2=k+3$ and the projection π_k contracts precisely $k+3$ curves on fibering over a section of $\mathcal{O}(2,1)$. □

Corollary 4.2.17. General sections of E are surfaces in the family $X_k^{(k+3)}$.

Proof. By Lemma 4.2.9, by contracting the strict transform of the conic obtain a surface in the family $X_k^{(k+3)}$. □

In the case $m=1$, this reduces to the case of $dP_5 \subset \mathbb{P}^2\times\mathbb{P}^1$ cut out by a section of $\mathcal{O}(2,1)$. Note however that we had to add an additional column $(1,1)$ to the weight matrix, and a line bundle $\mathcal{O}(1,1)$ before this construction generalises to arbitrary values of m.

In [65], Reid–Suzuki observe that (similarly to dP_5) the surface $X_3^{(6)}$ embeds in codimension three via a system of Pfaffians of a 5×5 matrix. In fact such a construction works in general, and corresponds to the anti-canonical scaffolding of P_k^{k+3} shown in Figure 8. Indeed, in the case $l = k+4$ there is a codimension two model of the surface $X_k^{(k+4)}$ and, making a suitable unprojection from this surface, it is possible to recover a codimension three surface $X_k^{(k+3)} \subset \mathbb{P}(1,1,1,m,m,k)$.

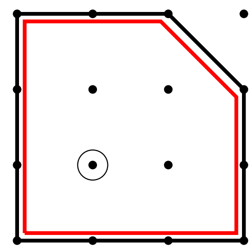

Figure 8: The anti-canonical scaffolding of P_k^{k+3} in the case $k = 3$.

Following the argument used in [65] this model works, taking a matrix:

$$\begin{pmatrix} x_1 & x_2 & b_{14} & b_{15} \\ & x_3 & b_{24} & b_{25} \\ & & b_{34} & b_{35} \\ & & & z \end{pmatrix} \text{ of degrees } \begin{pmatrix} 1 & 1 & m & m \\ & 1 & m & m \\ & & m & m \\ & & & k \end{pmatrix}$$

where x_i, $1 \leq i \leq 3$ and z are the co-ordinates on $\mathbb{P}(1,1,1,m,m,k)$ of degrees 1 and k respectively.

Case $\mathbf{l = k + 4}$:

The Hilbert series calculations would suggest a model for $X_k^{(k+4)}$ in weighted projective space of codimension ≤ 2 for all $k \in \mathbb{Z}_{\geq 1}$. These models should coincide with the model suggested by Laurent inversion applied to the anti-canonical scaffolding of a polygon associated to a toric degeneration of $X_k^{(k+4)}$. Figure 8 gives an example of polygons P_k^{k+4} for each parity of k.

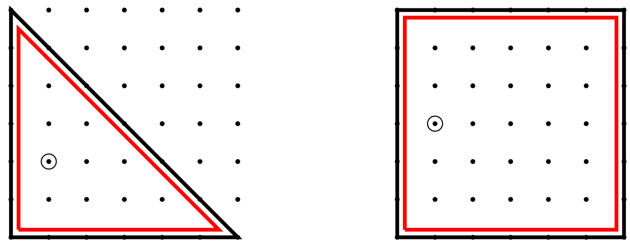

Figure 9: The anti-canonical scaffolding for $X_k^{(k+4)}$ in the case $k = 4$ and $k = 5$.

It is routine to verify that the singularities of a general section of each of these complete intersections is as expected. For $k = 2m - 1$ where $m \in \mathbb{Z}_{\geq 1}$, obtain the model:

$$X_{k+1,k+1} \subset \mathbb{P}(1, 1, m, m, k),$$

which, applying Theorem 4.2.2, is a quasismooth codimension two complete intersection. From this it is easy to verify that it has the correct singularities.

Contrary to previous, the case $k = 2m$ for some $m \in \mathbb{Z}_{\geq 1}$ is more complicated. The model

$$X_{k+2} \subset \mathbb{P}(1, 1, m, m + 1),$$

with co-ordinates x_1, x_2, y and z, is not quasismooth. Indeed, choosing a general section f of $\mathcal{O}(k+2)$, the affine variety $\{f = 0\} \subset \mathbb{A}^4$ is singular along the line $L = \{x_1 = x_2 = z = 0\}$. Setting $y = y_0$ the lowest order terms of f have degree two and the singularity in the affine slice $y = y_0$ is an ordinary double point. Taking the quotient by $\mathbb{G}_m$, the cyclic group of order m, maps $L \subset \mathbb{A}^4$ to a $\frac{1}{m}(1, 1, 1)$ singularity. Considering how this group action acts on $\{f = 0\}$, note the hypersurface in $\mathbb{P}(1, 1, m, m + 1)$ defined by f has a single singular point of type $\frac{1}{2m}(1, 1)$, as expected.

4.3 APPLICATION OF THE MINIMAL MODEL PROGRAM

We aim to prove that the surfaces that arise in Section 4.2 provide a complete classification of qG-deformation families of del Pezzo surfaces with a single $\frac{1}{k}(1,1)$ singularity. The proof is based on the *directed Minimal Model Program (MMP)* and has an identical structure to the classification of del Pezzo surfaces with $\frac{1}{3}(1,1)$ singularities derived in [27], although our current task is made considerably simpler by the assumption there is a single $\frac{1}{k}(1,1)$ singularity.

Definition 4.3.1. Given a del Pezzo surface X and rational curve $C \subset X$, then C is a *floating* (-1)*-curve* if C is contained in the smooth locus of X and $C^2 = -1$.

We rely heavily on the classification of extremal contractions for surfaces containing one singular point of the form $\frac{1}{k}(1,1)$. This classification is made in the following proposition and is directly analogous to [27, Theorem 31].

Proposition 4.3.2. Given a del Pezzo surface X with one singular point of the form $\frac{1}{k}(1,1)$, denote the exceptional curve of the minimal resolution $\widehat{X} \to X$ by E and let $f : X \to X_1$ be an extremal contraction. Exactly one of the following holds:

(i) the morphism f is the contraction of a floating (-1)-curve;

(ii) the morphism f is the contraction of a (-1)-curve in the minimal resolution of X meeting the curve E once. The surface X_1 has one singular point of the form $\frac{1}{k-1}(1,1)$ if $k > 2$ and is smooth if $k = 2$;

(iii) the morphism f is a Mori fibre space contraction. In this case X_1 is a single point and $X \cong \mathbb{P}(1,1,k)$.

Proof. Fix an integer $k > 1$, let X be a del Pezzo surface with one $\frac{1}{k}(1,1)$ singularity and let $\widehat{X} \to X$ be its minimal resolution with exceptional curve E. The surface $\widehat{X}$ is, by construction, a smooth projective surface with big anti-canonical class. Since $\widehat{X}$ has Kodaira dimension $-\infty$, $\widehat{X}$ is a ruled surface, that is, $\widehat{X}$ is birational to $\mathbb{P}^1 \times C$ for some curve C. However the only such surface with big anti-canonical class is $\mathbb{P}^1 \times \mathbb{P}^1$ and hence $\widehat{X}$ is rational.

By the classification of rational surfaces, see for example Beauville [14], if $\widehat{X}$ contains no (-1)-curves it is isomorphic to the Hirzebruch surface $\mathbb{F}_k$ (since $\widehat{X}$ contains a negative curve of self-intersection $-k$). Suppose now that $\widehat{X}$ contains a (-1)-curve C; after contracting all floating (-1)-curves and all curves C such that $C.C = -1$, and $C.E = 1$ we have a surface $\widehat{X}_1$. So if C is a rational curve in $\widehat{X}_1$ and $C.C = -1$, then $E.C \geq 2$. Contracting all such curves obtain a surface $\widehat{X}_2$ isomorphic to $\mathbb{F}_l$ for some $l \in \mathbb{Z}_{\geq 0}$, or $\mathbb{P}^2$. However the last contraction was the blow-up of a point on $\widehat{X}_2$ and this will not meet E in more than one point. $\square$

The list of extremal contractions appearing in the previous proposition is much shorter than that appearing in [27, Theorem 31] and consequently the analysis of the directed MMP is much more straightforward. This is due to the presence of exactly one singular point and the simple form of its minimal resolution.

It is also important to ensure that type (ii) divisorial contractions do not introduce more floating (-1)-curves. This is analogous to [27, Lemma 33] in our (simpler) context.

Lemma 4.3.3. Let X be a del Pezzo surface with a single $\frac{1}{k}(1,1)$ singularity which contains no floating (-1)-curves. Let $f : X \to X_1$ be an extremal contaction of type (ii). The surface X_1 contains no floating (-1)-curves.

Proof. Assume there is a floating (-1)-curve $C \subset X_1$. Since C is contained in the smooth locus of X_1 it does not meet the exceptional locus of f. Therefore f^{-1} is an isomorphism in a neighbourhood of C and $f^{-1}(C) \cdot f^{-1}(C) = -1$, a contradiction. $\square$

Theorem 4.3.4. Given an integer $k > 3$ there are precisely $k+6$ deformation classes of del Pezzo surfaces with a single $\frac{1}{k}(1,1)$ singularity. Of these, $k+5$ families are obtained by blowing up $\mathbb{P}(1,1,k)$ in general smooth points. The remaining surface is obtained by contracting an exceptional curve on $\mathbb{P}(1,1,k)$ blown up in $k+1$ smooth points. Moreover there is an embedding (not always quasismooth) of these surfaces, and a toric degeneration of each of these surfaces, into a toric variety with codimension ≤ 2.

Proof. Fix an integer $k > 1$, let X be a del Pezzo surface with a single $\frac{1}{k}(1,1)$ singularity, and let $\widehat{X} \to X$ be its minimal resolution with exceptional curve E. Assume that there are no floating (-1)-curves on X. Either there is a divisorial contraction (ii) of X, or X is the weighted projective space $\mathbb{P}(1,1,k)$. If X is equal to $\mathbb{P}(1,1,k)$ we are done. Assuming that X is not isomorphic to $\mathbb{P}(1,1,k)$ there is a sequence of divisorial contractions and taking the longest possible composition of these $\pi : \widehat{X} \to \widehat{X}_1$, $\pi(E) \cdot \pi(E) = l$ for some $0 \leq l < k$. If $l > 0$, $\widehat{X}_1$ must be isomorphic to $\mathbb{F}_l$. However blowing up a point in the negative curve of $\mathbb{F}_l$ introduces a floating (-1)-curve, so this cannot occur. If $l = 0$ then $\widehat{X} \cong \mathbb{P}^1 \times \mathbb{P}^1$; it is easily seen that the surface $B_k^{(k)}$ admits such a sequence of contractions. $\square$

4.4 ADDITIONAL SURFACES CONSTRUCTED USING LAURENT INVERSION

In this section we complete the proof of a classification of surfaces with $\frac{1}{3}(1,1)$ and $\frac{1}{6}(1,1)$ singularities or $\frac{1}{5}(1,1)$ singularities. In particular we classify families of locally $\mathbb{Q}$-Gorenstein rigid del Pezzo surfaces with residual baskets of the form:

$$\left\{ m_1 \times \frac{1}{3}(1,1), m_2 \times \frac{1}{5}(1,1), m_3 \times \frac{1}{6}(1,1) \right\},$$

such that:

$$m_1 = 0, m_2 > 0, m_3 = 0 \qquad \text{or} \qquad m_1 \geq 0, m_2 = 0, m_3 > 0,$$

which admit a $\mathbb{Q}$-Gorenstein toric degeneration. The toric varieties to which such a surface can degenerate are classified in [20]; applying Laurent inversion to these cases gives models for these surfaces. The main results of [20] show that either such a surface contains a single $\frac{1}{k}(1,1)$ singularity, for $k \in \{3,5,6\}$, or is one of three additional exceptional cases. In this section we show that all of these additional surfaces are hypersurfaces in weighted projective spaces. In particular, consider polygons 1.13 and 1.14 from [20]. While we use Laurent inversion here, we could also use the Ehrhart series of the dual polygons to guess the hypersurface model.

Polygon 1.13 is given by $\mathrm{conv}\{(-1,1),(1,1),(5,-1),(-5,-1)\}$. After mutating the T-singularities from the edge $\mathrm{conv}\{(-1,1),(1,1)\}$ obtain the polygon:

$$P = \mathrm{conv}\{(-6,-1),(0,1),(6,-1)\}.$$

Consider the following scaffolding of P consisting of two struts:

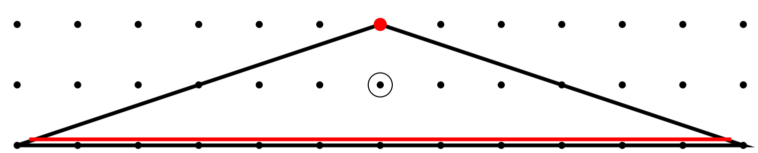

(i) the single point $\{(0,1)\}$;

(ii) the segment $\mathrm{conv}\{(-6,-1),(6,-1)\}$.

By Laurent inversion obtain the weight matrix:

$$\mathcal{M} = \begin{pmatrix} 1 & 6 & 6 & 1 \end{pmatrix}.$$

Therefore X_P is given by the general section of $\mathcal{O}(12)$ in $\mathbb{P}(1,1,6,6)$. By Theorem 4.2.1 , X_P is quasismooth and so X_P inherits two $\frac{1}{6}(1,1)$ from the ambient weighted projective space.

Via a different scaffold it is possible to obtain a different model. Mutate our original representativem $P_{1.13} := \operatorname{conv}\{(-1,1),(1,1),(5,-1),(-5,-1)\}$, to the representative $\operatorname{conv}\{(-3,1),(3,1),(3,-1),(-3,-1)\}$. Scaffold this new representative via a single strut as shown below:

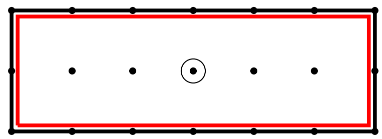

Laurent inversion gives the weight matrix:

$$\mathcal{M} = \begin{pmatrix} 1 & 1 & 1 & 3 & 3 \end{pmatrix},$$

and the corresponding toric variety is the complete intersection of the vanishing of two general sections of $\mathcal{O}(2)$ and $\mathcal{O}(6)$ in $\mathbb{P}(1,1,1,3,3)$. It is routine to check that this has the appropriate singularities.

In fact the two models:

$$(\mathbb{P}(1,1,6,6),\mathcal{O}(12)), \qquad \text{and} \qquad (\mathbb{P}(1,1,1,3,3),\mathcal{O}(2)\oplus\mathcal{O}(6)),$$

are isomorphic. This can be seen by observing that (possibly after a change of co-ordinates) the vanishing locus of a general section of $\mathcal{O}(2)$ on $\mathbb{P}(1,1,1,3,3)$ is isomorphic to the image of the degree 2 Veronese embedding of $\mathbb{P}(1,1,6,6)$ into $\mathbb{P}(1,1,1,3,3)$ defined by sending:

$$(x_1,x_2,y_1,y_2) \mapsto (x_1^2, x_1x_2, x_2^2, y_1, y_2).$$

In fact the hypersurface model of these surfaces generalises to the construction of a del Pezzo surface with a pair of R-singularities $\frac{1}{k_1}(1,1)$, $\frac{1}{k_2}(1,1)$ for any pair of positive integers $k_1, k_2 \in \mathbb{Z}_{>0} \setminus \{1,2,4\}$. Consider the polygon P with vertices $(0,1),(-k_1,-1),(k_2,-1)$. This polygon has two R-cones representing $\frac{1}{k_1}(1,1)$ and $\frac{1}{k_2}(1,1)$ cyclic quotient singularities. Scaffold using the struts as illustrated:

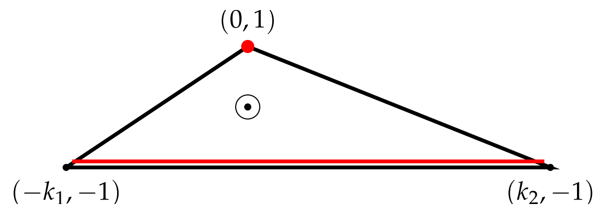

Laurent inversion gives us the weight matrix:

$$\mathcal{M} = \begin{pmatrix} 1 & k_1 & k_2 & 1 \end{pmatrix}.$$

Thus the toric variety X_P is a subvariety of $\mathbb{P}_{(x_1:x_2:y_1:y_2)}(1,1,k_1,k_2)$ cut out by the equation:

$$y_1y_2 - x_1^{k_1}x_2^{k_2}.$$

Consider the del Pezzo surface given by the vanishing of a general section of $\mathcal{O}(k_1+k_2)$ on $\mathbb{P}(1,1,k_1,k_2)$. By Theorem 4.2.1 the surface is quasismooth and the only singularities are inherited from the ambient space. Assume $k_1 \neq k_2$ and without loss of generality $k_1 < k_2$ so that $k_2 = nk_1 + r$. If $r = 0$, then a general section of $\mathcal{O}(k_1+k_2)$ is given by:

$$f = \sum_{i=0}^{n-1} f_{(1-i)k_1+k_2}(x_0,x_1)y^i + yz + y^n,$$

where x_0, x_1, y, z are coordinates on $\mathbb{P}(1,1,k_1,k_2)$. This surface intersects the orbifold locus at the points $[0:0:0:1]$ and $[0:0:1:-1]$ giving cyclic quotient singularities $\frac{1}{k_1}(1,1)$ and $\frac{1}{k_2}(1,1)$ respectively. If $r \neq 0$, then a general section of $\mathcal{O}(k_1+k_2)$ is given by:

$$f = \sum_{i=0}^{n} f_{(1-i)k_1+k_2}(x_0,x_1)y^i + yz.$$

The zero locus of f intersects the orbifold locus at $[0:0:0:1]$ and $[0:0:1:0]$ giving cyclic quotient singularities $\frac{1}{k_1}(1,1)$ and $\frac{1}{k_2}(1,1)$ on the del Pezzo surface. The case of $k_1 = k_2$ is treated similarly.

Corollary 4.4.1. There exists a del Pezzo surface admitting a toric degeneration with exactly two R-singularities $\frac{1}{k_1}(1,1)$ and $\frac{1}{k_2}(1,1)$ given by the vanishing of a general section of $\mathcal{O}(k_1 + k_2)$ on $\mathbb{P}(1,1,k_1,k_2)$. Considering the local models near the smoothable singularities of the respective toric varieties it is verifiable that this deformation is $\mathbb{Q}$-Gorenstein.

The polygons appearing in Theorems 3.0.1 and 3.0.2 with more than one R-singularity admit models as sections of $\mathcal{O}(k_1 + k_2)$ in $\mathbb{P}(1,1,k_1,k_2)$. There are four Fano polygons with two R-singularities $\frac{1}{k_1}(1,1)$ and $\frac{1}{k_2}(1,1)$ where $k_1, k_2 < 7$. These are the del Pezzo surfaces:

(i) $X_8 \subset \mathbb{P}(1,1,3,5)$ defined by a general section of $\mathcal{O}(8)$;

(ii) $X_9 \subset \mathbb{P}(1,1,3,6)$ defined by a general section of $\mathcal{O}(9)$;

(iii) $X_{10} \subset \mathbb{P}(1,1,5,5)$ defined by a general section of $\mathcal{O}(10)$;

(iv) $X_{11} \subset \mathbb{P}(1,1,5,6)$ defined by a general section of $\mathcal{O}(11)$.

Of these X_9 and X_{10} are needed to complete the desired classifications of Theorems 3.0.1 and 3.0.2.

5

RESTRICTIONS OF THE SINGULARITY CONTENT OF FANO POLYGONS

5.1 RESTRICTIONS USING MATRICES

The work of this section and the following one was completed in Cavey [18].

Let $P \subset N_{\mathbb{R}}$ be a Fano polygon with vertices $v_1, v_2, \ldots, v_k$ labelled anticlockwise. By convention subscripts are considered modulo k to be in the range $\{1, \ldots, k\}$. Consider the set of uniquely determined matrices $\{M_i \in GL(N)\}_{1 \leq i \leq k}$ satisfying:

$$M_i v_i = v_{i+1}, \qquad \text{and} \qquad M_i v_{i+1} = v_{i+2}.$$

It follows that:

$$M_k M_{k-1} \cdots M_1 = Id.$$

By specifying that the cones $\mathrm{span}_{\mathbb{R}_{\geq 0}}(v_i, v_{i+1})$ and $\mathrm{span}_{\mathbb{R}_{\geq 0}}(v_{i+1}, v_{i+2})$ describe particular cyclic quotient singularities, and understanding the corresponding matrices M_i, we create restrictions on when $M_k M_{k-1} \cdots M_1 = Id$ can hold.

Start with the simple case of a polygon P consisting entirely of $\frac{1}{3}(1,1)$ cones. Note we already know exactly one such polygon exists by Kasprzyk–Nill–Prince [48] and Theorem 2.5.18. Let E be an edge of P, that is, E is a $\frac{1}{3}(1,1)$

cone. Without loss of generality, E has vertices $(-1,3)$ and $(-2,3)$. Further consider the edge adjacent to E sharing the vertex $(-2,3)$, also a $\frac{1}{3}(1,1)$ cone. The corresponding matrix $M \in GL(N)$ satisfies:

$$M \begin{pmatrix} -1 \\ 3 \end{pmatrix} = \begin{pmatrix} -2 \\ 3 \end{pmatrix}, \qquad \text{and} \qquad \det(M) = 1.$$

The condition $\det(M) = 1$ follows from the fact that M maps a $\frac{1}{3}(1,1)$ cone onto a $\frac{1}{3}(1,1)$ cone, and so lattice length and lattice height must be preserved. Implementing these conditions shows M is of the form:

$$M = \begin{pmatrix} 3-2a & \frac{1-2a}{3} \\ 3a-3 & a \end{pmatrix}, \qquad \text{for some } a \in \mathbb{Z}.$$

The only remaining restriction is that $(1-2a)/3 \in \mathbb{Z}$ and so $a \equiv 2 \pmod 3$. Substituting $a = 3n+2$, obtain the set of matrices:

$$A_n := \begin{pmatrix} -6n-1 & -2n-1 \\ 9n+3 & 3n+2 \end{pmatrix}, \qquad \text{where } n \in \mathbb{Z}.$$

The image of the point $(-2,3)$ under A_n, that is the second vertex of the second $\frac{1}{3}(1,1)$ cone, is given by:

$$A_n \begin{pmatrix} -2 \\ 3 \end{pmatrix} = \begin{pmatrix} 6n-1 \\ -9n \end{pmatrix}.$$

Note if $n < 0$, convexity of the Fano polygon is broken. Therefore we have a 1-dimensional family of suitable matrices parametrised by $\mathbb{Z}_{\geq 0}$ each giving a point v such that $\operatorname{span}_{\mathbb{R}_{\geq 0}}((-2,3), v)$ is a cone representing a $\frac{1}{3}(1,1)$ singularity. For example:

$$
\begin{aligned}
n = 0 &\longleftrightarrow \begin{pmatrix} -1 \\ 0 \end{pmatrix}, \\
n = 1 &\longleftrightarrow \begin{pmatrix} 5 \\ -9 \end{pmatrix}, \\
n = 2 &\longleftrightarrow \begin{pmatrix} 11 \\ -18 \end{pmatrix}, \\
&\vdots
\end{aligned}
$$

Lemma 5.1.1. A Fano polygon consisting only of $\frac{1}{3}(1,1)$ R-cones satisfies:

$$M_k M_{k-1} \cdots M_1 = A_{n_1} A_{n_2} \cdots A_{n_k}.$$

Proof. We have that:

$$
\begin{aligned}
M_1 =& A_{n_1}, \\
M_2 =& M_1 A_{n_2} M_1^{-1} = A_{n_1} A_{n_2} A_{n_1}^{-1}, \\
M_3 =& M_2 M_1 A_{n_2} M_1^{-1} M_2^{-1} = A_{n_1} A_{n_2} A_{n_3} A_{n_2}^{-1} A_{n_1}^{-1}, \\
&\vdots \\
M_i =& A_{n_1} A_{n_2} \cdots A_{n_{i-1}} A_{n_i} A_{n_{i-1}}^{-1} \cdots A_{n_2}^{-1} A_{n_1}^{-1}.
\end{aligned}
$$

The desired identity then follows by substitution. □

The problem remains to test when the identity $A_{n_1}A_{n_2}\cdots A_{n_k} = Id$ holds. First consider multiplication of the matrices A_{n_i} modulo 3:

$$\begin{aligned}
A_{n_1} &\equiv \begin{pmatrix} 2 & n_1+2 \\ 0 & 2 \end{pmatrix} \pmod 3\,, \\
A_{n_1}A_{n_2} &\equiv \begin{pmatrix} 2 & n_1+2 \\ 0 & 2 \end{pmatrix} \begin{pmatrix} 2 & n_2+2 \\ 0 & 2 \end{pmatrix} \\
&\equiv \begin{pmatrix} 1 & 2n_1+2n_2+1 \\ 0 & 1 \end{pmatrix} \pmod 3\,, \\
A_{n_1}A_{n_2}A_{n_3} &\equiv \begin{pmatrix} 1 & 2n_1+2n_2+1 \\ 0 & 1 \end{pmatrix} \begin{pmatrix} 2 & n_3+2 \\ 0 & 2 \end{pmatrix} \\
&\equiv \begin{pmatrix} 2 & n_1+n_2+n_3+1 \\ 0 & 2 \end{pmatrix} \pmod 3\,, \\
&\;\vdots
\end{aligned}$$

Note that the multiplication of three A_{n_i} matrices can never equal the identity matrix modulo 3, since the upper left entry of $A_{n_1}A_{n_2}A_{n_3}$ is $2 \not\equiv 1 \pmod 3$. Indeed note $A_{n_1}A_{n_2}A_{n_3} \equiv A_{n_1+n_2+n_3-1} \pmod 3$, and then by induction the identity $A_{n_1}A_{n_2}\cdots A_{n_k} = Id$ cannot hold when k is odd. Therefore we assume k is even. Looking at the multiplication of A_{n_i} matrices modulo 9 further narrows down the possibilities for k. Calculate that:

$$\begin{aligned}
A_{n_1}A_{n_2} &\equiv \begin{pmatrix} * & * \\ 6 & * \end{pmatrix} \not\equiv Id \pmod 9\,, \\
A_{n_1}A_{n_2}A_{n_3}A_{n_4} &\equiv \begin{pmatrix} * & * \\ 3 & * \end{pmatrix} \not\equiv Id \pmod 9\,.
\end{aligned}$$

Therefore the smallest possible value of k satisfying $A_{n_1}A_{n_2}\cdots A_{n_k} = Id$ is 6.

To finish the argument, we use the fact that for a Fano polygon, its boundary is a closed loop that wraps around the origin once. We shall use the winding number defined by Poonen–Rodriguez-Villegas [61]:

Considering $SL_2(\mathbb{R})$ as a topological space, the fundamental group is given by $\pi_1\left(SL_2(\mathbb{R})\right) = \mathbb{Z}$. The universal cover, denoted $\widetilde{SL_2(\mathbb{R})}$, is the connected topological group fitting into the exact sequence:

$$0 \longrightarrow \mathbb{Z} \longrightarrow \widetilde{SL_2(\mathbb{R})} \longrightarrow SL_2(\mathbb{R}) \longrightarrow 0.$$

There is no description of $\widetilde{SL_2(\mathbb{R})}$ as a group of matrices subject to a set of algebraic conditions. The commonly used description for $\widetilde{SL_2(\mathbb{R})}$ is that of pairs $(M, [\gamma])$, where:

$$M = \begin{pmatrix} a & b \\ c & d \end{pmatrix} \in SL_2(\mathbb{R}),$$

and $[\gamma]$ is a homotopy equivalence class of paths in $\mathbb{R}^2 \backslash \{\mathbf{0}\}$ from $(0, 1)$ to (c, d). It follows that $\widetilde{SL_2(\mathbb{R})}$ has the structure of a group via the composition law:

$$(M_1, [\gamma_1]) \cdot (M_2, [\gamma_2]) = (M_1 M_2, [M_1(\gamma_2) \star \gamma_1]),$$

where $\star$ denotes concatenation.

Define $\widetilde{SL_2(\mathbb{Z})}$ to be the inverse image of $SL_2(\mathbb{Z})$ under the map $\widetilde{SL_2(\mathbb{R})} \to SL_2(\mathbb{R})$. Note this is not a covering space of $SL_2(\mathbb{Z})$ since it is not a connected topological space. Lift each matrix A_{n_i} to $\widetilde{SL_2(\mathbb{Z})}$ by equipping it with the appropriate straight line path denoted γ_i. The algebraic condition $A_{n_1} A_{n_2} \ldots A_{n_k} = Id$ lifted to $\widetilde{SL_2(\mathbb{R})}$, then becomes:

$$(A_{n_1}, [\gamma_1]) \cdot (A_{n_2}, [\gamma_2]) \cdot \cdots \cdot (A_{n_k}, [\gamma_k]) = (Id, [\text{anticlockwise loop}]). \quad (4)$$

In [61], a homomorphism $\Phi : \widetilde{SL_2(\mathbb{Z})} \to \mathbb{Z}$ is introduced to act as a winding number. The aim is to apply Φ to both sides of equation (4) to obtain an extra condition on k.

Similarly to how $SL_2(\mathbb{Z})$ is generated by:

$$S = \begin{pmatrix} 0 & -1 \\ 1 & 0 \end{pmatrix}, \qquad \text{and} \qquad T = \begin{pmatrix} 1 & 1 \\ 0 & 1 \end{pmatrix},$$

it is known that $\widetilde{SL_2(\mathbb{Z})}$ is generated by the two elements $\tilde{S}$ and $\tilde{T}$ obtained from lifting S and T to $\widetilde{SL_2(\mathbb{R})}$ by equipping them with the straight line path from $(0,1)$ to $(1,0)$ and the trivial path respectively. Furthermore it is shown in [61] that:

$$\Phi(\tilde{S}) = -3, \qquad \text{and} \qquad \Phi(\tilde{T}) = 1.$$

It is routine to check that $(\tilde{S})^4 = (Id, [\text{anticlockwise loop}])$ and so

$$\Phi\left(Id, [\text{anticlockwise loop}]\right) = -12.$$

It remains to calculate $\Phi\left(A_{n_i}, [\gamma_i]\right)$. By using an algorithm of Conrad [26], we obtain the expression:

$$A_{n_i} = TS^{-1}T^{-2}S^{-1}T^{-(n_i+1)}ST^{-3}.$$

After lifting to $\widetilde{SL_2(\mathbb{Z})}$ and applying the winding number homomorphism we obtain:

$$\Phi\left(A_{n_i}, [\gamma_i]\right) = -2 - n_i.$$

Therefore applying Φ to both sides of (4) gives the expression:

$$\sum_{i=1}^{k} n_i = 12 - 2k.$$

If $k > 6$ this implies $\sum\limits_{i=1}^{k} n_i < 0$, but convexity determines that $n_i \geq 0$ and so there are no solutions. The only remaining case is $k = 6$, for which the equation becomes:

$$\sum_{i=1}^{k} n_i = 0.$$

Therefore there is a single possible solution given by $k = 6$ and $n_i = 0$. This recovers the known Fano polygon consisting of six $\frac{1}{3}(1,1)$ R-cones shown in Figure 10.

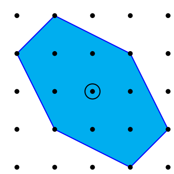

Figure 10: Fano polygon with singularity content $\left(0, \left\{6 \times \frac{1}{3}(1,1)\right\}\right)$.

We now generalise our approach to consider a Fano polygon consisting only of $\frac{1}{r}(1,1)$ cones, for some fixed value of $r \in \mathbb{Z}_{>0} \backslash \{1,2,4\}$.

Theorem 5.1.2. There are no Fano polygons with singularity content:

$$\left(0, \left\{k \times \frac{1}{r}(1,1)\right\}\right), \qquad \text{where } k \in \mathbb{Z}_{>0}, r \in \mathbb{Z}_{\geq 5}.$$

Proof. Suppose such a Fano polygon exists. First assume r odd. Consider the standard position of the $\frac{1}{r}(1,1)$ cone to have vertices $(-(r+1)/2, r)$ and $(-(r-1)/2, r)$. Then we consider a matrix $M \in GL(N)$ such that:

$$M \begin{pmatrix} -\frac{r-1}{2} \\ r \end{pmatrix} = \begin{pmatrix} -\frac{r+1}{2} \\ r \end{pmatrix}, \qquad \text{and} \qquad \det(M) = 1.$$

Therefore M takes the form:

$$M = \begin{pmatrix} \frac{-ar-a+2r}{r-1} & \frac{r-ar-a-1}{2r} \\ \frac{2r(a-1)}{r-1} & a \end{pmatrix}.$$

The entries of M belong to $\mathbb{Z}$ if and only if:

$$a \equiv 1 \pmod{(r-1)/2}, \qquad \text{and} \qquad a \equiv -1 \pmod{r}.$$

This implies that $a = 2r - 1 + n((r-1)r)/2$ for some $n \in \mathbb{Z}$. Making this substitution gives M of the form:

$$A_n^{(r)} := \begin{pmatrix} -n\frac{r+1}{2}r - 2r - 1 & -n\frac{r^2-1}{4} - r \\ nr^2 + 4r & 2r - 1 + n\frac{r-1}{2}r \end{pmatrix}, \qquad \text{where } n \in \mathbb{Z}.$$

By using a generalised version of Lemma 5.1.1, the problem is reduced to testing when the identity:

$$A_{n_1}^{(r)} A_{n_2}^{(r)} \cdots A_{n_k}^{(r)} = Id, \tag{5}$$

can hold. Studying $A_{n_i}^{(r)}$ modulo r:

$$A_{n_1}^{(r)} \equiv \begin{pmatrix} -1 & -(\frac{r^2-1}{4})n_1 \\ 0 & -1 \end{pmatrix} \not\equiv Id \pmod{r},$$

$$A_{n_1}^{(r)} A_{n_2}^{(r)} \equiv \begin{pmatrix} 1 & \frac{r^2-1}{4}(n_1+n_2) \\ 0 & 1 \end{pmatrix} \equiv Id, \qquad \text{if } n_1+n_2 \equiv 0 \pmod{r},$$

$$A_{n_1}^{(r)} A_{n_2}^{(r)} A_{n_3}^{(r)} \equiv \begin{pmatrix} -1 & -\frac{r^2-1}{4}(n_1+n_2+n_3) \\ 0 & -1 \end{pmatrix} \equiv A_{n_1+n_2+n_3}^{(r)} \not\equiv Id \pmod{r}.$$

Continuing inductively shows there cannot be a solution if k is odd as in the case $r = 3$. Furthermore for k even, the identity $A_{n_1}^{(r)} A_{n_2}^{(r)} \cdots A_{n_k}^{(r)} = Id$ holds if and only if $\sum_{i=1}^{k} n_i \equiv 0 \pmod{r}$. Alternatively studying a product of $A_{n_i}^{(r)}$ matrices modulo r^2, observe that:

$$\prod_{i=1}^{k} A_{n_i}^{(r)} \equiv \begin{pmatrix} * & * \\ (-1)^k 4kr & * \end{pmatrix} \left(\operatorname{mod} r^2\right),$$

and so $A_{n_1}^{(r)} A_{n_2}^{(r)} \cdots A_{n_k}^{(r)} = Id$ holds only if k is a multiple of r. Therefore the smallest possible value for k in (5) is $2r$. Finally, appealing to the winding number argument as in the case $r = 3$, calculate by [26] that:

$$A_n^{(r)} = TS^{-1}(T^{-2}S^{-1})^{\frac{r-3}{2}} T^{-2} S^{-1} T^{-(n+2)} S^{-1} (T^{-2}S^{-1})^{\frac{r-5}{2}} T^{-2} S T^{-3},$$

and so $\Phi\left(A_n^{(r)}, [\gamma_i]\right) = -6 + r - n$. Applying Φ to (5) obtain:

$$\sum_{i=1}^{k} n_i = 12 - (r-6)\, k.$$

Since k must be a multiple of $2r$, and $\sum_{i=1}^{k} n_i$ must be congruent to 0 modulo r:

$$12 \equiv 0 \pmod{r}.$$

This implies $r \mid 12$ and since r is odd and greater or equal 5, there are no solutions. The case where r is even follows similarly. □

Note that $r = 3$ satisfies the congruence $12 \equiv 0 \pmod{r}$ corresponding to the fact that there is a solution in this case.

5.2 RESTRICTIONS USING CONTINUED FRACTIONS

In this section, we use results on continued fractions to provide a second example of a singularity content that cannot occur for a Fano polygon. The geometry of continued fractions can be studied in Karpenkov [46].

Definition 5.2.1. Given $a_0, a_1, \cdots, a_k \in \mathbb{R}$, define the *continued fraction* by:

$$[a_0 : a_1 : \cdots : a_k] := a_0 + \cfrac{1}{a_1 + \cfrac{1}{a_2 + \cfrac{1}{\dots + \frac{1}{a_k}}}}.$$

The numbers a_i are called the *elements* of the continued fraction. A continued fraction is *odd/even* if there are an odd/even number of elements.

It is worth noting the difference between a continued fraction and the Hirzeburch-Jung continued fraction of Section 3.1.

There uniquely exist polynomials P_k and Q_k in variables a_i satisfying:

$$[a_0 : a_1 : \cdots : a_k] = \frac{P_k(a_0, \dots, a_k)}{Q_k(a_0, \dots, a_k)}, \qquad \text{and} \qquad P_k(0, \dots, 0) + Q_k(0, \dots, 0) = 1.$$

The first few of these polynomials are:

$$[a_0] = \frac{P_0(a_0)}{Q_0(a_0)} = \frac{a_0}{1},$$
$$[a_0 : a_1] = \frac{P_1(a_0, a_1)}{Q_1(a_0, a_1)} = \frac{a_0 a_1 + 1}{a_1},$$
$$[a_0 : a_1 : a_2] = \frac{P_2(a_0, a_1, a_2)}{Q_2(a_0, a_1, a_2)} = \frac{a_0 a_1 a_2 + a_0 + a_2}{a_1 a_2 + 1}.$$

The polynomials P_k and Q_k satisfy the recursions:

$$P_k = a_k P_{k-1} + P_{k-2}, \qquad \text{and} \qquad Q_k = a_k Q_{k-1} + Q_{k-2}.$$

Continued fractions have applications to integer geometry.

Definition 5.2.2 ([46, Definition 2.7])**.** Consider an integer triangle ΔABC, that is a triangle whose vertices are the integer points A, B and C. The *integer area* of ΔABC, denoted $l\text{Area}(\Delta ABC)$, is given by the index of the sublattice generated by the line segments AB and AC thought of as vectors in the integer lattice.

Definition 5.2.3 ([46, Definition 4.1])**.** Consider an integer angle $\angle ABC$, that is an angle between two integer lines; the line through the primitive line segment AB and similarly the line through BC, based at the integer point B. The *integer sine* of $\angle ABC$, denoted $l\sin(\angle ABC)$, is given by:

$$l\sin(\angle ABC) := \frac{l\text{Area}(\Delta ABC)}{l(AB)l(BC)}.$$

Note that the integer sine is independent of the orientation of the integer angle, that is, $l\sin(\angle ABC) = l\sin(\angle CBA)$.

Definition 5.2.4 ([46, Definition 11.1])**.** A *broken line* is defined by $L = A_0 A_1 \cdots A_n = \bigcup_{i=0}^{n-1} L_i$, where L_i is the line segment between the integer points A_i and A_{i+1}. Let L be an integer broken line that does not contain the origin $\mathbf{0} \in \mathbb{Z}^2$. If all the line segments L_i are at lattice height 1, then L is called an $\mathbf{0}$-*broken line*.

Definition 5.2.5 ([46, Definition 11.2])**.** Let $A_0A_1 \cdots A_n$ be an $\mathbf{0}$-broken line. Associate to the broken line its *lattice-signed-length-sine (LSLS) sequence* given by $(a_0, a_1, \ldots, a_{2n-2})$ where

$$\begin{aligned}
a_0 &:= \operatorname{sign}(A_0\mathbf{0}A_1) \cdot l(A_0A_1),\\
a_1 &:= \operatorname{sign}(A_0\mathbf{0}A_1) \cdot \operatorname{sign}(A_1\mathbf{0}A_2) \cdot \operatorname{sign}(A_0A_1A_2) \cdot l\sin(\angle A_0A_1A_2),\\
a_2 &:= \operatorname{sign}(A_1\mathbf{0}A_2) \cdot l(A_1A_2),\\
&\vdots\\
a_{2n-3} &:= \operatorname{sign}(A_{n-2}\mathbf{0}A_{n-1}) \cdot \operatorname{sign}(A_{n-1}\mathbf{0}A_n) \cdot\\
&\qquad \operatorname{sign}(A_{n-2}A_{n-1}A_n) \cdot l\sin(\angle A_{n-2}A_{n-1}A_n),\\
a_{2n-2} &:= \operatorname{sign}(A_{n-1}\mathbf{0}A_n) \cdot l(A_{n-1}A_n),
\end{aligned}$$

and $\operatorname{sign}(ABC)$ is defined for arbitrary integer points A, B, C by:

$$\operatorname{sign}(ABC) := \begin{cases} 1, & \text{if } (BA, BC) \text{ is orientated positively;}\\ 0, & \text{if } A, B, C \text{ are collinear;}\\ -1, & \text{if } (BA, BC) \text{ is orientated negatively.} \end{cases}$$

Given an $\mathbf{0}$-broken line the LSLS sequence measures alternatively the lattice length of the line segments and lattice sine of the angles as we travel along the broken line, up to some change in sign for each value. Since lattice length and lattice sign are invariant under $GL_2(\mathbb{Z})$ transformations, so is the LSLS sequence of an $\mathbf{0}$-broken line.

A strong link between LSLS sequences of $\mathbf{0}$-broken lines and continued fractions is made via the following theorem from [46]:

Theorem 5.2.6 ([46, Theorem 11.10])**.** Consider an $\mathbf{0}$-broken line $A_0 \ldots A_n$ with LSLS sequence $(a_0, a_1, \ldots, a_{2n})$. Suppose also $A_0 = (1, 0)$ and $A_1 = (1, a_0)$. Then:

$$A_n = \left(Q_{2n+1}(a_0, a_1, \ldots, a_{2n}), P_{2n+1}(a_0, a_1 \ldots, a_{2n})\right).$$

Corollary 5.2.7 ([46, Corollary 11.14])**.** Consider a broken line $A_0A_1 \cdots A_n$ with the LSLS sequence $(a_0, a_1, \ldots, a_{2n})$. Then the broken line is closed if and only if:

$$P_{2n+1}(a_0, a_1, \ldots, a_{2n}) = 0, \qquad \text{and} \qquad Q_{2n+1}(a_0, a_1, \ldots, a_{2n}) = 1.$$

Let C be the cone over an edge of a Fano polygon $P \subseteq N_{\mathbb{R}}$.

Definition 5.2.8. The *sail* $S(C)$ of C is given by $\operatorname{conv}(C \backslash \{\mathbf{0}\} \cap N)$.

Lemma 5.2.9. The boundary $\partial S(C)$ of the sail of a cone C defines an $\mathbf{0}$-broken line.

Proof. Let $\partial S(C) = A_0A_1 \cdots A_n$. We need to show that each component L_i of the broken line is at lattice height 1. Consider the line segment L_i with vertices A_i and A_{i+1}. By the definition of $S(C)$, there are no interior points in $\operatorname{conv}\{\mathbf{0}, A_i, A_{i+1}\}$. Therefore the Euclidean area of $\operatorname{conv}\{\mathbf{0}, A_i, A_{i+1}\}$ is $1/2$ which is equivalent to the lattice height of L_i being 1. □

Using this lemma, associate to a cone an LSLS sequence.

Example 5.2.10. Consider a $\frac{1}{r}(1,1)$ R-singularity. First suppose r is even. Since $\frac{1}{2}(1,1)$ and $\frac{1}{4}(1,1)$ are T-singularities, assume $r \geq 6$. Without loss of generality, assume the $\frac{1}{r}(1,1)$ cone has ray generators $(-1, r/2)$ and $(1, r/2)$. The corresponding broken line, that is the boundary of the sail of the cone, then has integer points $(-1, r/2)$, $(0,1)$ and $(1, r/2)$ giving a LSLS sequence of $[1 : r-2 : 1]$. The odd case with $r > 3$ is treated similarly by considering the cone $C_{\frac{1}{r}(1,1)}$ with ray generators $(-(r+1)/2, r)$ and $(-(r-1)/2, r)$. The LSLS sequence is again $[1 : r-2 : 1]$.

Observe that the sum of the elements of the LSLS sequence of a $\frac{1}{r}(1,1)$ singularity is equal to r; the Gorenstein index. This is not a property that generalises to arbitrary cyclic quotient singularities. For example, consider a $\frac{1}{9}(1,2)$ cone with rays generated by $(-1,3)$ and $(2,3)$. The LSLS sequence of the cone is $[1:3:2]$; the sum of the elements is not equal to the Gorenstein index 9.

Example 5.2.11. Consider the unique Fano polygon P with six $\frac{1}{3}(1,1)$ cones. By glueing the broken line of adjacent cones together along common vertices of P, obtain a broken line associated to P and through this an LSLS sequence. It is routine to check for this example that the integer sine for the angles at each vertex of P is -1, and that the LSLS sequence satisfies:

$$\left[1:1:1:-1:1:1:1:-1:1:1:1:-1:\cdots:1:1:1\right] = \frac{0}{1}.$$

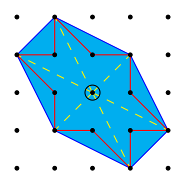

Figure 11: The broken line associated to the unique Fano polygon with singularity content $\left(0, \left\{6 \times \frac{1}{3}(1,1)\right\}\right)$.

Corollary 5.2.7 provides a test as to whether it is possible to glue together combinations of R-cones to form a Fano polygon. Namely if there exists a Fano polygon made of cones, cyclically ordered and corresponding to the cyclic quotient singularities $\frac{1}{r_1}(1,1), \frac{1}{r_2}(1,1), \ldots, \frac{1}{r_k}(1,1)$ respectively, then there is a solution to the identity:

$$[1:r_1-2:1:m_1:1:r_2-2:1:m_2:\cdots:m_{k-1}:1:r_k-2:1] = \frac{0}{1},$$

where $m_i \in \mathbb{Z}$ is the integer sine of the angle of the associated broken line lying between consecutive cones. Furthermore the convexity of the Fano polygon dictates that $m_i < 0$. Note this variable m_i is analogous to the 1-dimensional family of matrices parametrised by $\mathbb{Z}_{\geq 0}$ obtained in Section 5.1.

The association of a broken line to a polygon is not unique. The choice of starting point for the broken line may change the continued fraction of the broken line since the integer sine of the angle at this vertex is omitted from the LSLS sequence. However the choice of starting point does not affect that the associated continued fraction should evaluate to $0/1$. Indeed this condition is required to hold for all possible choices of starting point for the broken line.

Theorem 5.2.12. There are no Fano polygons with singularity content:

$$\left(0, \left\{\frac{1}{r_1}(1,1), \frac{1}{r_2}(1,1), \frac{1}{r_3}(1,1)\right\}\right), \qquad \text{where } r_i \in \{3\} \cup \mathbb{Z}_{\geq 5}.$$

Proof. If such a Fano polygon did exist, then by Corollary 5.2.7 there would be a solution $(m_1, m_2) \in \mathbb{Z}^2_{<0}$ to the following identity:

$$[1 : r_1 - 2 : 1; m_1 : 1 : r_2 - 2 : 1 : m_2 : 1 : r_3 - 2 : 1] = \frac{0}{1}.$$

By calculating the polynomials $P_{10}(a_0, \cdots, a_{10})$ and $Q_{10}(a_0, \cdots, a_{10})$ and substituting appropriately for the a_i the condition of the continued fraction translates to the simultaneous equations:

$$\begin{aligned} P_{10}(1, r_1 - 2, 1, m_1, 1, r_2 - 2, 1, m_2, 1, r_3 - 2, 1) &= \\ &Am_1m_2 + Bm_1 + Cm_2 + D = 0, \\ Q_{10}(1, r_1 - 2, 1, m_1, 1, r_2 - 2, 1, m_2, 1, r_3 - 2, 1) &= \\ &Em_1m_2 + Fm_1 + Gm_2 + H = 1, \end{aligned}$$

where:

$$
\begin{aligned}
A &= r_1r_2r_3, \\
B &= 2r_1r_2r_3 - r_1r_3 - r_2r_3, \\
C &= 2r_1r_2r_3 - r_1r_2 - r_1r_3, \\
D &= 4r_1r_2r_3 - 2r_1r_2 - 4r_1r_3 - 2r_2r_3 + r_1 + r_2 + r_3 - 12, \\
E &= r_1r_2r_3 - r_2r_3, \\
F &= 2r_1r_2r_3 - r_1r_2 - r_1r_3 - 2r_2r_3 + r_2 + r_3, \\
G &= 2r_1r_2r_3 - r_1r_3 - 3r_2r_3 + r_3, \\
H &= 4r_1r_2r_3 - 2r_1r_2 - 4r_1r_3 - 6r_2r_3 + r_1 - 3r_2 + 5r_3 + 1.
\end{aligned}
$$

Solving the simultaneous equations for m_2 gives:

$$m_2 = \frac{-(CF + DE + A - G) \pm \sqrt{(CF + DE + A - G)^2 - 4CE(DF + B - H)}}{2CE}.$$

This expression is not integer for $r_i \in \{3\} \cup \mathbb{Z}_{\geq 5}$. $\square$

5.3 RESTRICTIONS USING r-MODULAR SEQUENCES

Intuitively the *winding number* of a planar piecewise linear curve, which is defined by a sequence of points, is the number of times that the curve travels anticlockwise around the origin. In this section we adapt the formula of the winding number of a unimodular sequence proved in [41] to a more general setting, and use it to discern a new winding number formula for a Fano polygon. The new winding number is then used to find more restricted singularity contents. Indeed this section includes a stronger version of Theorem 5.1.2. The material of this section was joint work with Akihiro Higashitani [19].

Definition 5.3.1. A sequence of vectors $v_1, \ldots, v_k$, where each $v_i \in \mathbb{Z}^2$ is primitive, is said to be *r-modular* if the parallelogram $\operatorname{conv}\{\mathbf{0}, v_i, v_{i+1}, v_i + v_{i+1}\}$ contains exactly $r-1$ lattice points in its interior, for each $i \in \{1, \ldots, k\}$, where $v_{k+1} = v_1$.

Note that the case $r = 1$ is exactly the notion of unimodular sequences. Indeed this definition is equivalent to $v_i \wedge v_{i+1} = \pm r, \forall i \in \{1, \ldots, k\}$. In this vain set $\epsilon_i = \frac{v_i \wedge v_{i+1}}{r}$. This variable indicates whether the sequence is moving in an anticlockwise or clockwise direction.

As in the case of unimodular sequences, for each successive pair of vectors (v_{i-1}, v_i) and (v_i, v_{i+1}) of an r-modular sequence, there exists a matrix $M \in GL(N)$ such that:

$$\begin{pmatrix} v_i & v_{i+1} \end{pmatrix} = \begin{pmatrix} v_{i-1} & v_i \end{pmatrix} M.$$

Necessarily $\det(M) = \epsilon_{i-1}\epsilon_i$, and so M takes the form:

$$M = \begin{pmatrix} 0 & -\epsilon_{i-1}\epsilon_i \\ 1 & -\epsilon_i a_i \end{pmatrix},$$

for some $a_i \in \mathbb{Q}$. In fact, since each v_i is primitive, by taking an appropriate unimodular transformation, we can assume that:

$$v_{i-1} = \begin{pmatrix} r \\ -s \end{pmatrix}, \qquad \text{and} \qquad v_i = \begin{pmatrix} 0 \\ 1 \end{pmatrix},$$

for some $s \in \mathbb{Z}$ such that $0 \leq s < r$. Then:

$$\begin{pmatrix} v_{i-1} & v_i \end{pmatrix} M = \begin{pmatrix} r & 0 \\ -s & 1 \end{pmatrix} \begin{pmatrix} 0 & -\epsilon_{i-1}\epsilon_i \\ 1 & -\epsilon_i a_i \end{pmatrix} = \begin{pmatrix} 0 & -\epsilon_{i-1}\epsilon_i r \\ 1 & \epsilon_{i-1}\epsilon_i s - \epsilon_i a_i \end{pmatrix}.$$

Since $\epsilon_{i-1}, \epsilon_i \in \{\pm 1\}$, we conclude that $a_i \in \mathbb{Z}$.

The definition of a_i is equivalent to:

$$\epsilon_{i-1} v_{i-1} + \epsilon_i v_{i+1} + a_i v_i = \begin{pmatrix} 0 \\ 0 \end{pmatrix}. \tag{6}$$

We use a general version of a lemma used to study unimodular sequences in Higashitani–Masuda [41]. The proof of this generalised statement is identical to that of the original proof.

Lemma 5.3.2 ([41, Lemma 1.3])**.** Consider an r-modular sequence $v_1, \dots, v_k$, and let v_j be the vector among the sequence with maximal Euclidean norm. Then $a_j \in \{0, \pm 1\}$.

Theorem 5.3.3. Given an r-modular sequence $v_1, \dots, v_k$ where $k \geq 2$, its winding number is:

$$\frac{1}{12}\left(\sum_{i=1}^{k} a_i + 3\sum_{i=1}^{k} \epsilon_i\right).$$

Proof. The proof uses induction on the length of the r-modular sequence k.

For the base case $k = 2$, it is easy to see that $\epsilon_1 = -\epsilon_2$, and so from (6) that $a_1 = a_2 = 0$. The winding number is 0, and so the required identity holds trivially.

For $k = 3$, by an orientation preserving unimodular transformation assume (v_1, v_2) is equal to either $((r, -s), (0, 1))$ or $((0, 1), (r, -s))$, where $1 \leq s < r$ and $\gcd(r, s) = 1$. In both these cases since $v_2 \wedge v_3 = v_3 \wedge v_1 = \pm r$, necessarily v_3 is given by one of $(r, 1-s), (r, -1-s), (-r, 1+s)$ or $(-r, s-1)$. The desired formula can be routinely checked for each of these four possibilities.

Suppose $k \geq 4$, and that by inductive assumption all r-modular sequences with less than k vertices satisfies the desired identity. Now choose v_j to be the vertex with maximal Euclidean norm. By Lemma 5.3.2 we know $a_j \in \{0, \pm 1\}$. The inductive step is split into cases based on the value of a_j and the proof follows exactly as in [41, Theorem 1.2] from this point onwards. □

Can this statement be generalised to any sequence of integer points, that is, allowing the value $r_i = v_i \wedge v_{i+1}$ to be arbitrary for all i? A major obstacle is that when repeating the above matrix calculation for this general case, results in the conclusion that $-a_i + s\frac{r_i}{r_{i-1}} \in \mathbb{Z}$. It follows that the a_j corresponding to the vector of maximal Euclidean norm belongs to $\frac{1}{r_{j-1}}\mathbb{Z}$. The proof for Lemma

5.3.2 then adapts to tell us that $|a_j| \leq 1$, but this results in a more complicated problem when compared to the case $r_1 = r_2 = \ldots = r_k$.

We seek to provide a classification of Fano polygons consisting of cones $\{C_i\}_{i=1}^k$ such that each C_i represents a $\frac{1}{r}(1, s_i)$ cyclic quotient singularity where r is some fixed positive integer and $1 \leq s_i < r$ with $\gcd(r, s_i) = 1$, for all i. Such a cone is referred to as a determinant r cone. The key observation here is that given a Fano polygon P with determinant r cones only, then the anticlockwise ordered set of primitive ray generators of each cone, denoted $\{v_1, \ldots, v_k\}$, forms an associated r-modular sequence with winding number 1. Therefore Theorem 5.3.3 provides a condition that the vertices of the Fano polygon must satisfy.

Furthermore properties of Fano polygons translate to properties of the associated r-modular sequence:

Lemma 5.3.4. The r-modular sequence associated to a Fano polygon with determinant r cones only, has the property that $\epsilon_i = 1, \forall i$.

Proof. This is trivial since the vertices are traversed in an anticlockwise fashion. □

Lemma 5.3.5. The r-modular sequence $v_1, \ldots, v_k$ associated to a Fano polygon with determinant r cones only, has the property $a_i \geq -2, \forall i$. Furthermore the case $a_i = -2$ means that cones C_{i-1} and C_i share an edge of the Fano polygon, that is v_i does not necessarily need to be listed as a vertex.

Proof. The statement follows trivially from the identity $v_{i-1} + v_{i+1} = -a_i v_i$. □

In the case where each cone represents a $\frac{1}{r}(1, 1)$ R-singularity, it is derived in Section 5.1 that k must be a multiple of $2r$. Furthermore since all cones of P

are R-cones and so cannot share an edge with another cone, each $a_i > -2$ by Lemma 5.2.6. So for some $l \in \mathbb{Z}_{>0}$:

$$12 = \sum_{i=1}^{2rl} a_i + 3\sum_{i=1}^{2rl} \epsilon_i \geq \sum_{i=1}^{2rl}(-1) + 3\sum_{i=1}^{2rl}(1) \geq -2rl + 6rl = 4rl.$$

Therefore:

$$r \leq \frac{3}{l}.$$

Introducing r-modular sequences has provided a simpler way to complete the proof of Theorem 5.1.2 by using this identity. Namely the identity is satisfied by $(r, l) = (3, 1)$ only.

Note further that the winding number of the r-modular sequence associated to a Fano polygon P with determinant r cones only is enough to provide a statement on $\#\mathcal{V}(P)$. Assume P is a Fano polygon with $\mathcal{V}(P) = \{v_1, \ldots, v_k\}$ where all the v_i are necessary (no three consecutive vertices are collinear), and the determinant of each cone is r. Then:

$$12 = \sum_{i=1}^{k} a_i + 3\sum_{i=1}^{k} \epsilon_i \geq \sum_{i=1}^{k}(-1) + 3\sum_{i=1}^{k}(1) \geq -k + 3k = 2k.$$

So the maximum number of vertices for a Fano polygon is 6. By investigating case by case each value $k \in \{3, 4, 5, 6\}$, we construct all Fano polygons satisfying the necessary conditions allowing us to provide the classification of all Fano polygons with only cones of determinant r. For an arbitrary Fano polygon, we introduce the notation $\sigma_i = \mathrm{Cone}(v_i, v_{i+1})$.

We recall a similar notion to r-modular sequence arising from a Fano polygon.

Definition 5.3.6 ([51, Definition 1.1])**.** A Fano polygon P is ℓ-reflexive if every edge is of height ℓ.

As a natural generalisation of reflexive polygons, the class of ℓ-reflexive polygons is of great interest. Kasprzyk–Nill [51] provide a classification of ℓ-reflexive polygons for $\ell \leq 200$.

Case k = 3

By a $\mathrm{GL}(N)$-transformation, assume $v_1 = \begin{pmatrix} r \\ -s \end{pmatrix}$ where $1 \leq s < r$ with $\gcd(r,s) = 1$, and $v_2 = \begin{pmatrix} 0 \\ 1 \end{pmatrix}$. It follows that $v_3 = \begin{pmatrix} a \\ b \end{pmatrix}$ satisfies:

$$\det \begin{pmatrix} 0 & a \\ 1 & b \end{pmatrix} = r, \qquad \Longrightarrow \qquad a = -r,$$

and:

$$\det \begin{pmatrix} -r & r \\ b & -s \end{pmatrix} = r, \qquad \Longrightarrow \qquad b = s - 1.$$

So $v_3 = \begin{pmatrix} -r \\ s-1 \end{pmatrix}$, meaning $\gcd(r, s-1) = 1$ is also required. Therefore this describes a unique model for appropriate Fano polygons in the case $k = 3$.

	$\mathcal{V}(P)$	Conditions on variables	Cyclic quotient singularities
Family 1	$(-r,s-1)$, $(0,1)$, $(r,-s)$.	$\gcd(r,s)=1$, $\gcd(r,s-1)=1$.	$\sigma_1=\frac{1}{r}(1,s)$, $\sigma_2=\frac{1}{r}(1,r+1-s)$, $\sigma_3=\frac{1}{r}\left(r-(s-1)\left\lfloor\frac{r}{s}\right\rfloor,r-s\left\lfloor\frac{r}{s}\right\rfloor\right)$.

Figure 12: Unique family of Fano polygons with only determinant r cones on 3 vertices.

A model for this family of polygons is illustrated:

$k = 3,$ Family 1 :

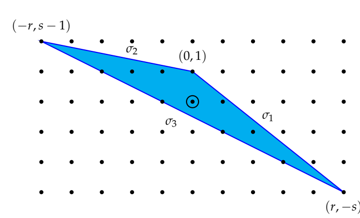

It is worth noting at this point that this classification will overlap with the classification of ℓ-reflexive polygons by Kasprzyk–Nill [51]. Not all the Fano polygons that arise in family 1 of Figure 12 are ℓ-reflexive polygons for some $\ell \in \mathbb{Z}$. Indeed if $(r,s) = (35,12)$, the polygon consists of 3 R-singularities $\frac{1}{35}(1,3)$, $\frac{1}{35}(1,17)$ and $\frac{1}{35}(1,19)$, however two edges are of height 7 and the other is of height 35.

Case $\mathbf{k} = 4$

Assume without loss of generality that:

$$v_1 = \begin{pmatrix} r \\ -s \end{pmatrix}, \qquad \text{and} \qquad v_2 = \begin{pmatrix} 0 \\ 1 \end{pmatrix}$$

where $1 \leq s < r$ and $\gcd(r,s) = 1$. As before in the case $k = 3$, if $v_3 = \begin{pmatrix} a \\ b \end{pmatrix}$, then $v_2 \wedge v_3 = r$ implies that $a = -r$. Let $v_4 = \begin{pmatrix} c \\ d \end{pmatrix}$, and by $v_4 \wedge v_1 = r$ deduce that $d = -1 - \frac{cs}{r}$. Finally v_3 and v_4 are subject to the condition:

$$\det \begin{pmatrix} -r & c \\ b & -\frac{cs}{r} - 1 \end{pmatrix} = r, \qquad \Longrightarrow \qquad c(s-b) = 0.$$

Therefore either $c = 0$ or $s = b$.

Suppose $c = 0$. In this case the vertices of P are given by:

$$v_1 = \begin{pmatrix} r \\ -s \end{pmatrix}, \qquad v_2 = \begin{pmatrix} 0 \\ 1 \end{pmatrix}, \qquad v_3 = \begin{pmatrix} -r \\ \alpha \end{pmatrix}, \qquad \text{and} \qquad v_4 = \begin{pmatrix} 0 \\ -1 \end{pmatrix}$$

where $\gcd(r,s) = \gcd(r,\alpha) = 1$. The final condition that needs checked is that the vertices satisfy convexity. This is easily checked in the language of r-modular sequences by calculating:

$$a_1 = 0, \qquad a_2 = s - \alpha, \qquad a_3 = 0, \qquad \text{and} \qquad a_4 = \alpha - s.$$

Using Lemma 5.3.5 convexity is equivalent to $a_i > -2, \forall i$, and so imposing the condition $|s - \alpha| < 2$ arising from $a_2, a_4 > -2$ is enough here. Note the case $\alpha = s - 1$ is isomorphic to the case $\alpha = s + 1$ by reflection in both axes. The cases $s = \alpha$ and $s = \alpha + 1$ provide the first two families shown in Figure 13.

Now suppose $s = b$. The vertices of P are of the form:

$$v_1 = \begin{pmatrix} r \\ -s \end{pmatrix}, \qquad v_2 = \begin{pmatrix} 0 \\ 1 \end{pmatrix}, \qquad v_3 = \begin{pmatrix} -r \\ s \end{pmatrix}, \qquad \text{and} \qquad v_4 = \begin{pmatrix} c \\ -\frac{cs}{r} - 1 \end{pmatrix}$$

where $1 \leq s < r$ and $\gcd(r, s) = 1$. Note that necessarily v_4 is an integer point, so $\frac{cs}{r} \in \mathbb{Z}$. Furthermore since $\gcd(s, r) = 1$, it follows that $r \mid c$. Set $c = \tilde{c}r$ so that:

$$v_4 = \begin{pmatrix} r\tilde{c} \\ -\tilde{c}s - 1 \end{pmatrix}.$$

It follows that:

$$a_1 = -\tilde{c}, \qquad \text{and} \qquad a_3 = \tilde{c},$$

and the convexity condition $a_i > -2, \forall i$, implies that $|\tilde{c}| \leq 1$. If $\tilde{c} = 0$, we have reduced to the previous case $c = 0$. Therefore assume that $\tilde{c} = 1$ and $v_4 = \begin{pmatrix} r \\ -s-1 \end{pmatrix}$, or $\tilde{c} = -1$ and $v_4 = \begin{pmatrix} -r \\ s-1 \end{pmatrix}$. This describes the third and fourth $k = 4$ families seen in Figure 13.

Models for each of these families are illustrated:

$k = 4,$ Family 1 :

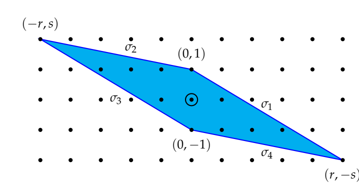

$k = 4,$ Family 2 :

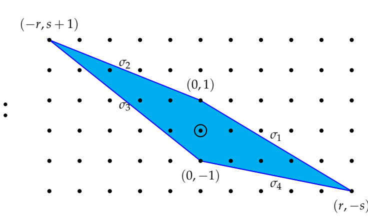

	$\mathcal{V}(P)$	Conditions on variables	Cyclic quotient singularities
Family 1	$(-r,s)$, $(0,1)$, $(r,-s)$, $(0,-1)$.	$1 \leq s < r$, $\gcd(r,s)=1$.	$\sigma_1=\frac{1}{r}(1,s)$, $\sigma_2=\frac{1}{r}(1,r-s)$, $\sigma_3=\frac{1}{r}(1,s)$, $\sigma_4=\frac{1}{r}(1,r-s)$
Family 2	$(-r,s+1)$, $(0,1)$, $(r,-s)$, $(0,-1)$.	$1 \leq s < r$, $\gcd(r,s)=1$, $\gcd(r,s+1)=1$.	$\sigma_1=\frac{1}{r}(1,s)$, $\sigma_2=\frac{1}{r}(1,r-1-s)$, $\sigma_3=\frac{1}{r}(1,s+1)$, $\sigma_4=\frac{1}{r}(1,r-s)$.
Family 3	$(-r,s)$, $(0,1)$, $(r,-s)$, $(r,-s-1)$.	$1 \leq s < r$, $\gcd(r,s)=1$, $\gcd(r,s+1)=1$.	$\sigma_1=\frac{1}{r}(1,s)$, $\sigma_2=\frac{1}{r}(1,r-s)$, $\sigma_3=\frac{1}{r}(r-s\left\lfloor\frac{r}{s+1}\right\rfloor,r-(s+1)\left\lfloor\frac{r}{s+1}\right\rfloor)$, σ_4 is an indeterminable R-singularity.
Family 4	$(-r,s)$, $(0,1)$, $(r,-s)$, $(-r,s-1)$.	$1 \leq s < r$, $\gcd(r,s)=1$, $\gcd(r,s-1)=1$.	$\sigma_1=\frac{1}{r}(1,s)$, $\sigma_2=\frac{1}{r}(1,r-s)$, σ_3 is an indeterminable R-singularity, $\sigma_4=\frac{1}{r}(r-(s-1)\left\lfloor\frac{r}{s}\right\rfloor,r-s\left\lfloor\frac{r}{s}\right\rfloor)$.

Figure 13: Four families of Fano polygons with only determinant r cones on 4 vertices.

$k = 4,$ Family 3 :

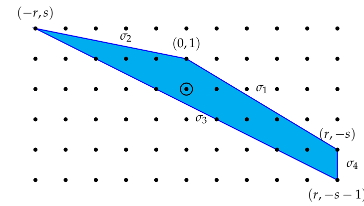

$k = 4,$ Family 4 :

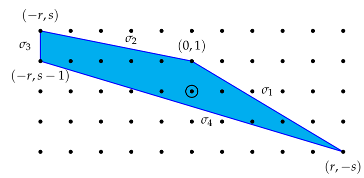

Similarly to when $k = 3$, not every Fano polygon here is ℓ-reflexive. Indeed this is not even true of any individual family: consider $(r,s) = (15,2)$ for Family 1, $(r,s) = (15,7)$ for Family 2, $(r,s) = (15,13)$ for Family 3 and $(r,s) = (15,2)$ for Family 4. Each of these four explicit Fano polygons have four R-cones which are not all of equal height.

Case k $= 5$

Assume:

$$v_1 = \begin{pmatrix} r \\ -s \end{pmatrix}, \qquad \text{and} \qquad v_2 = \begin{pmatrix} 0 \\ 1 \end{pmatrix}.$$

We then have:

$$\begin{aligned} v_2 \wedge v_3 = r \qquad &\Longrightarrow \qquad v_3 = \begin{pmatrix} -r \\ \alpha \end{pmatrix}, \\ v_3 \wedge v_4 = r \qquad &\Longrightarrow \qquad v_4 = \begin{pmatrix} r\beta \\ -\alpha\beta - 1 \end{pmatrix}, \\ v_5 \wedge v_1 = r \qquad &\Longrightarrow \qquad v_5 = \begin{pmatrix} r\gamma \\ -s\gamma - 1 \end{pmatrix} \end{aligned}$$

with the vertices further subject to the condition $v_4 \wedge v_5 = r$.

First suppose $\beta = 0$. From the equation:

$$v_3 + v_5 + a_4 v_4 = \begin{pmatrix} -r \\ \alpha \end{pmatrix} + \begin{pmatrix} r\gamma \\ -s\gamma - 1 \end{pmatrix} + a_4 \begin{pmatrix} 0 \\ -1 \end{pmatrix} = \begin{pmatrix} 0 \\ 0 \end{pmatrix},$$

obtain that necessarily $\gamma = 1$. Therefore the vertices are given by:

$$v_1 = \begin{pmatrix} r \\ -s \end{pmatrix}, \qquad v_2 = \begin{pmatrix} 0 \\ 1 \end{pmatrix}, \qquad v_3 = \begin{pmatrix} -r \\ \alpha \end{pmatrix},$$

$$v_4 = \begin{pmatrix} 0 \\ -1 \end{pmatrix}, \qquad \text{and} \qquad v_5 = \begin{pmatrix} r \\ -s-1 \end{pmatrix}.$$

Calculating that $a_2 = s - \alpha > -2$ and $a_4 = \alpha - s - 1 > -2$ implies that $\alpha \in \{s, s+1\}$. This gives rise to two families of Fano polygons, shown in Figure 14, on five vertices such that each cone has determinant r.

The case where $\gamma = 0$ is addressed similarly. The equation $v_4 + v_1 + a_5 v_5 = 0$ implies that $\beta = -1$, and so the vertices of the polygon are given by:

$$v_1 = \begin{pmatrix} r \\ -s \end{pmatrix}, \qquad v_2 = \begin{pmatrix} 0 \\ 1 \end{pmatrix}, \qquad v_3 = \begin{pmatrix} -r \\ \alpha \end{pmatrix},$$

$$v_4 = \begin{pmatrix} -r \\ \alpha - 1 \end{pmatrix}, \qquad \text{and} \qquad v_5 = \begin{pmatrix} 0 \\ -1 \end{pmatrix}.$$

The convexity conditions for a_2 and a_5 imply that $\alpha \in \{s, s+1\}$ and we obtain two more families of Fano polygons, however these are both respectively isomorphic (with some relabelling) to one of the two families that occurred when $\beta = 0$.

Having completed these two cases, instead assume $\beta, \gamma \neq 0$. The values a_i for the associated r-modular sequence are:

$$a_1 = -\gamma, \qquad a_2 = s - \alpha, \qquad a_3 = \beta,$$

$$a_4 = \frac{1-\gamma}{\beta}, \qquad \text{and} \qquad a_5 = \frac{-1-\beta}{\gamma}.$$

We split into four sub-cases:

(i) $\beta, \gamma > 0$, (ii) $\beta, \gamma < 0$,

(iii) $\beta > 0, \gamma < 0$, (iv) $\beta < 0, \gamma > 0$.

In case (i), $a_1 = -\gamma > -2$ implies that $0 < \gamma < 2$ and so $\gamma = 1$. It follows that

$$a_5 = -1 - \beta > -2 \qquad \Longrightarrow \qquad \beta < 1$$

and since $\beta > 0$, there are no possible integer solutions for case (i). Similarly in case (ii), $a_3 > -2$ implies $-2 < \beta < 0$ and so $\beta = -1$. Manipulation of a_4, gives that $\gamma > -1$ and there are no integer solutions here either.

Suppose a polygon exists in case (iii). By Theorem 5.3.3, and by calculating $a_2 = s - \alpha > -2$:

$$\begin{aligned} -3 &= 12 - 3(5) \\ &= 12 - 3\sum_{i=1}^{5} \epsilon_i \\ &= \sum_{i=1}^{5} a_i \\ &= -\gamma + (s - \alpha) + \beta + \frac{1-\gamma}{\beta} + \frac{-1-\beta}{\gamma} \\ &> 0 + (-2) + 0 + 0 + 0 \\ &= -2. \end{aligned}$$

This is an obvious contradiction and no such Fano polygon can exist.

Finally for case (iv), by the same method as in case (i) and case (ii), obtain bounds $-2 < \beta < 0 < \gamma < 2$, and hence $(\beta, \gamma) = (-1, 1)$. Calculation of the winding number of Theorem 5.3.3 reduces to $\alpha = s + 1$, and we obtain a final family in the case $k = 5$ with vertices:

$$v_1 = \begin{pmatrix} r \\ -s \end{pmatrix}, \qquad v_2 = \begin{pmatrix} 0 \\ 1 \end{pmatrix}, \qquad v_3 = \begin{pmatrix} -r \\ s+1 \end{pmatrix},$$

$$v_4 = \begin{pmatrix} -r \\ s \end{pmatrix}, \qquad \text{and} \qquad v_5 = \begin{pmatrix} r \\ -s-1 \end{pmatrix}.$$

	$\mathcal{V}(P)$	Conditions on variables	Cyclic quotient singularities
Family 1	$(-r,s+1)$, $(0,1)$, $(r,-s)$, $(0,-1)$, $(-r,s)$.	$1 \leq s < r$, $\gcd(r,s)=1$, $\gcd(r,s+1)=1$.	$\sigma_1 = \frac{1}{r}(1,s)$, $\sigma_2 = \frac{1}{r}(1,r-1-s)$, σ_3 is an indeterminable R-singularity, $\sigma_4 = \frac{1}{r}(1,s)$, $\sigma_5 = \frac{1}{r}(1,r-s)$.
Family 2	$(-r,s)$, $(0,1)$, $(r,-s)$, $(0,-1)$, $(-r,s-1)$.	$1 \leq s < r$, $\gcd(r,s)=1$, $\gcd(r,s-1)=1$.	$\sigma_1 = \frac{1}{r}(1,s)$, $\sigma_2 = \frac{1}{r}(1,r-s)$, σ_3 is an indeterminable R-singularity, $\sigma_4 = \frac{1}{r}(1,s-1)$, $\sigma_5 = \frac{1}{r}(1,r-s)$.
Family 3	$(-r,s+1)$, $(0,1)$, $(r,-s)$, $(r,-s-1)$, $(-r,s)$.	$1 \leq s < r$, $\gcd(r,s)=1$, $\gcd(r,s+1)=1$.	$\sigma_1 = \frac{1}{r}(1,s)$, $\sigma_2 = \frac{1}{r}(1,r-1-s)$, σ_3 is an indeterminable R-singularity, $\sigma_4 = \frac{1}{r}(r-s\left\lfloor\frac{r}{s+1}\right\rfloor, r-(s+1)\left\lfloor\frac{r}{s+1}\right\rfloor)$, σ_5 is an indeterminable R-singularity.

Figure 14: Three families of Fano polygons with only determinant r cones on 5 vertices.

All derived families on five vertices are shown in Figure 14.

Models for these families of polygons are also illustrated:

$k = 5$, Family 1 :

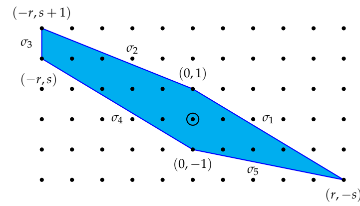

$k = 5$, Family 2 :

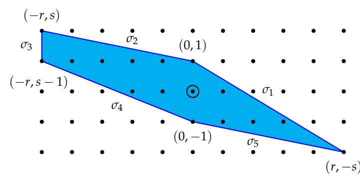

$k = 5$, Family 3 :

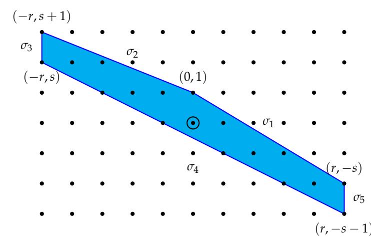

Again each family here contains a Fano polygon that has five R-cones and is not ℓ-reflexive: consider $(r, s) = (15, 7)$ for Family 1, $(r, s) = (15, 2)$ for Family 2 and $(r, s) = (15, 13)$ for Family 3.

Case $\mathbf{k} = 6$

Consider a Fano polygon on six vertices all of whose cones have determinant r. By studying the winding number equation given in Theorem 5.3.3 obtain:

$$\sum_{i=1}^{6} a_i + 3\sum_{i=1}^{6}(1) = 12, \qquad \Longrightarrow \qquad \sum_{i=1}^{6} a_i = -6.$$

Since by convexity $a_i > -2$, there is a unique solution to this equation given by $a_i = -1, \forall i$. Hence having fixed σ_1, that is, $v_1 = \begin{pmatrix} r \\ -s \end{pmatrix}$ where $1 \leq s < r$

	$\mathcal{V}(P)$	Conditions on variables	Cyclic quotient singularities
Family 1	$(-r,s+1)$, $(0,1)$, $(r,-s)$, $(r,-s-1)$, $(0,-1)$, $(-r,s)$.	$1 \leq s < r$, $\gcd(r,s)=1$, $\gcd(r,s+1)=1$.	$\sigma_1=\frac{1}{r}(1,s)$, $\sigma_2=\frac{1}{r}(1,r-1-s)$, σ_3 is an indeterminable R-singularity, $\sigma_4=\frac{1}{r}(1,s)$, $\sigma_5=\frac{1}{r}(1,r-1-s)$, σ_6 is an indeterminable R-singularity.

Figure 15: Unique familiy of Fano polygons with only determinant r cones on 6 vertices.

with $\gcd(r,s) = 1$, and $v_2 = \begin{pmatrix} 0 \\ 1 \end{pmatrix}$, all other vertices are determined by the identity:

$$\begin{pmatrix} v_i & v_{i+1} \end{pmatrix} = \begin{pmatrix} v_{i-1} & v_i \end{pmatrix} \begin{pmatrix} 0 & -1 \\ 1 & 1 \end{pmatrix}.$$

Namely

$$v_3 = \begin{pmatrix} -r \\ s+1 \end{pmatrix}, \qquad v_4 = \begin{pmatrix} -r \\ s \end{pmatrix},$$

$$v_5 = \begin{pmatrix} 0 \\ -1 \end{pmatrix}, \qquad \text{and} \qquad v_6 = \begin{pmatrix} r \\ -s-1 \end{pmatrix}.$$

Convexity is already satisfied by construction and therefore the only required conditions are that $\gcd(r,s) = \gcd(r,s+1) = 1$. This unique model for the $k = 6$ case is shown in Figure 15.

A model for this family of polygons is illustrated:

$k = 6$, Family 1 : 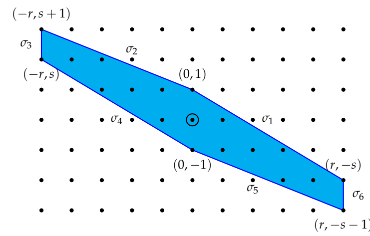

This $k = 6$ family is the only family appearing in the paper for which every entry is ℓ-reflexive for some $\ell \in \mathbb{Z}_{>0}$. More specifically the pair of conditions $\gcd(r, s) = \gcd(r, s+1) = 1$ guarentee every Fano polygon here is r-reflexive.

Each of these cases together prove the following theorem:

Theorem 5.3.7. Let $r \in \mathbb{Z}_{>0} \backslash \{1, 2, 4\}$. Any Fano polygon P with singularity content:

$$\mathrm{SC}(P) = \left(0, \left\{\frac{1}{r}(1, s_1), \frac{1}{r}(1, s_2), \ldots, \frac{1}{r}(1, s_k)\right\}\right),$$

has $k \in \{3, 4, 5, 6\}$ and vertex set unimodular equivalent to one of the following:

- $\{(0,1), (-r, s-1), (r, -s)\}$, where $\gcd(r, s) = \gcd(r, s-1) = 1$;
- $\{(0,1), (-r, s), (0, -1), (r, -s)\}$, where $\gcd(r, s) = 1$;
- $\{(0,1), (-r, s+1), (0, -1), (r, -s)\}$, where $\gcd(r, s) = \gcd(r, s+1) = 1$;
- $\{(0,1), (-r, s), (r, -s-1), (r, -s)\}$, where $\gcd(r, s) = \gcd(r, s+1) = 1$;
- $\{(0,1), (-r, s), (-r, s-1), (r, -s)\}$,
  where $\gcd(r, s) = \gcd(r, s-1) = 1$;
- $\{(0,1), (-r, s+1), (-r, s), (0, -1), (r, -s)\}$,
  where $\gcd(r, s) = \gcd(r, s+1) = 1$;
- $\{(0,1), (-r, s), (-r, s-1), (0, -1), (r, -s)\}$,
  where $\gcd(r, s) = \gcd(r, s-1) = 1$;
- $\{(0,1), (-r, s+1), (-r, s), (r, -s-1), (r, -s)\}$,
  where $\gcd(r, s) = \gcd(r, s+1) = 1$;

- $\{(0,1),(-r,s+1),(-r,s),(0,-1),(r,-s-1),(r,-s)\}$,
  where $\gcd(r,s)=\gcd(r,s+1)=1$.

In geometric terms this result is as follows:

Theorem 5.3.8. The existence of a qG-rigid orbifold del Pezzo surface that admits a toric degeneration, has topological Euler number 0 and has singular locus equal to a collection of isolated points $\left\{k \times \frac{1}{r}(1,s)\right\}$ where $r \in \mathbb{Z}_{>0} \backslash \{1,2,4\}$ is understood in terms of necessary and sufficient conditions on k, r, s. These conditions are listed in Theorem 5.3.7.

Given Theorem 5.3.7 we can provide a classification of Fano polygons with singularity content of the form $\left(0, \left\{k \times \frac{1}{r}(1,s)\right\}\right)$. Since the cone $C_{\frac{1}{r}(1,s)}$ has determinant r, every object in this classification will appear as one of the models above. Note any polygon appearing in this classification, arises as an l-reflexive polygon in [51]. We analyse each of the derived eight families of Fano polygons from Theorem 5.3.7 with only determinant r cones, and deduce conditions on the parameters r, s under which every cone of a family member corresponds to the same $\frac{1}{r}(1,s)$ cyclic quotient R-singularity. Note immediately that necessarily $r > 2$ since $\frac{1}{r}(1,1)$ is a T-singularity for $r \in \{1,2\}$.

We state three results that will be used repeatedly. These lemmas provide conditions on the variables r and s as to when certain collections of R-singularities will be isomorphic to each other.

Lemma 5.3.9. Fix $r \in \mathbb{Z}_{>0} \backslash \{1,2,4\}$, and $s \in \mathbb{Z}_{>0}$ such that $0 < s < r$. The cones representing the R-singularities $\frac{1}{r}(1,s)$ and $\frac{1}{r}(1,r-s\pm 1)$ are isomorphic if and only if either $s = \frac{r\pm1}{2}$, or $p \equiv 1 \pmod 6$ for all primes $p \mid r$ and $s^2 \mp s + 1 \equiv 0 \pmod r$.

Proof. There are two conditions under which the cones $C_{\frac{1}{r}(1,s)}$ and $C_{\frac{1}{r}(1,r\pm1-s)}$ are isomorphic, namely:

(i) $s = r - s \pm 1$,

(ii) $s(r-s+1) \equiv 1 \pmod r$.

In case (i) it follows trivially that $s = \frac{r\pm 1}{2}$.

Now consider case (ii):

$$s(r-s\pm 1) \equiv 1 \pmod r \qquad \Longleftrightarrow \qquad s^2 \mp s + 1 \equiv 0 \pmod r\,.$$

Techniques in number theory tell us that a quadratic congruence has a solution if and only if the square root of the discriminant of the quadratic exists in the finite field. In this case the square root of the discriminant is given by $\sqrt{(\pm 1)^2 - 4(1)(1)} = \sqrt{-3}$. It is a well known result concerning Legendre symbols that for an odd prime p, then:

$$\left(\frac{-3}{p}\right) = \begin{cases} 1, & \text{if } p \equiv 1 \pmod 3\,, \\ -1, & \text{if } p \equiv -1 \pmod 3\,. \end{cases}$$

Combining this identity with the Chinese remainder theorem (CRT) and the fact that we know r to be odd (since $\gcd(r,s) = \gcd(r, s-1) = 1$), means s exists if and only $p \equiv 1 \pmod 6$ for all primes $p \mid r$. It is not clear however how to express s in terms of r with this information. □

Lemma 5.3.10. Fix $r \in \mathbb{Z}_{>0} \backslash \{1,2,4\}$, and $s \in \mathbb{Z}_{>0}$ such that $0 < s < r$. The cones representing cyclic quotient R-singularities $\frac{1}{r}(1,s)$ and $\frac{1}{r}(1,r-s)$ are isomorphic if and only if $p \equiv 1 \pmod 4$ for all primes $p \mid r$, and $s^2 \equiv -1 \pmod r$.

Proof. The argument is similar to the proof of Lemma 5.3.9. Note that the singularities $\frac{1}{r}(1,s)$ and $\frac{1}{r}(1,r-s)$ are isomorphic if and only if either:

(i) $s = r-s$;

(ii) $s(r-s) \equiv 1 \pmod r$.

If (i) holds it follows that $r = 2s$, and since $\gcd(r,s) = 1$, that $s = 1$ and $r = 2$ which is not of interest. Therefore the cones are isomorphic R-cones if and only if $s(r-s) \equiv 1 \pmod r$, which is equivalent to the quadratic congruence:

$$s^2 \equiv -1 \pmod r .$$

Similarly to the proof of Lemma 5.3.9, we want to understand when the discriminant -1 is a square in the finite ring $\mathbb{Z}/r\mathbb{Z}$. It is well known that for an odd prime p that:

$$\left(\frac{-1}{p}\right) = \begin{cases} 1, & \text{if } p \equiv 1 \pmod 4 , \\ -1, & \text{if } p \equiv 3 \pmod 4 . \end{cases}$$

By the CRT a solution for s exists if and only if $p \equiv 1 \pmod 4$ holds for all primes dividing r. $\square$

Lemma 5.3.11. Fix $r \in \mathbb{Z}_{>0} \backslash \{1,2,4\}$, and $s \in \mathbb{Z}_{>0}$ such that $0 < s < r$. Consider three cones representing R-singularities $\frac{1}{r}(1,s)$, $\frac{1}{r}(1,r-s)$ and $\frac{1}{r}(1,r-s-1)$. Then all three cones are isomorphic if and only if $(r,s) = (5,2)$.

Proof. Suppose the three cones are isomorphic. The $\frac{1}{r}(1,s)$ and $\frac{1}{r}(1,r-1-s)$ cones imply by Lemma 5.3.9 that either $s = \frac{r-1}{2}$ or $s^2+s+1 \equiv 0 \pmod r$. Similarly the cones $\frac{1}{r}(1,s)$ and $\frac{1}{r}(1,r-s)$ imply that $s^2 \equiv -1 \pmod r$ by Lemma 5.3.10. It follows that:

$$0 \equiv s^2 + s + 1 \pmod r , \qquad \Longrightarrow \qquad s \equiv 0 \pmod r ,$$

which is not possible since $\gcd(r,s) = 1$ and $r > 2$. Hence the only remaining possibility is $s = \frac{r-1}{2}$, which means:

$$\begin{aligned} \left(\frac{r-1}{2}\right)^2 &\equiv -1 \pmod r , \\ (-1)^2 &\equiv -4 \pmod r , \\ 0 &\equiv 5 \pmod r . \end{aligned}$$

Therefore $(r,s) = (5,2)$. $\square$

It remains to analyse each family appearing in Theorem 5.3.7. We do so looking at k case by case.

Proposition 5.3.12. Fix $r \in \mathbb{Z}_{>0} \backslash \{1,2,4\}$, and $s \in \mathbb{Z}_{>0}$ such that $0 < s < r$. There exists a Fano polygon P such that

$$\mathrm{SC}(P) = \left(0, \left\{3 \times \frac{1}{r}(1,s)\right\}\right),$$

if and only if $p \equiv 1 \pmod 6$ for all primes $p \mid r$, and $s^2 - s + 1 \equiv 0 \pmod r$.

Proof. There is a unique family of Fano polygons on three vertices all of whose cones have determinant r, shown in Figure 1. Consider

$$\sigma_1 = \frac{1}{r}(1,s), \qquad \text{and} \qquad \sigma_2 = \frac{1}{r}(1, r-s+1).$$

By Lemma 5.3.9 there are two possibilies: $s = \frac{r+1}{2}$ or $s^2 - s + 1 \equiv 0 \pmod r$. Suppose $s = \frac{r+1}{2}$, and look at σ_3 under this assumption:

$$\begin{aligned}
\sigma_3 &= \frac{1}{r}\left(r + \left(1 - \frac{r+1}{2}\right)\left\lfloor \frac{r}{\frac{r+1}{2}} \right\rfloor, r - \frac{r+1}{2}\left\lfloor \frac{r}{\frac{r+1}{2}} \right\rfloor\right) \\
&= \frac{1}{r}\left(\frac{r+1}{2}, \frac{r-1}{2}\right) \\
&= \frac{1}{r}\left(1, \frac{r+1}{2}\left(\frac{r-1}{2}\right)^{-1}\right) \\
&= \frac{1}{r}\left(1, r-1\right).
\end{aligned}$$

which is a T-singularity, since it is represented by the cone $\mathrm{span}_{\mathbb{R}_{\geq 0}}((0,1),(r,1))$. Hence there is no polygon contributed to our classification here.

Alternatively consider σ_3 in the case $s^2 - s + 1 \equiv 0 \pmod r$:

$$\begin{aligned}
\sigma_3 &= \frac{1}{r}\left(r - (s-1)\left\lfloor \frac{r}{s} \right\rfloor, r - s\left\lfloor \frac{r}{s} \right\rfloor\right), \\
&\cong \frac{1}{r}\left(1, \left(r - (s-1)\left\lfloor \frac{r}{s} \right\rfloor\right)\left(r - s\left\lfloor \frac{r}{s} \right\rfloor\right)^{-1}\right), \\
&= \frac{1}{r}\left(1, *\right).
\end{aligned}$$

As previously $\sigma_3 \cong \sigma_1$ if and only if either

- $* \equiv s \pmod r$,
- $* \equiv s^{-1} \pmod r$.

We claim the first of these two alternatives always holds:

$$\begin{aligned} * &\equiv s \pmod r, \\ r - (s-1)\left\lfloor \frac{r}{s} \right\rfloor &\equiv s\left(r - s\left\lfloor \frac{r}{s} \right\rfloor\right) \pmod r, \\ -(s-1)\left\lfloor \frac{r}{s} \right\rfloor &\equiv -s^2\left\lfloor \frac{r}{s} \right\rfloor \pmod r, \\ (s^2 - s + 1)\left\lfloor \frac{r}{s} \right\rfloor &\equiv 0 \pmod r. \end{aligned}$$

which is true by our condition on s, and so $\sigma_1 \cong \sigma_2 \cong \sigma_3$ for such a choice of r and s. □

Proposition 5.3.13. Fix $r \in \mathbb{Z}_{>0} \setminus \{1, 2, 4\}$, and $s \in \mathbb{Z}_{>0}$ such that $0 < s < r$. There exists a Fano polygon P such that

$$\mathrm{SC}(P) = \left(0, \left\{4 \times \frac{1}{r}(1, s)\right\}\right),$$

if and only if $p \equiv 1 \pmod 4$ for all primes $p \mid r$, and $s^2 \equiv -1 \pmod r$. Furthermore this polygon is unique up to isomorphism, except in the case $(r, s) = (5, 2)$ where there are two non-isomorphic polygons with the described singularity content.

Proof. There are four families to analyse for $k = 4$. We check all four in turn and determine when all the cones are isomorphic as $\frac{1}{r}(1, s)$ R-cones. The first family of Fano polygons with $k = 4$ shown in Figure 13, has 4 cones representing two different singularities in total. By Lemma 5.3.10 applied to this family there is a collection of Fano polygons all of whose cones represent $\frac{1}{r}(1, s)$ singularities when $s^2 \equiv -1 \pmod r$ and $p \equiv 1 \pmod 4$ for all primes $p \mid r$.

Lemma 5.3.11 shows that the only possibility for the second family is when $(r, s) = (5, 2)$. It is routine to check that for $(r, s) = (5, 2)$ the only other remaining cone σ_3 is also isomorphic to the others, and so a single polygon arises from this family. This Fano polygon has singularity content $\left(0, \left\{4 \times \frac{1}{5}(1,2)\right\}\right)$, the same singularity content as the polygon arising when $(r,s) = (5,2)$ in family 1, however these are two non-isomorphic Fano polygons.

We now look at the third family of polygons shown in Figure 13. As in the previous family, the cones σ_1 and σ_2 representing the singularities $\frac{1}{r}(1,s)$ and $\frac{1}{r}(1,r-s)$ imply by Lemma 5.3.10, that $s^2 \equiv -1 \pmod r$ and all primes dividing r satisfy $p \equiv 1 \pmod 4$. It remains to check σ_3 and σ_4. The cone σ_3 can be written as:

$$\sigma_3 = \frac{1}{r}\left(1, \left(r - (s+1)\left\lfloor \frac{r}{s+1} \right\rfloor\right)\left(r - s\left\lfloor \frac{r}{s+1} \right\rfloor\right)^{-1}\right) = \frac{1}{r}\left(1, *\right)$$

and is isomorphic to σ_1 if and only if either:

(i) $* \equiv s \pmod r$;

(ii) $* \equiv s^{-1} \equiv -s \pmod r$.

Note in both cases that $\gcd\left(r, \left\lfloor \frac{r}{s+1} \right\rfloor\right) = 1$, since the singularity σ_3 is well-defined, and so $\left\lfloor \frac{r}{s+1} \right\rfloor$ is invertible modulo r.

Consider (ii) first:

$$\begin{aligned}
\left(r - (s+1)\left\lfloor \frac{r}{s+1} \right\rfloor\right)\left(r - s\left\lfloor \frac{r}{s+1} \right\rfloor\right)^{-1} &\equiv -s \pmod r, \\
-(s+1)\left\lfloor \frac{r}{s+1} \right\rfloor &\equiv s^2 \left\lfloor \frac{r}{s+1} \right\rfloor \pmod r, \\
-s-1 &\equiv -1 \pmod r, \\
s &\equiv 0 \pmod r.
\end{aligned}$$

This is not possible since $\gcd(s,r) = 1$, and $r > 2$.

Alternatively for (i):

$$\begin{aligned}\left(r-(s+1)\left\lfloor\frac{r}{s+1}\right\rfloor\right)\left(r-s\left\lfloor\frac{r}{s+1}\right\rfloor\right)^{-1} \equiv& s \pmod r,\\ -(s+1)\left\lfloor\frac{r}{s+1}\right\rfloor \equiv& -s^2\left\lfloor\frac{r}{s+1}\right\rfloor \pmod r,\\ -s-1 \equiv& 1 \pmod r,\\ s \equiv& -2 \pmod r.\end{aligned}$$

Therefore $s = r-2$. We require $s^2 \equiv (r-2)^2 \equiv (-2)^2 \equiv -1 \pmod r$ which implies $r = 5$ and $s = 3$. For these values, σ_4 has vertices $(5,-3)$ and $(5,-4)$ which we know to describe a $\frac{1}{5}(1,2)$ cyclic quotient singularity. Therefore $(r,s) = (5,3)$ describes a suitable Fano polygon. However it is easy to check that this polygon is isomorphic to the $k = 4$, family 2 polygon for the values $(r,s) = (5,2)$.

The fourth family of Figure 13 follows very similarly to the third. The cones σ_1 and σ_2 being isomorphic is equivalent to $s^2 \equiv -1 \pmod r$ by Lemma 5.3.10. Then $\sigma_4 = \frac{1}{r}(r-(s-1)\left\lfloor\frac{r}{s}\right\rfloor, r-s\left\lfloor\frac{r}{s}\right\rfloor)$ is isomorphic to σ_1 and σ_2 if and only if either:

(i) $r-s\left\lfloor\frac{r}{s}\right\rfloor \equiv s\left(r-(s-1)\left\lfloor\frac{r}{s}\right\rfloor\right) \pmod r$;

(ii) $r-s\left\lfloor\frac{r}{s}\right\rfloor \equiv s^{-1}\left(r-(s-1)\left\lfloor\frac{r}{s}\right\rfloor\right) \pmod r$.

Consider (ii):

$$\begin{aligned}r-s\left\lfloor\frac{r}{s}\right\rfloor \equiv& s^{-1}\left(r-(s-1)\left\lfloor\frac{r}{s}\right\rfloor\right) \pmod r,\\ -s\left\lfloor\frac{r}{s}\right\rfloor \equiv& s(s-1)\left\lfloor\frac{r}{s}\right\rfloor \pmod r,\\ -s \equiv& s^2-s \pmod r,\\ 0 \equiv& -1 \pmod r,\end{aligned}$$

which is uninteresting since we specify $r > 2$. Finally for (i):

$$\begin{aligned}
r - s\left\lfloor \frac{r}{s} \right\rfloor \equiv& s\left(r - (s-1)\left\lfloor \frac{r}{s} \right\rfloor\right) \pmod r,\\
-s\left\lfloor \frac{r}{s} \right\rfloor \equiv& -s(s-1)\left\lfloor \frac{r}{s} \right\rfloor \pmod r,\\
-s \equiv& -s^2 + s \pmod r,\\
s^2 \equiv& 2s \pmod r,\\
s \equiv& 2 \pmod r,\\
-1 \equiv s^2 \equiv& 4 \pmod r,\\
0 \equiv& 5 \pmod r.
\end{aligned}$$

Therefore either $(r, s) = (5, 2)$ for which the polygon is isomorphic to when $(r, s) = (5, 2)$ in family 2 of Figure 13, or $(r, s) = (5, 3)$ for which σ_4 is not then isomorphic to the other cones of the polygon. □

Proposition 5.3.14. For all $r \in \mathbb{Z}_{>0} \backslash \{1, 2, 4\}$, and $s \in \mathbb{Z}_{>0}$ such that $0 < s < r$, there does not exist a Fano polygon P such that

$$\mathrm{SC}(P) = \left(0, \left\{5 \times \frac{1}{r}(1, s)\right\}\right).$$

Proof. Consider the first family of Fano polygons with cones of determinant r shown in Figure 14. By Lemma 5.3.11, the only possibility is $(r, s) = (5, 2)$. The ray generators of σ_5 are now $(5, -3)$ and $(5, -2)$ and describe a $\frac{1}{5}(1, 1)$ cone which is not isomorphic to the other σ_i cones. No polygons of interest arise in the first $k = 5$ family.

Consider the second $k = 5$ family shown in Figure 14 whose analysis follows very similarly to that of the first family. An application of Lemma 5.3.9 implies $s^2 \equiv -1 \pmod r$. Additionally in order for $\sigma_1 = \frac{1}{r}(1, s)$ and $\sigma_4 = \frac{1}{r}(1, s-1)$ to be isomorphic, we require $s(s-1) \equiv 1 \pmod r$, since $s \equiv s-1 \pmod r$ will clearly not giving rise to an interesting polygon. So:

$$\begin{aligned} s(s-1) \equiv& 1 \pmod r, \\ s^2 - s \equiv& 1 \pmod r, \\ -1 - s \equiv& 1 \pmod r, \\ s \equiv& -2 \pmod r. \end{aligned}$$

We have already seen that $s \equiv -2 \pmod r$ combined with $s^2 \equiv -1 \pmod r$ leads to $(r,s) = (5,3)$. It follows though that σ_3 is not isomorphic to the other cones for these values of r and s. No suitable polygons arise here either.

There is a final remaining family for $k = 5$ shown in Figure 14. In order for $\sigma_1 = \frac{1}{r}(1,s)$ and $\sigma_2 = \frac{1}{r}(1, r-s-1)$ to be isomorphic it is required by Lemma 5.3.9 that either:

(i) $s = \frac{r-1}{2}$,

(ii) $s^2 + s + 1 \equiv 0 \pmod r$.

Studying σ_4 in (i):

$$\begin{aligned} \sigma_4 =& \frac{1}{r}\left(r - \left(\frac{r-1}{2}\right)\left\lfloor \frac{r}{\frac{r+1}{2}} \right\rfloor, r - \left(\frac{r+1}{2}\right)\left\lfloor \frac{r}{\frac{r+1}{2}} \right\rfloor\right) \\ =& \frac{1}{r}\left(\frac{r+1}{2}, \frac{r-1}{2}\right) \\ =& \frac{1}{r}\left(1, \left(\frac{r+1}{2}\right)^{-1}\left(\frac{r-1}{2}\right)\right) \\ =& \frac{1}{r}(1, r-1) \end{aligned}$$

which is a T-singularity and so is not of interest.

Alternatively in (ii) where $s^2 + s + 1 \equiv 0 \pmod r$, we can write:

$$\sigma_4 = \frac{1}{r}\left(1, \left(r - (s+1)\left\lfloor \frac{r}{s+1} \right\rfloor\right)\left(r - s\left\lfloor \frac{r}{s+1} \right\rfloor\right)^{-1}\right).$$

Suppose:

$$\begin{aligned}
\left(r-(s+1)\left\lfloor\frac{r}{s+1}\right\rfloor\right)\left(r-s\left\lfloor\frac{r}{s+1}\right\rfloor\right)^{-1} &\equiv s \pmod{r}, \\
-(s+1) &\equiv -s^2 \pmod{r}, \\
s^2-s-1 &\equiv 0 \pmod{r}.
\end{aligned}$$

However this equation alongside $s^2+s+1 \equiv 0 \pmod{r}$ implies $2s^2 \equiv 0 \pmod{r}$, and we know $r>2$ and $\gcd(r,s)=1$. Instead suppose:

$$\begin{aligned}
\left(r-(s+1)\left\lfloor\frac{r}{s+1}\right\rfloor\right)\left(r-s\left\lfloor\frac{r}{s+1}\right\rfloor\right)^{-1} &\equiv s^{-1} \equiv r-s-1 \pmod{r}, \\
-(s+1)\left\lfloor\frac{r}{s+1}\right\rfloor &\equiv (-s-1)\left(-s\left\lfloor\frac{r}{s+1}\right\rfloor\right) \pmod{r}, \\
-s-1 &\equiv s^2+s \pmod{r}, \\
s^2+2s+1 &\equiv 0 \pmod{r}, \\
s &\equiv 0 \pmod{r},
\end{aligned}$$

which we know to be contradictory. Therefore there are no cases of a Fano polygon all of whose cones represent the same R-singularity in this final family.

$\square$

Proposition 5.3.15. Fix $r \in \mathbb{Z}_{>0}\backslash\{1,2,4\}$, and $s \in \mathbb{Z}_{>0}$ such that $0<s<r$. There exists a Fano polygon P such that

$$\mathrm{SC}(P) = \left(0, \left\{6 \times \frac{1}{r}(1,s)\right\}\right),$$

if and only if either $(r,s)=(3,1)$ or $p \equiv 1 \pmod{6}$ for all primes $p \mid r$, and $s^2+s+1 \equiv 0 \pmod{r}$. Furthermore this polygon is unique up to isomorphism.

Proof. There is a unique family of Fano polygons with $k=6$ shown in Figure 15, each with 3 different isomorphism classes of cones since $\sigma_1 \cong \sigma_4$, $\sigma_2 \cong \sigma_5$ and $\sigma_3 \cong \sigma_6$. By Lemma 5.3.9, $\sigma_1 \cong \sigma_2$ if and only if either:

(i) $s = \frac{r-1}{2}$;

(ii) $s^2 + s + 1 \equiv 0 \pmod r$.

In (i), we study σ_3 and when it is isomorphic to a $\frac{1}{r}\left(1, \frac{r-1}{2}\right)$ cone. Note that here, σ_3 has ray generators $\left(-r, \frac{r+1}{2}\right)$ and $\left(-r, \frac{r-1}{2}\right)$, and hence is a $\frac{1}{r}(1,1)$ cone. Therefore σ_3 is a $\frac{1}{r}(1, \frac{r-1}{2})$ cone if and only if $r = 3$. Hence $(r,s) = (3,1)$ gives rise to a Fano polygon with six $\frac{1}{3}(1,1)$ cones which appears in the known classification of [48] and in Section 5.1. This is later discussed in Example 5.3.18.

Alternatively for (ii) when $s^2 + s + 1 \equiv 0 \pmod r$:

$$s^2 + s + 1 = nr, \text{ for some } n \in \mathbb{Z}.$$

The linear map determined by the matrix:

$$\begin{pmatrix} 1+s & r \\ -n & -s \end{pmatrix} \in \mathrm{GL}(N),$$

maps $\sigma_3 \mapsto \sigma_4$ and $\sigma_6 \mapsto \sigma_1$. Hence all the cones σ_i represent $\frac{1}{r}(1,s)$ cyclic quotient singularities. We have shown the following proposition: □

Propositions 5.3.12, 5.3.13, 5.3.14 and 5.3.15 together prove the following result:

Theorem 5.3.16. Fix $r \in \mathbb{Z}_{>0} \backslash \{1,2,4\}$ and $s,k \in \mathbb{Z}_{>0}$ such that $0 < s < r$. Then there exists a Fano polygon P such that

$$\mathrm{SC}(P) = \left(0, \left\{k \times \frac{1}{r}(1,s)\right\}\right),$$

if and only if one of the following holds:

- $k = 3$, $p \equiv 1 \pmod 6$ for all primes $p \mid r$, and $s^2 - s + 1 \equiv 0 \pmod r$;
- $k = 4$, $p \equiv 1 \pmod 4$ for all primes $p \mid r$, and $s^2 + 1 \equiv 0 \pmod r$;
- $k = 6$, $r = 3$ and $s = 1$;
- $k = 6$, $p \equiv 1 \pmod 6$ for all primes $p \mid r$, and $s^2 + s + 1 \equiv 0 \pmod r$.

Furthermore in each of these cases P is unique up to isomorphism with the exception of the case $(k,r,s) = (4,5,2)$ in which there are two non-isomorphic models for P.

In geometric terms this result is as follows:

Theorem 5.3.17. The existence of a qG-rigid orbifold del Pezzo surface that admits a toric degeneration, has topological Euler number 0 and has singular locus equal to a collection of isolated points $\left\{k \times \frac{1}{r}(1,s)\right\}$ where $r \in \mathbb{Z}_{>0}\backslash\{1,2,4\}$ is understood in terms of necessary and sufficient conditions on k,r,s. These conditions are as listed in Theorem 5.3.16.

Note that the condition $r \in \mathbb{Z}_{>0}\backslash\{1,2,4\}$ in Theorems 5.3.7, 5.3.8, 5.3.16 and 5.3.17 comes from the geometric fact that the cyclic quotient singularities $\frac{1}{1}(1,1)$, $\frac{1}{2}(1,1)$ and $\frac{1}{4}(1,1)$ and $\frac{1}{4}(1,3)$ are T-singularities and hence are smoothable on the toric variety which corresponds to a Fano polygon with the prescribed singularity content. This is made precise in the theorems by the statement that the topological Euler number is 0. From a purely combinatorial approach, we could generalise the theorems to remove this condition.

For a fixed value of r there is a significant overlap between the Fano polygons of Theorem 5.3.7 and the set of r-reflexive polygons, though neither set is contained in the other. The Fano polygons of Theorem 5.3.16 are all r-reflexive.

Example 5.3.18. Consider when $(k,r,s) = (6,3,1)$. By Theorem 5.3.16 there exists a unique polygon with singularity content $\mathrm{SC}(P) = \left(0, \left\{6 \times \frac{1}{3}(1,1)\right\}\right)$, and by Theorem 5.3.7 a model for this polygon has vertices given by:

$$\mathcal{V}(P) = \{(0,1),(-3,2),(-3,1),(0,-1),(3,-2)(3,-1)\}.$$

This polygon appears in [48] as the unique Fano polygon with singularity content of the form $\mathrm{SC}(P) = \left(n, \left\{6 \times \frac{1}{3}(1,1)\right\}\right)$ where $n \in \mathbb{Z}_{\geq 0}$, and also appears in Section 5.1 as the unique Fano polygon with singularity content of the form $\mathrm{SC}(P) = \left(0, \left\{k \times \frac{1}{r}(1,1)\right\}\right)$ where $k, r \in \mathbb{Z}_{>0}$.

6

MUTATION GRAPH OF $\mathbb{P}^1 \times \mathbb{P}^1$

6.1 MUTATION GRAPH OF WEIGHTED PROJECTIVE PLANES

Akhtar–Kasprzyk [6] efficiently describe the effect of a mutation on a weighted projective plane. This description is subsequently used to understand the graph of mutations, or *mutation graph*, of a weighted projective plane via links to Diophantine equations.

Consider a Fano triangle $P = \operatorname{conv}\{v_0, v_1, v_2\} \subset N_{\mathbb{Q}}$ such that v_0, v_1, v_2 generate the lattice N. By Borisov-Borisov [16, Proposition 2], X_P is a weighted projective space. More specifically, there exists pairwise coprime $\lambda_0, \lambda_1, \lambda_2$ such that:

$$\lambda_0 v_0 + \lambda_1 v_1 + \lambda_2 v_2 = \begin{pmatrix} 0 \\ 0 \end{pmatrix}.$$

The toric surface X_P is $\mathbb{P}(\lambda_0, \lambda_1, \lambda_2)$.

Proposition 6.1.1 ([6, Proposition 3.3, Lemma 3.8, Proposition 3.9])**.** Let X_P be the weighted projective plane $\mathbb{P}(\lambda_0, \lambda_1, \lambda_2)$. Then there exists a one-step mutation from the Fano polygon P to the Fano polygon Q representing a weighted projective plane X_Q if and only if up to relabelling $\lambda_0 \mid (\lambda_1 + \lambda_2)^2$ and $X_Q = \mathbb{P}\left(\lambda_1, \lambda_2, \frac{(\lambda_1+\lambda_2)^2}{\lambda_0}\right)$.

This is exactly the case in Example 2.5.13. Iterating this simple test and calculating weights via Proposition 6.1.1 allows the mutation graph of a weighted projective space to be computed. The mutation graph of $\mathbb{P}^2$ is shown to depth four in [6]. Here Figure 16 shows the trivalent structure of the $\mathbb{P}^2$ mutation graph: each polygon of the mutation graph can be mutated with respect to the three primitive T-singularities.

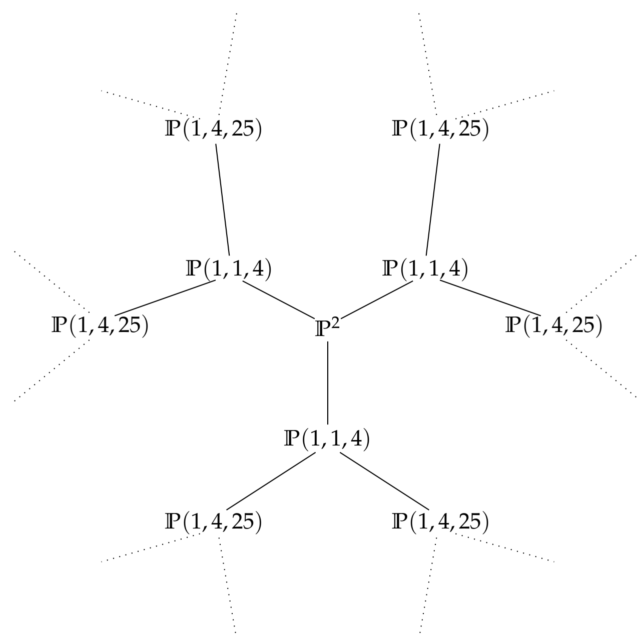

Figure 16: Mutation graph of $\mathbb{P}^2$

Figure 17 demonstrates the $\mathbb{P}^2$ mutation graph modulo isomorphism with the toric variety of each vertex shown:

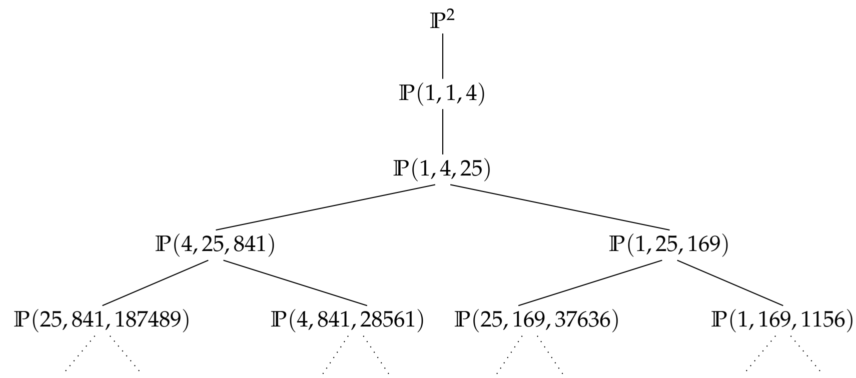

Figure 17: Mutation graph of $\mathbb{P}^2$ modulo isomorphism

For $\mathbb{P}(1,1,1)$ it does not matter which weight is chosen as λ_0 when testing for a mutation; up to reordering we obtain the weights $(1,1,4)$. Hence the vertex $\mathbb{P}^2$ in Figure 17 has valency one. This is reflected in the symmetries of the Fano polygon $P_{\mathbb{P}^2}$. Mutating the weights of $\mathbb{P}(1,1,4)$ by choosing $\lambda_0 = 4$ brings us back to $\mathbb{P}^2$. Choosing $\lambda_0 = 1$, then $\mathbb{P}(1,1,4)$ mutates to $\mathbb{P}(1,4,25)$ after relabelling. Hence the point $\mathbb{P}(1,1,4)$ has valency two. Every other point has valency three and again this is reflected in the combinatorics of the Fano polygons.

The weights that appear in the mutation graph of a weighted projective space correspond to solutions of an associated Diophantine equation.

Theorem 6.1.2 ([6, Lemma 3.11, Proposition 3.12])**.** Consider the weighted projective space $X_P = \mathbb{P}(\lambda_0, \lambda_1, \lambda_2)$. Set:

- $\lambda_i = c_i a_i^2$ where c_i is square-free, for $i \in \{0,1,2\}$;
- $\frac{(\lambda_0+\lambda_1+\lambda_2)^2}{\lambda_0\lambda_1\lambda_2} = \frac{m^2}{rk^2}$, where $m,k,r \in \mathbb{Z}_{>0}$ and r is square-free.

Then (a_0, a_1, a_2) is a solution to the Diophantine equation:

$$m x_0 x_1 x_2 = k\left(c_0 x_0^2 + c_1 x_1^2 + c_2 x_2^2\right).$$

Furthermore the weights of any mutation of P also provide a solution to the same Diophantine equation.

The proof of this theorem involves exploiting the fact that the anticanonical degree of a Fano variety is invariant under mutation.

The Diophantine equation corresponding to $\mathbb{P}^2$ is given by:

$$3x_0x_1x_2 = x_0^2 + x_1^2 + x_2^2.$$

It is routine to check that the triples (a_0, a_1, a_2) corresponding to weighted projective spaces $\mathbb{P}(a_0^2, a_1^2, a_2^2)$ appearing in Figure 17 are solutions to this Diophantine equation. For example the solutions $(1,1,1), (1,1,2)$ and $(1,2,5)$ correspond to the weighted projective planes $\mathbb{P}^2, \mathbb{P}(1,1,4)$ and $\mathbb{P}(1,4,25)$ respectively.

We aim to find analogous results for $\mathbb{P}^1 \times \mathbb{P}^1$ to those for weighted projective planes, and to gain a similar understanding of the $\mathbb{P}^1 \times \mathbb{P}^1$ mutation graph.

6.2 CLUSTER ALGEBRAS

The definition and basics of cluster algebras are recalled in this section. Cluster algebras are much more involved in the study of mutation graphs than one may initially perceive. We focus on material from Chapter 2 of the book by Marsh [55].

Let $n, m \in \mathbb{Z}_{>0}$ with $n \leq m$.

Definition 6.2.1 ([55, Definition 2.1.1])**.** A *seed* is a pair $(\tilde{u}, \tilde{B})$ where:

- $\tilde{u} = \{u_1, \ldots, u_m\}$ is a free generating set of $\mathbb{Q}(x_1, \ldots, x_m)$ over $\mathbb{Q}$;
- $\tilde{B} = (b_{i,j})_{1 \leq i \leq m, 1 \leq j \leq n}$ is an integer matrix, known as the *exchange matrix*;

- The submatrix of $\tilde{B}$ given by $B = (b_{i,j})_{1\leq i,j\leq n}$, known as the *principal part* of B, is skew-symmetric.

The elements of $\{u_1, \dots, u_n\}$ are called the *cluster variables* of the seed, and the elements of $\{u_{n+1}, \dots, u_m\}$ are called the *cluster coefficients*.

Definition 6.2.2 ([55, Definition 2.1.3])**.** Let $k \in \{1, \dots, n\}$. The *mutation* $\mu_k(\tilde{u}, \tilde{B}) = (\tilde{u'}, \tilde{B'})$ in the direction k of the seed $(\tilde{u}, \tilde{B})$, is defined as follows:

- $\tilde{u'} = \{u'_1 \dots u'_m\}$, where $u'_i = u_i$ for $i \neq k$, and u'_k satisfies the exchange relation:
$$u_k u'_k = \prod_{j\in\{1,\dots,m\}:b_{kj}>0} u_j^{b_{kj}} + \prod_{j\in\{1,\dots,m\}:b_{kj}<0} u_j^{-b_{kj}}; \tag{7}$$

- $\tilde{B'} = (b'_{i,j})_{1\leq i\leq m, 1\leq j\leq n}$ where:
$$b'_{i,j} = \begin{cases} -b_{i,j}, & \text{if } i = k \text{ or } j = k, \\ b_{i,j} + \frac{|b_{i,k}|b_{k,j} + b_{i,k}|b_{k,j}|}{2}, & \text{otherwise.} \end{cases}$$

Since $b_{k,k} = 0$ by definition, it follows that u_k does not appear on the right hand side of the exchange relation (7). The mutation terminology of this definition is not coincidental. Also note that cluster coefficients do not change under mutation but cluster variables can.

Lemma 6.2.3 ([55, Lemma 2.1.5])**.** The mutation μ_k of a seed is self-inversing, that is:
$$\mu_k^2(\tilde{u}, \tilde{B}) = (\tilde{u}, \tilde{B}).$$

Two seeds are said to be mutation equivalent if there is a sequence of mutations taking one to the other.

Definition 6.2.4 ([55, Definition 2.1.6])**.** The *cluster algebra* with initial seed $(\tilde{u}, \tilde{B})$, denoted $\mathcal{A}(\tilde{u}, \tilde{B})$, is the subring of $\mathbb{Q}(x_1, \dots, x_m)$ generated by the cluster coefficients and all the cluster variables of the seeds mutation equivalent to $(\tilde{u}, \tilde{B})$.

The principle part B of an exchange matrix can be recorded as a directed graph, known as a *quiver* and denoted $\mathcal{Q}(B)$, as follows:

- Vertices correspond to elements of $\{1, \dots, n\}$;
- If $b_{i,j} > 0$, then there are $b_{i,j}$ arrows from i to j;

Note the final point here implies by skew-symmetry that if $b_{i,j} < 0$, then there are $-b_{i,j} = b_{j,i}$ arrows from j to i. It follows that $\mathcal{Q}(B)$ will not have any loops or 2-cycles.

Lemma 6.2.5 ([55, Definition 2.3.1])**.** There is a one-to-one correspondence between $n \times n$ skew-symmetric integer matrices and quivers without loops or 2-cycles.

This association can be extended to obtaining a quiver $\mathcal{Q}(\tilde{B})$ from the whole exchange matrix $\tilde{B}$ as follows:

- Vertices correspond to elements of $\{1, \dots, m\}$;
- The subquiver on vertices $1, \dots, n$ is $\mathcal{Q}(B)$;
- For $i \in \{n+1, \dots, m\}$ and $j \in \{1, \dots, n\}$, then if $b_{i,j} > 0$ there are $b_{i,j}$ arrows from i to j and if $b_{i,j} < 0$ there are $-b_{j,i}$ arrows from j to i.

Example 6.2.6. The exchange matrix:

$$\tilde{B} = \begin{pmatrix} 0 & 0 & -2 & 2 \\ 0 & 0 & 2 & -2 \\ 2 & -2 & 0 & 0 \\ -2 & 2 & 0 & 0 \end{pmatrix},$$

corresponds to the quiver:

$$\mathcal{Q}(B) = \begin{tikzcd} v_3 \arrow[r, "2"] & v_1 \arrow[d, "2"] \\ v_2 \arrow[u, "2"] & v_4 \arrow[l, "2"] \end{tikzcd}$$

The notion of mutation can be defined for these quivers such that a mutation of an exchange matrix corresponds to a mutation of a quiver.

Definition 6.2.7 ([55, Definition 2.3.2])**.** The mutation of a quiver at a vertex v_k, for $k \in \{1, \dots n\}$, is defined by the following steps:

(i) For all paths $v_i \to v_k \to v_j$, counted up to multiplicity, add an arrow from $v_i \to v_j$;

(ii) Cancel a maximal set of disjoint 2-cycles that now exist;

(iii) All arrows incident with v_k are reversed.

Note we do not allow ourselves to mutate with respect to a vertex $v_k \in \{v_{n+1}, \dots, v_m\}$. These are known as *frozen vertices*.

Example 6.2.8. We mutate the exchange matrix of Example 6.2.6 in direction 1, and the corresponding quiver with respect to v_1:

$$\begin{tikzcd}
\begin{pmatrix} 0 & 0 & -2 & 2 \\ 0 & 0 & 2 & -2 \\ 2 & -2 & 0 & 0 \\ -2 & 2 & 0 & 0 \end{pmatrix} \arrow[r, leftrightarrow] \arrow[d, mapsto, "\mu_1"] & \begin{tikzcd}[ampersand replacement=\&] v_3 \arrow[r, "2"] \& v_1 \arrow[d, "2"] \\ v_2 \arrow[u, "2"] \& v_4 \arrow[l, "2"] \end{tikzcd} \arrow[d, mapsto, "\mu_1"] \\
\begin{pmatrix} 0 & 0 & 2 & -2 \\ 0 & 0 & 2 & -2 \\ -2 & -2 & 0 & 4 \\ 2 & 2 & -4 & 0 \end{pmatrix} \arrow[r, leftrightarrow] & \begin{tikzcd}[ampersand replacement=\&] v_3 \arrow[dr, "4"] \& v_1 \arrow[l, "2"'] \\ v_2 \arrow[u, "2"] \& v_4 \arrow[l, "2"] \arrow[u, "2"'] \end{tikzcd}
\end{tikzcd}$$

Lemma 6.2.9 ([48, Proposition 3.17])**.** Let $\tilde{B}$ be an exchange matrix. Then:

$$\mathcal{Q}\left(\mu_k(\tilde{B})\right) = \mu_k\left(\mathcal{Q}(B)\right).$$

It follows that a cluster algebra can be defined using a quiver as opposed to an exchange matrix. This is of vital importance when quivers are associated to Fano polygons in Section 6.4.

Definition 6.2.10 ([55, Definition 2.5.1])**.** The *mutation graph of a cluster algebra* is defined as having vertices corresponding to seeds, and edges corresponding to mutations.

Example 6.2.11. Consider the following mutation graph of a cluster algebra which has only finitely many seeds:

$$\begin{tikzcd}
 & \left(\{x_1, x_2, x_3, x_4\} \quad , \quad \begin{pmatrix} 0 & 1 \\ -1 & 0 \\ 1 & 0 \\ 0 & 1 \end{pmatrix}\right) \arrow[dl, dash] \arrow[dr, dash] & \\
\left(\left\{\frac{x_1x_4+1}{x_2}, x_1, x_3, x_4\right\} \quad , \quad \begin{pmatrix} 0 & 1 \\ -1 & 0 \\ 0 & 1 \\ -1 & 0 \end{pmatrix}\right) \arrow[d, dash] & & \left(\left\{\frac{x_2+x_3}{x_1}, x_2, x_3, x_4\right\} \quad , \quad \begin{pmatrix} 0 & -1 \\ 1 & 0 \\ -1 & 1 \\ 0 & 1 \end{pmatrix}\right) \arrow[d, dash] \\
\left(\left\{\frac{x_1x_4+1}{x_2}, \frac{x_1x_3x_4+x_2+x_3}{x_1x_2}, x_3, x_4\right\} \quad , \quad \begin{pmatrix} 0 & -1 \\ 1 & 0 \\ 0 & -1 \\ -1 & 0 \end{pmatrix}\right) \arrow[rr, dash] & & \left(\left\{\frac{x_2+x_3}{x_1}, \frac{x_1x_3x_4+x_2+x_3}{x_1x_2}, x_3, x_4\right\} \quad , \quad \begin{pmatrix} 0 & 1 \\ -1 & 0 \\ 0 & -1 \\ 1 & -1 \end{pmatrix}\right)
\end{tikzcd}$$

It follows from the association of a quiver to a Fano polygon that the mutation graph of a Fano polygon describes exactly a cluster algebra, and so the classification of the $\mathbb{P}^1 \times \mathbb{P}^1$ mutation graph is equivalent to calculating the cluster algebra associated to $\mathbb{P}^1 \times \mathbb{P}^1$.

6.3 MUTATION GRAPH OF $\mathbb{P}^1 \times \mathbb{P}^1$

Consider the Fano polygon $P_{\mathbb{P}^1\times\mathbb{P}^1}$ which has four primitive T-cones labelled a, b, c, d each lying on a distinct edge. Hence there are four possible one-step mutations that can be applied to $P_{\mathbb{P}^1\times\mathbb{P}^1}$.

$P_{\mathbb{P}^1\times\mathbb{P}^1} =$ 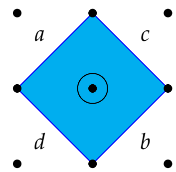

First we try to find the underlying shape of the mutation graph of $\mathbb{P}^1 \times \mathbb{P}^1$, similar to that of $\mathbb{P}^2$ in Figure 16. If we ignore isomorphisms of Fano polygons within the graph, then at every node there are four mutations that can be applied, all of which are self-inversing. The mutation graph is the free product of four copies of $\mathbb{Z}/2\mathbb{Z}$ as shown in Figure 18.

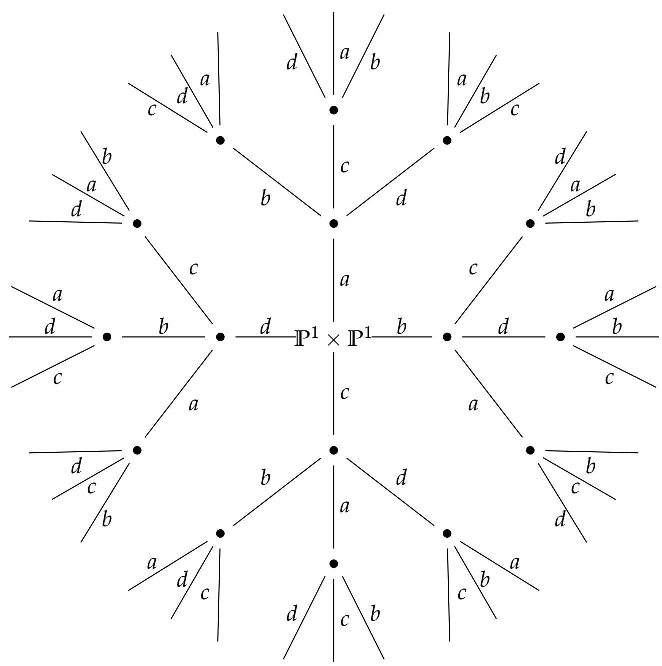

Figure 18: Mutation graph of $\mathbb{P}^1 \times \mathbb{P}^1$ without isomorphic equivalence

By abuse of notation, we often refer to a to mean the mutation of a polygon with respect to the T-cone a, and likewise for b, c and d. More specifically the free group of four copies of $\mathbb{Z}/2\mathbb{Z}$ is a group G which acts on the set of all Fano polygons that are mutation equivalent to $\mathbb{P}^1 \times \mathbb{P}^1$. So for an element $g = g_1 g_2 \cdots g_k \in G$, where $g_i \in \{a, b, c, d\}$, and a polygon P belonging to the mutation graph of $\mathbb{P}^1 \times \mathbb{P}^1$, we define $gP = \mu_{g_k} \cdots \mu_{g_1}(P)$.

By exploiting the combinatorics and symmetries of the Fano polygon $P_{\mathbb{P}^1 \times \mathbb{P}^1}$, we determine isomorphisms between polygons in the mutation graph of Figure 18.

As a result of the rotational symmetry of $P_{\mathbb{P}^1 \times \mathbb{P}^1}$, the first mutation performed will map to $P_{\mathbb{P}(1,1,2)}$ irrespective of which mutation is chosen. As a result the four branches from $\mathbb{P}^1 \times \mathbb{P}^1$ are isomorphic and we need only consider one. Without loss of generality assume a is the first mutation.

$P_{\mathbb{P}(1,1,2)} =$ 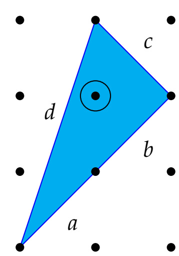

At this point the mutation a is the inverse of the first mutation and so takes us back to $P_{\mathbb{P}^1 \times \mathbb{P}^1}$. Since the T-cone b lies on the same edge as a in $P_{\mathbb{P}(1,1,2)}$, the mutation b also maps to $P_{\mathbb{P}^1 \times \mathbb{P}^1}$ so we discount this branch of the mutation graph by isomorphism. By a $GL(N)$-transformation the T-cones c and d are indistinguishable. Therefore the only new edge of the mutation graph modulo isomorphism from $P_{\mathbb{P}(1,1,2)} = aP_{\mathbb{P}^1 \times \mathbb{P}^1}$ is c.

The T-cones c and d are now distinguishable. However a and b are T-cones on the same edge and so are not distinguishable in $caP_{\mathbb{P}^1 \times \mathbb{P}^1}$. Hence the branches obtained by applying a or b are isomorphic. Therefore the new edges from the $P_{\mathbb{P}(1,1,2)}$ vertex that occur are a and d. Indeed this argument continues if we alternatively apply c and d to $aP_{\mathbb{P}^1\times\mathbb{P}^1}$ to study the Fano polygons $(dc)^n aP_{\mathbb{P}^1\times\mathbb{P}^1}$ and $c(dc)^n aP_{\mathbb{P}^1\times\mathbb{P}^1}$ which form a *spine* of the mutation graph: the T-cones a and b are bound along the same edge, the T-cones c and d are distinguishable and there are two new Fano polygons obtained by applying a, and either c or d respectively at each stage.

What if we choose to apply a along this spine, namely consider the Fano polygon $a(dc)^n aP_{\mathbb{P}^1\times\mathbb{P}^1}$. Any argument for $a(dc)^n aP_{\mathbb{P}^1\times\mathbb{P}^1}$ can be identically applied to $ac(dc)^n aP_{\mathbb{P}^1\times\mathbb{P}^1}$. At this point all four T-cones have separate edges, the only caveat being that the edges of the T-cones a and b are parallel. The mutations c and d (either of which are possible) break this parallel property for the edges of the T-cones a and b, so the mutation graph from this point on has valency four. Instead if we mutate b (we do not perform a as this was the last mutation), then a and b are again bound together and indistinguishable.

The polygon $ba(dc)^n aP_{\mathbb{P}^1\times\mathbb{P}^1}$ is similar to the Fano polygon $aP_{\mathbb{P}^1\times\mathbb{P}^1} = P_{\mathbb{P}(1,1,2)}$. Applying either mutation a or mutation b takes us back to $a(dc)^n aP_{\mathbb{P}^1\times\mathbb{P}^1}$, whereas c and d are both permitted. For either polygon $cba(dc)^n aP_{\mathbb{P}^1\times\mathbb{P}^1}$ or $dba(dc)^n aP_{\mathbb{P}^1\times\mathbb{P}^1}$, there is no distinction between a and b, and so we disregard the mutation b as isomorphic to the mutation a. The only other possible mutation for $cba(dc)^n aP_{\mathbb{P}^1\times\mathbb{P}^1}$ and $dba(dc)^n aP_{\mathbb{P}^1\times\mathbb{P}^1}$ are d or c respectively. There are two new spines consisting of polygons of the form $c^i(dc)^{n_2}bad^i(cd)^{n_1}caP_{\mathbb{P}^1\times\mathbb{P}^1}$ and $d^j(cd)^{n_2}bad^i(cd)^{n_1}caP_{\mathbb{P}^1\times\mathbb{P}^1}$ where $i, j \in \{0,1\}$ and $n_1, n_2 \in \mathbb{Z}_{\geq 0}$. The whole argument repeats inductively to this spine, either applying ba to some entry of a spine producing two new spines, or applying either ca or da to some entry producing a valency four subgraph.

This discussion is summarised by the following proposition:

Proposition 6.3.1. Every Fano polygon in the mutation graph of $\mathbb{P}^1 \times \mathbb{P}^1$ modulo isomorphism is represented by a word in the alphabet $\{a, b, c, d\}$ which obeys the following rules:

- $a^2 = b^2 = c^2 = d^2 = 1$;
- All words must start with the letter a;
- The second letter (if it exists) must be c;
- The second occurrence of a (if it exists) must be before a first occurrence of b;
- If a second occurrence of a is followed immediately by b, then the third occurrence of a (if it exists) must be before a second occurrence of b. This rule repeats inductively until an a is not followed by a b.

This is shown in Figure 19. We conjecture that this representation is unique.

The structure here is certainly less simple than that of $\mathbb{P}^2$ in Figure 17, and certainly does not appear to be particularly natural. For this reason one may propose that looking modulo isomorphism is not the correct way to study mutation graphs. In general I suspect that mutation graphs modulo isomorphism are Tits buildings, see [1, 66].

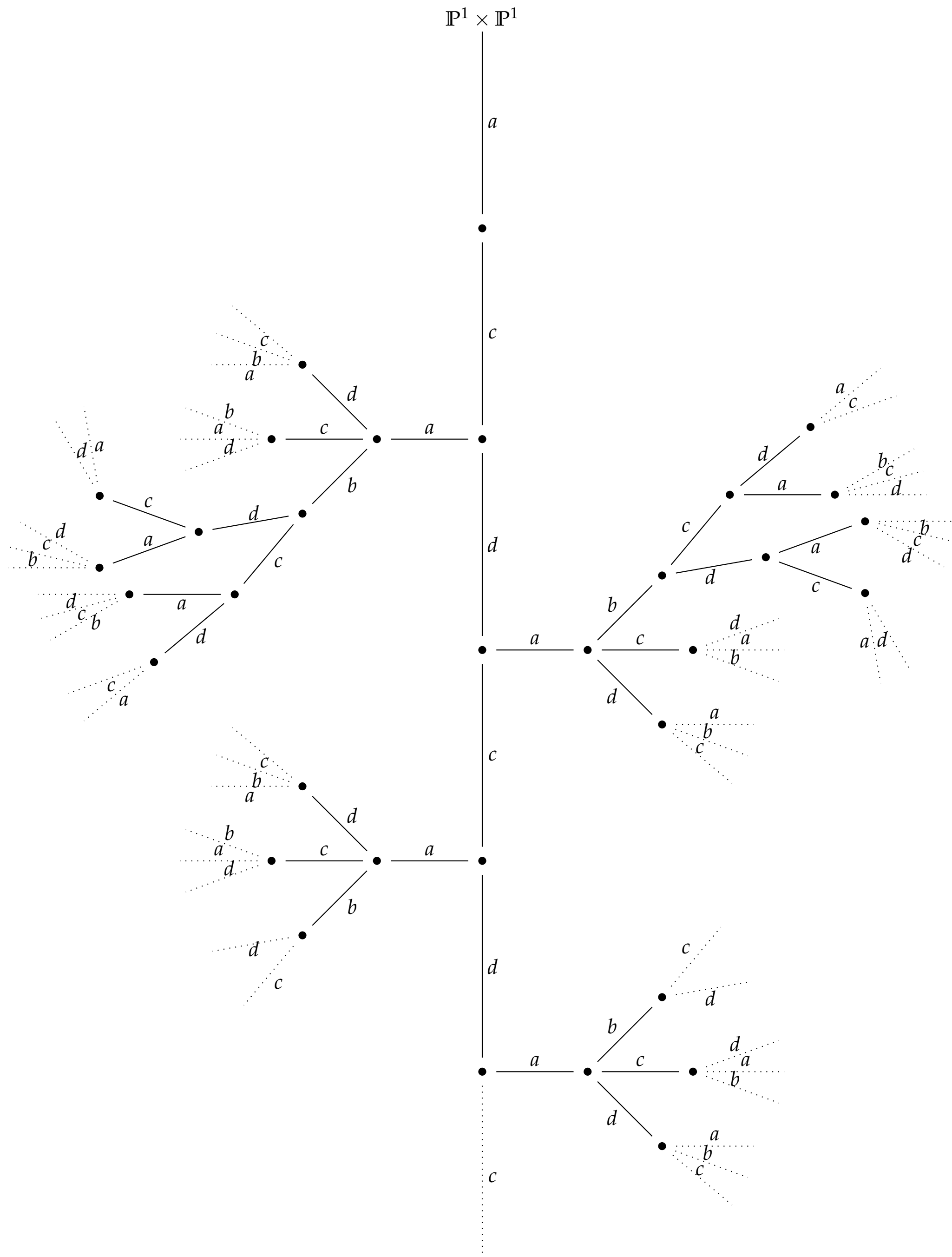

Figure 19: Mutation graph of $\mathbb{P}^1 \times \mathbb{P}^1$ modulo isomorphic equivalence

It is interesting at this point to consider the work of Hacking–Prokhorov [38] who give a classification of del Pezzo surfaces with quotient singularities of Picard rank 1 which admit a qG-smoothing. In particular [38, Theorem 4.1] links a family of toric surfaces of the form $\mathbb{P}(a^2, b^2, 2c^2)$ to solutions (a, b, c) of the Markov equation $a^2 + b^2 + 2c^2 = 4abc$, in similar fashion to that of Proposition 6.1.1. Note that $\mathbb{P}(1, 1, 2)$ is one such of these surfaces. Similarly to $\mathbb{P}^2$, the mutation graph of $\mathbb{P}(1, 1, 2)$ is valency three. The mutation graph of $\mathbb{P}(1, 1, 2)$ modulo isomorphism is shown in Figure 20.

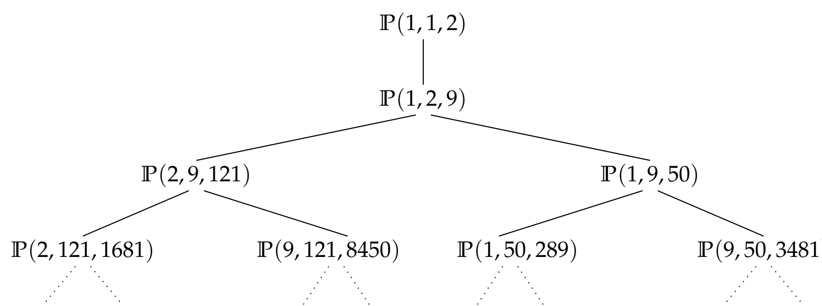

Figure 20: Mutation graph of $\mathbb{P}(1, 1, 2)$ modulo isomorphism

In particular the solution $(a, b, c) = (1, 1, 1)$ to the Markov equation gives rise to the surface $\mathbb{P}(1, 1, 2)$, which is obtained by any one step mutation of $\mathbb{P}^1 \times \mathbb{P}^1$. Therefore the toric surfaces in this classification will appear in the mutation tree of $\mathbb{P}^1 \times \mathbb{P}^1$. Figure 21 shows how infinitely many copies of the $\mathbb{P}(1, 1, 2)$ mutation graph sit inside the $\mathbb{P}^1 \times \mathbb{P}^1$ mutation graph. Note that when attempting to place the mutation graph of $\mathbb{P}(1, 1, 2)$ inside the $\mathbb{P}^1 \times \mathbb{P}^1$ mutation graph, it may not at a glance appear to be valency three. The reason for this is that when two primitive T-cones, say a and b, share the same edge, there is no distinction in the $\mathbb{P}(1, 1, 2)$ mutation graph between the two-step mutations ab and ba, whereas there is in the $\mathbb{P}^1 \times \mathbb{P}^1$ mutation graph. In Figure 21, entries of the $\mathbb{P}^1 \times \mathbb{P}^1$ mutation graph that are of Picard rank 2 are in black, and copies of the $\mathbb{P}(1,1,2)$ mutation graph are shown in red. The mutation graph is show up to depth 4 except in selected areas.

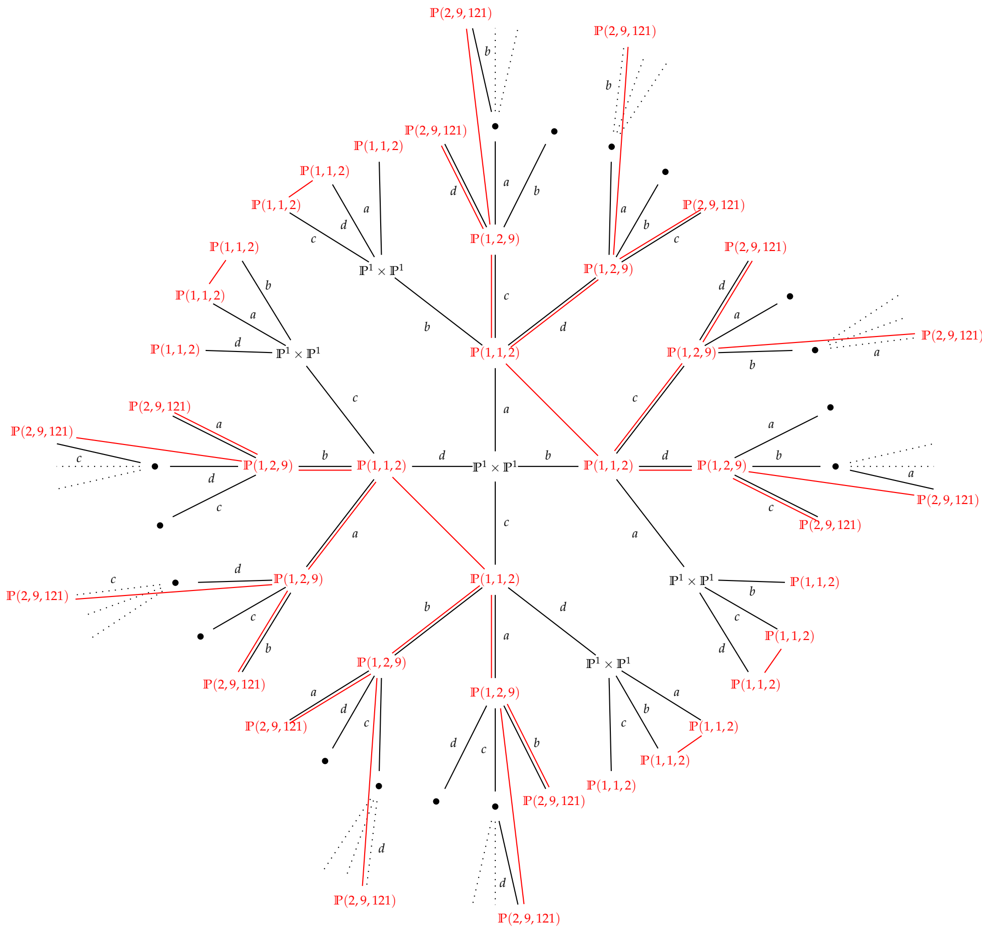

Figure 21: Mutation graphs of $\mathbb{P}(1,1,2)$ lying in the mutation graph of $\mathbb{P}^1 \times \mathbb{P}^1$

6.4 QUIVERS AND HAMILTONIAN CYCLES

As mentioned in Section 6.2, given a Fano polygon P, by [15, 34] we can associate a quiver $\mathcal{Q}_P$. Namely take a partial crepant resolution to divide the Fano polygon into primitive T-cones and R-cones; each vertex of $\mathcal{Q}_P$ is indexed by one of these cones. The frozen vertices are exactly those corresponding to

R-cones. Consider two vertices v and v' of $\mathcal{Q}_P$ corresponding to cones C_v and $C_{v'}$ respectively. The number of arrows from v to v' is given by $\max(n \wedge n', 0)$ where n and n' are the inward pointing normals of the edges E_v and $E_{v'}$ of the two respective cones.

Example 6.4.1. Consider $\mathbb{P}^1 \times \mathbb{P}^1$ and calculate the quiver $\mathcal{Q}_{\mathbb{P}^1 \times \mathbb{P}^1}$. Note there are no frozen vertices since $\mathrm{SC}\left(P_{\mathbb{P}^1 \times \mathbb{P}^1}\right) = (4, \varnothing)$.

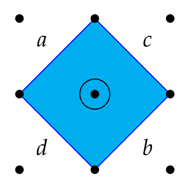

$P_{\mathbb{P}^1 \times \mathbb{P}^1}$

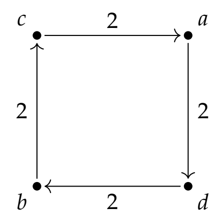

$\mathcal{Q}_{P_{\mathbb{P}^1 \times \mathbb{P}^1}}$

Definition 6.4.2 ([49, Definition 1.7])**.** A quiver $\mathcal{Q}$ is *weighted* if for each vertex $v \in \mathcal{V}(\mathcal{Q})$ there is an associated non-negative integer, denoted $\mathrm{weight}(v)$, known as the *weight of* v. The *weight of an edge* $v \to v'$ is the product of the source weight and the target weight:

$$\mathrm{weight}\left(v \to v'\right) = \mathrm{weight}(v) \cdot \mathrm{weight}(v').$$

Definition 6.4.3 ([49, Definition 1.7])**.** A weighted quiver $\mathcal{Q}$ is *balanced* if:

$$\sum_{v' \to v} \mathrm{weight}(v' \to v) = \sum_{v \to v''} \mathrm{weight}(v \to v''), \qquad \forall v \in \mathcal{V}(\mathcal{Q}).$$

That is informally, at any vertex the number of arrows going in equals the number of arrows coming out counted up to weight and multiplicity.

Note that the condition for a quiver to be balanced is equivalent to:

$$\sum_{v' \to v} \mathrm{weight}(v') = \sum_{v \to v''} \mathrm{weight}(v''), \qquad \forall v \in \mathcal{V}(\mathcal{Q}).$$

For a quiver associated to a Fano polygon there is always a choice of integers at each vertex to balance the quiver:

Lemma 6.4.4 ([49, Lemma 2.3])**.** Let P be a Fano polygon, and $\mathcal{Q}_P$ be the associated quiver. If each vertex $v \in \mathcal{V}(\mathcal{Q}_P)$ is given weight $\ell(E_v)$, where E_v is the edge of the cone C_v, then the resulting weighted quiver, denoted $\mathcal{Q}_P^{(b)}$ is balanced.

Proof. Let $\{p_1, p_2, \ldots, p_k\}$ be the vertices of a partial crepant resolution of P into its primitive T-cones and R-cones ordered anticlockwise so that p_i and p_{i+1} are the primitive points define the generating rays of C_{v_i}. Let d_i be the primitive direction vector from p_i to p_{i+1}, that is the primitive vector lying on E_{v_i} with appropriate orientation, and let n_i be the inward pointing normal of E_{v_i}. Since P is closed:

$$\ell(E_{v_1})d_1 + \ldots + \ell(E_{v_k})d_k = 0.$$

Taking the symplectic product on this identity:

$$\ell(E_{v_1})n_1 + \ldots + \ell(E_{v_k})n_k = 0,$$

and then taking the wedge product with n_i, for $1 \leq i \leq k$ gives the result. $\square$

Example 6.4.5. The balanced quiver $\mathcal{Q}^{(b)}_{\mathbb{P}^1\times\mathbb{P}^1}$ is as follows:

$$\begin{tikzcd}
c\,(1) \arrow[r, "2"] & a\,(1) \arrow[d, "2"] \\
b\,(1) \arrow[u, "2"] & d\,(1) \arrow[l, "2"]
\end{tikzcd}$$

$\mathcal{Q}^{(b)}_{P_{\mathbb{P}^1\times\mathbb{P}^1}}$

A final piece of information that can be associated to a quiver $\mathcal{Q}_P$ is a choice of Hamiltonian cycle. Recall that a Hamiltonian cycle of a quiver $\mathcal{Q}$ is a cycle that visits each vertex exactly once.

Definition 6.4.6. The Hamiltonian cycle associated to a balanced quiver of the form $\mathcal{Q}_P^{(b)}$ is the unique path through the v_i in the order determined by the anticlockwise orientation of the corresponding cones C_{v_i}. We denote the balanced quiver of a Fano polygon with Hamiltonian cycle equip by $\mathcal{Q}_P^{(b,H)}$.

By definition, a Hamiltonian cycle will not travel against an arrow of a quiver. More specfically , consider two cones C_1, C_2 lying adjacently in an anticlockwise orientation. It follows that $n_1 \wedge n_2 \geq 0$, and so there is not an arrow from v_2 to v_1 in the quiver. It is however possible for the Hamiltonian cycle to pass between two vertices that do not have an arrow between them. Indeed this is exactly the case when C_1, C_2 belong to the same edge.

Example 6.4.7. The balanced quiver with Hamiltonian cycle of $\mathbb{P}^1 \times \mathbb{P}^1$ is given by:

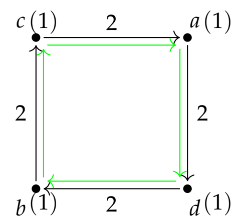

$\mathcal{Q}^{(b,H)}_{\mathbb{P}^1 \times \mathbb{P}^1}$

Lemma 6.4.8. Given a balanced quiver with Hamiltonian cycle $\mathcal{Q}_P^{(b,H)}$ belonging to the mutation graph of $\mathcal{Q}^{(b,H)}_{\mathbb{P}^1 \times \mathbb{P}^1}$, it is possible to recover the corresponding Fano polygon P.

Proof. This is a simple exercise in linear algebra to reconstruct the affine loop which forms the boundary of the Fano polygon. Since every edge of P represents a primitive T-singularity, this determines where the origin is. $\square$

This lemma is almost true in greater generality. If a Fano polygon P has singularity content $(n, \mathcal{B})$ where $\mathcal{B} \neq \varnothing$, then we can recover P from the balanced quiver with Hamiltonian cycle $\mathcal{Q}_P^{(b,H)}$, if one knows which vertices of $\mathcal{Q}_P^{(b,H)}$ are frozen.

It is understood how to mutate a quiver, see Bernstein–Gelfand–Ponomarev and Fomin–Zelevinsky [15, 34], and we recall this definition from Section 6.2.

Definition 6.4.9. Let $\mathcal{Q}$ be a quiver and $v \in \mathcal{V}(\mathcal{Q})$. Define the *mutation* of Q at v, denoted $\mathrm{mut}_v(\mathcal{Q})$, to be the quiver obtained from $\mathcal{Q}$ by:

(i) For every pair of arrows $v' \to v$ and $v \to v''$, add an arrow $v' \to v''$;

(ii) Delete a maximal set of disjoint two-cycles;

(iii) Reverse all arrows incident to v.

Suppose $\mathcal{Q}_P$ is the quiver associated to a Fano polygon P. By convention we do not mutate with respect to frozen vertices.

Proposition 6.4.10 ([48])**.** Consider a Fano polygon P and the corresponding quiver $\mathcal{Q}_P$. Let $v \in \mathcal{V}(\mathcal{Q}_P)$, and E be the edge of the T-cone corresponding to v. Then

$$\mathrm{mut}_v(\mathcal{Q}_p) = \mathcal{Q}_{\mathrm{mut}_{(n_E,F)}(P)}.$$

This notion of quiver mutation can be extended to the mutation of a weighted quiver as shown in [49].

Definition 6.4.11. Consider a balanced quiver $\mathcal{Q}^{(b)}$, and $v \in \mathcal{V}(\mathcal{Q}^{(b)})$. Let $\mathcal{Q}$ by the underlying quiver of $\mathcal{Q}^{(b)}$, that is, the quiver obtained from $\mathcal{Q}^{(b)}$ by ignoring the weights of the vertices. Set $\mathcal{Q}' = \mathrm{mut}_v(Q)$. The quiver $\mathcal{Q}'$ can be balanced by assigning the weights of $\mathcal{Q}^{(b)}$ to every vertex $v' \neq v$, and then using any arrow of Q' incident to v to obtain a balancing condition that uniquely determines weight(v). This new balanced quiver, denoted $\mathrm{mut}_v(\mathcal{Q}^{(b)})$, is called the *mutation of the balanced quiver* $\mathcal{Q}^{(b)}$.

Mutation of a balanced quiver is well-defined by Lemma 6.4.4.

We look to extend this notion to the mutation of a balanced quiver with a Hamiltonian cycle $\mathcal{Q}_P^{(b,H)}$ associated to a Fano polygon P.

Definition 6.4.12. Choose a vertex $v \in \mathcal{V}(\mathcal{Q}_P^{(b,H)})$. By starting at $u_1 = v$ and following the Hamiltonian cycle, label the vertices of $\mathcal{Q}_P^{(b,H)}$ by $u_1, \ldots, u_k$. For $2 \leq i \leq k$, set

$$n_i = \#(\text{arrows from } u_i \text{ to } v) - \#(\text{arrows from } v \text{ to } u_i).$$

Choose j to be the smallest integer such that $\text{sign}(n_j) \neq \text{sign}(n_{j+1})$, where

$$\text{sign}(n) = \begin{cases} 1, & \text{if } n > 0, \\ 0, & \text{if } n = 0, \\ -1, & \text{if } n < 0. \end{cases}$$

Define a Hamilton cycle H' on the vertices of $\mathcal{Q}_P^{(b,H)}$ by $u_2 u_3 \ldots u_j u_1 u_{j+1} \ldots u_k$. The *mutation of* $\mathcal{Q}_P^{(b,H)}$ *with respect to* v, denoted by $\text{mut}_v\left(\mathcal{Q}_P^{(b,H)}\right)$, is the quiver $\text{mut}_v\left(Q_P^{(b)}\right)$ equipped with the Hamiltonian cycle H'.

Example 6.4.13. Consider the quiver $\mathcal{Q}_{\mathbb{P}^1\times\mathbb{P}^1}^{(b,H)}$ from Example 6.4.7 and mutate with respect to v_1. With the above notation, the Hamiltonian cycle of $\mathcal{Q}_{\mathbb{P}^1\times\mathbb{P}^1}^{(b,H)}$ is $u_1 u_2 u_3 u_4$ = adbc. Mutating the Hamiltonian cycle with $j = 3$, it follows that the new Hamiltonian cycle is $u_2 u_3 u_1 u_4 = dbac$.

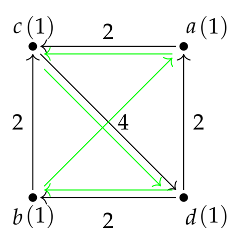

$$\text{mut}_a\left(Q_{\mathbb{P}^1\times\mathbb{P}^1}^{(b,H)}\right)$$

In some cases there may not be a unique choice for j. When there is more than one vertex of P with respect to the inward pointing normal used in the mutation, then the choice of j is akin to the choice of primitive slice $F = \operatorname{conv}\{\mathbf{0}, v_E\}$ in Definition 2.5.12.

Proposition 6.4.14. Consider a Fano polygon P and the corresponding quiver $\mathcal{Q}_P^{(b,H)}$. Let $v \in \mathcal{V}(\mathcal{Q}_P^{(b,H)})$, and E be the edge of the T-cone corresponding to v. Then

$$\operatorname{mut}_v(\mathcal{Q}_p^{(b,H)}) = \mathcal{Q}^{(b,H')}_{\operatorname{mut}_{(n_E,F)}(P)}.$$

Proof. Using Lemma 6.4.4 and Proposition 6.4.10 it remains only to check the Hamiltonian cycle. Informally we have seen that mutation lifts a T-cone C over an edge E, and places it onto the vertex of P that is maximal with respect to the grading induced by the inward pointing normal n_E. It follows that this vertex will be the end point of two edges E_1 and E_2 such that $\operatorname{sign}(n_E \wedge n_{E_1}) \neq \operatorname{sign}(n_E \wedge n_{E_2})$. The two cones either side of C will then lie adjacent. Therefore the Hamiltonian cycle of $\operatorname{mut}_v(\mathcal{Q}_p^{(b,H)})$ is the correct one. $\square$

By Lemma 6.4.8 and Proposition 6.4.14, studying the mutation graph of $\mathbb{P}^1 \times \mathbb{P}^1$ is equivalent to studying the mutation graph of the quiver $\mathcal{Q}^{(b,H)}_{\mathbb{P}^1\times\mathbb{P}^1}$. From Section 6.3, the shape of the mutation graph of $\mathcal{Q}^{(b,H)}_{\mathbb{P}^1\times\mathbb{P}^1}$ is known. With this in mind we study the central spine of the $\mathbb{P}^1 \times \mathbb{P}^1$ mutation graph, that is polygons of the general form $(dc)^n a\mathbb{P}^1 \times \mathbb{P}^1$ and $c(dc)^n a\mathbb{P}^1 \times \mathbb{P}^1$, where $n \in \mathbb{Z}_{\geq 0}$.

We have already seen $\mathcal{Q}^{(b,H)}_{a\mathbb{P}^1\times\mathbb{P}^1}$ in Example 6.4.13. In particular, $\mathcal{Q}^{(H)}_{a\mathbb{P}^1\times\mathbb{P}^1}$ is of the form

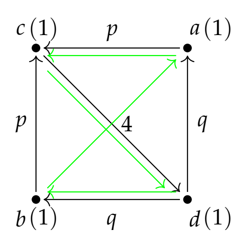

for some $p, q \in \mathbb{Z}_{>0}$. Mutate this quiver with respect to c followed by the mutation with respect to d:

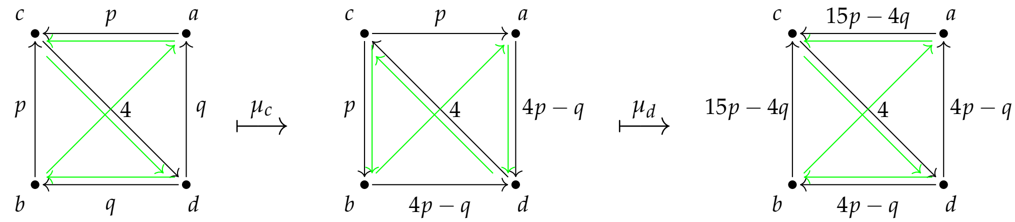

Note that the underlying shape of the quiver has been preserved under mutation. Hence $\mathcal{Q}^{(H)}_{(dc)^n a \mathbb{P}^1 \times \mathbb{P}^1}$ is given by

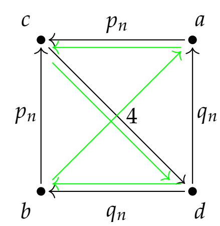

where p_n and q_n satisfy the linear recursions

$$\begin{aligned} p_n &= 15p_{n-1} - 4q_{n-1}, & p_0 &= 2, & p_1 &= 22, \\ q_n &= 4p_{n-1} - q_{n-1}, & q_0 &= 2, & q_1 &= 6. \end{aligned}$$

Uncoupling the two linear recursions we obtain:

$$\begin{aligned} p_n &= 14p_{n-1} - p_{n-2}, \\ q_n &= 14q_{n-1} - q_{n-2}. \end{aligned}$$

The sequence $\{p_n\}_{n\in\mathbb{Z}_{\geq 0}}$ has characteristic equation $x^2 - 14x + 1 = 0$ which has roots $x_1 = 7 + 4\sqrt{3}$ and $x_2 = 7 - 4\sqrt{3}$. Using the conditions $p_0 = 2, p_1 = 22$ to find the constants in the expression $p_n = C_1(7+4\sqrt{3})^n + C_2(7-4\sqrt{3})^n$, we find that $C_1 = \frac{3+\sqrt{3}}{3}$ and $C_2 = \frac{3-\sqrt{3}}{3}$. Therefore

$$p_n = \frac{1}{3}\left[(3+\sqrt{3})(7+4\sqrt{3})^n + (3-\sqrt{3})(7-4\sqrt{3})^n\right].$$

Similarly calculate that

$$q_n = \frac{1}{3}\left[(3-\sqrt{3})(7+4\sqrt{3})^n + (3+\sqrt{3})(7-4\sqrt{3})^n\right].$$

Consider the quiver $\mathcal{Q}^{(H)}_{(dc)^n a\mathbb{P}^1\times\mathbb{P}^1}$:

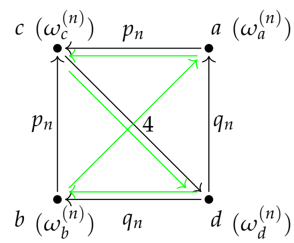

The balancing weights of $\mathcal{Q}^{(H)}_{(dc)^n a\mathbb{P}^1\times\mathbb{P}^1}$ on the vertices a and b are the same as those for $\mathcal{Q}^{(H)}_{a\mathbb{P}^1\times\mathbb{P}^1}$ by Definition 6.4.11, that is $\omega_a = \omega_b = 1$. Deriving a linear equation for ω_c and ω_d by balancing about d and c respectively gives:

$$\omega_c^{(n)} = \frac{1}{6}\left[(3-\sqrt{3})(7+4\sqrt{3})^n + (3+\sqrt{3})(7-4\sqrt{3})^n\right],$$
$$\omega_d^{(n)} = \frac{1}{6}\left[(3+\sqrt{3})(7+4\sqrt{3})^n + (3-\sqrt{3})(7-4\sqrt{3})^n\right].$$

The quiver $\mathcal{Q}^{(H)}_{c(dc)^n a\mathbb{P}^1\times\mathbb{P}^1}$ can be found by mutating the quiver $\mathcal{Q}^{(H)}_{(dc)^n a\mathbb{P}^1\times\mathbb{P}^1}$ about the vertex c. It is of the form

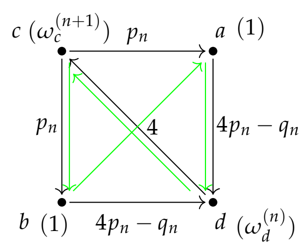

The toric variety associated to either $\mathcal{Q}^{(H)}_{(dc)^n a\mathbb{P}^1\times\mathbb{P}^1}$ or $\mathcal{Q}^{(H)}_{c(dc)^n a\mathbb{P}^1\times\mathbb{P}^1}$ by Lemma 6.4.8 is the weighted projective space given by $\mathbb{P}(2, \omega_c^2, \omega_d^2)$. Note that ω_c and ω_d are increasing functions in n so there will be no further index two toric varieties along this mutation line.

Additionally consider the following quiver, which is a general form of the quivers $\mathcal{Q}^{(H)}_{(dc)^n a\mathbb{P}^1\times\mathbb{P}^1}$, and two mutations with respect to a then b.

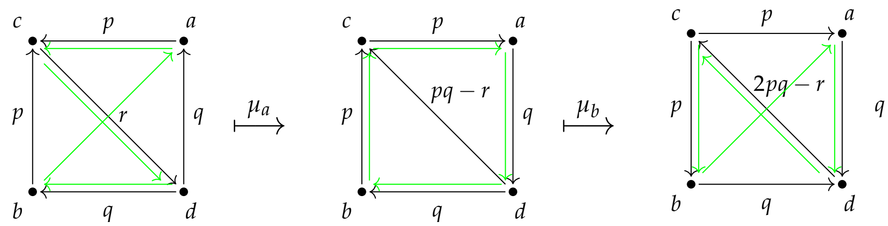

It follows that the quivers $\mathcal{Q}^{(H)}_{ba(dc)^n a\mathbb{P}^1\times\mathbb{P}^1}$ have a very similar form to the quivers $\mathcal{Q}^{(H)}_{(dc)^n a\mathbb{P}^1\times\mathbb{P}^1}$, and so we know how to alternatively apply the mutations c and d to $\mathcal{Q}^{(H)}_{ba(dc)^n a\mathbb{P}^1\times\mathbb{P}^1}$. The same analysis holds when for calculating $\mathcal{Q}^{(H)}_{bac(dc)^n a\mathbb{P}^1\times\mathbb{P}^1}$. Repeating this inductively allows to to understand large portions of the mutation graph, namely we understand the mutation graph while the cones a and b either share an edge or are parallel.

As an interesting aside we highlight a link between the weights of the quivers in the central spine of the $\mathbb{P}^1 \times \mathbb{P}^1$ mutation graph, and the domino tilings of a $3 \times 2n$ grid. This link was noticed using [45].

A domino tiling of a grid of squares is a covering with 2×1 grid-sized tiles such that every tile covers exactly two squares of the grid and none of the tiles overlap. Milchev–Karamfilova [58] outline various dependencies between the number of domino tilings between grids. In particular they produce a formula for the number of domino tilings, denoted A_n of a $3 \times 2n$ grid where $n \in \mathbb{Z}_{>0}$, namely:

$$A_n = \frac{1}{6}\left[(3+\sqrt{3})(2+\sqrt{3})^n + (3-\sqrt{3})(2-\sqrt{3})^n\right].$$

Proposition 6.4.15. The integer sequence $(\omega_d^{(0)}, \omega_c^{(0)}, \omega_d^{(1)}, \omega_c^{(1)}, \omega_d^{(2)}, \ldots)$ of new balancing conditions appearing in the central spine of the $\mathbb{P}^1 \times \mathbb{P}^1$ mutation graph is equal to the integer sequence $(A_0, A_1, A_2, \ldots)$.

Proof. By calculating $(2+\sqrt{3})^{2n} = (7+4\sqrt{3})^n$, it follows that $A_{2n} = \omega_d^{(n)}$. We also have that

$$\begin{aligned} A_{2n-1} &= \frac{1}{6}\left[(3+\sqrt{3})(2+\sqrt{3})^{2n-1} + (3-\sqrt{3})(2-\sqrt{3})^{2n-1}\right] \\ &= \frac{1}{6}\left[\frac{(3+\sqrt{3})}{(2+\sqrt{3})}(7+4\sqrt{3})^n + \frac{(3-\sqrt{3})}{(2-\sqrt{3})}(7-4\sqrt{3})^n\right] \\ &= \frac{1}{6}\left[(3-\sqrt{3})(7+4\sqrt{3})^n + (3+\sqrt{3})(7-4\sqrt{3})^n\right] \\ &= \omega_c^{(n)}. \end{aligned}$$

□

At the level of Fano polygons, Proposition 6.4.15 is a statement about the changing lattice lengths of the edges of $P_{\mathbb{P}^1\times\mathbb{P}^1}$ under a certain sequence of mutations.

6.5 plücker coordinates of $\mathbb{P}^1 \times \mathbb{P}^1$

We recall the construction of a toric variety which generalises the well-known construction of projective space. This is well documented and can be studied in [2, 29, 30] among others.

Let X_Σ be a Fano toric variety given by the complete fan $\Sigma \subset N_\mathbb{R} \cong \mathbb{R}^n$, where the minimal ray generators u_ρ of Σ span $N_\mathbb{R}$. Consider the $n \times |\Sigma(1)|$ matrix B whose columns are given by the generators u_ρ, $\rho \in \Sigma(1)$. Let A be the $|\Sigma(1)| \times (|\Sigma(1)| - n)$ matrix which is the dual of B, that is, the rows of A give relations among the u_ρ. These matrices define the functions in the short exact sequence of Theorem 1.4.1:

$$0 \longrightarrow M \xrightarrow{B} \mathrm{CDiv}_T(X_\Sigma) \cong \mathbb{Z}^n \xrightarrow{A} \mathrm{Pic}(X) \longrightarrow 0. \tag{8}$$

The matrix A is uniquely determined up to the action of $\mathrm{GL}\left(n - |\Sigma(1)|\right)$. So we always assume A contains a submatrix of the form $\lambda I_{|\Sigma(1)|}$, for some $\lambda \in \mathbb{Z}_{>0}$.

Definition 6.5.1 ([29]). For each $\rho \in \Sigma(1)$, define a variable x_ρ. Set $S = \mathbb{C}\left[x_\rho : \rho \in \Sigma(1)\right]$. Define the degree of a monomial $\prod_{\rho \in \Sigma(1)} x_\rho^{d_\rho}$ as:

$$\deg\left(\prod_{\rho\in\Sigma(1)} x_\rho^{d_\rho}\right) = \left[\sum_{\rho\in\Sigma(1)} d_\rho D_\rho\right],$$

where D_ρ is the divisor corresponding to ρ, and $[D]$ is the class of the divisor D in $\mathrm{Pic}\left(X_\Sigma\right)$. The ring S with this grading is called the Cox ring of X_Σ.

Example 6.5.2. Let $X = \mathbb{P}^n$. Then the Cox ring S is the homogeneous coordinate ring $\mathbb{C}[x_0, \ldots, x_n]$ where all variables x_i have weight 1.

Example 6.5.3. Let $X = \mathbb{P}(a_0, \ldots, a_n)$. Then the Cox ring S is the ring $\mathbb{C}[x_0, \ldots, x_n]$ where x_i has weight a_i.

Indeed the Cox ring is the generalisation of the homogeneous coordinate ring to toric varieties.

Since $\mathrm{Pic}(X_\Sigma)$ depends only on $\Sigma(1)$, so does S. Indeed we can reconstruct $\Sigma(1)$ from the Cox ring. In dimension $n = 2$, this is enough to find Σ (using completeness) but if $n \geq 3$, Σ cannot be recovered from $\Sigma(1)$.

Let $\sigma \in \Sigma$. Set $x^{\hat{\sigma}} = \prod_{\rho \notin \sigma(1)} x_\rho$.

Definition 6.5.4. The irrelevant ideal of X is given by:

$$I = \langle x^{\hat{\sigma}} : \sigma \in \Sigma \rangle \subset S.$$

Lemma 6.5.5. For a Fano variety, only the maximal full dimensional cones need to be considered when defining the irrelevant ideal, that is:

$$I = \langle x^{\hat{\sigma}} : \sigma \in \Sigma(n) \rangle.$$

Theorem 6.5.6. The data A and I determine Σ, and hence X_Σ.

Proof. The matrix A determines the rays of Σ. The ideal determines the maximal cones. Together this is enough to determine Σ. $\square$

Applying $\mathrm{Hom}_{\mathbb{Z}}(-, \mathbb{C}^*)$ to the short exact sequence of (8), we obtain:

$$1 \longrightarrow G = \mathrm{Hom}_{\mathbb{Z}}\left(\mathrm{Cl}(X_\Sigma), \mathbb{C}^*\right) \xrightarrow{M} \left(\mathbb{C}^*\right)^n \longrightarrow T \longrightarrow 1, \tag{9}$$

where $M = A^T$.

Definition 6.5.7. M is called the GIT matrix of X_Σ.

Note the columns of M are the ray generators of the secondary fan of X_Σ. The ideal I can also be read off the secondary fan. The anticanonical divisor $-K_{X_\Sigma}$ is given by the sum of the columns of M. This can be marked on the secondary fan.

Lemma 6.5.8. The irrelevant ideal is given by:

$$I = \left\langle x_{\rho_{j_1}} x_{\rho_{j_2}} \dots x_{\rho_{j_n}} : -K_{X_\Sigma} \in \mathrm{Cone}\left(x_{\rho_{j_1}}, x_{\rho_{j_2}}, \dots, x_{\rho_{j_n}}\right)\right\rangle.$$

The short exact sequence (9) describes an action of $G = \mathrm{Hom}_{\mathbb{Z}}\left(\mathrm{Cl}\left(X\right), \mathbb{C}^*\right)$ on $\left(\mathbb{C}^*\right)^n$. Namely:

$$\left(\lambda_1, \dots, \lambda_{n-|\Sigma(1)|}\right) \cdot (x_1, \dots, x_n) = \left(\left(\prod_{i=1}^{n-|\Sigma(1)|} \lambda_i^{a_{i,1}}\right) x_1, \dots, \left(\prod_{i=1}^{n-|\Sigma(1)|} \lambda_i^{a_{i,n}}\right) x_n\right).$$

The significance of all these definitions lie in the following theorem.

Theorem 6.5.9. The toric variety X_Σ is isomorphic to the categorical quotient $\left(\mathbb{C}^{\Sigma(1)} \backslash \mathbb{V}(I)\right) / G$.

Example 6.5.10. Consider $\mathbb{P}^1 \times \mathbb{P}^1$, and the corresponding Fano polygon $P_{\mathbb{P}^1 \times \mathbb{P}^1}$:

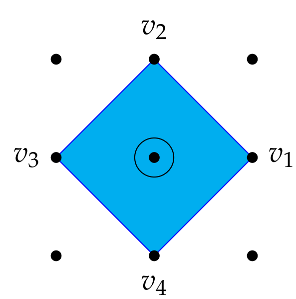

The columns of B are given by the vertices of P, that is:

$$B = \begin{pmatrix} 1 & 0 & -1 & 0 \\ 0 & 1 & 0 & -1 \end{pmatrix}.$$

Calculating the dual matrix and transposing gives the GIT matrix:

v_1	v_2	v_3	v_4
1	0	1	0
0	1	0	1

This determines that $-K_{\mathbb{P}^1 \times \mathbb{P}^1} = \begin{pmatrix} 2 \\ 2 \end{pmatrix}$, and the secondary fan is given by:

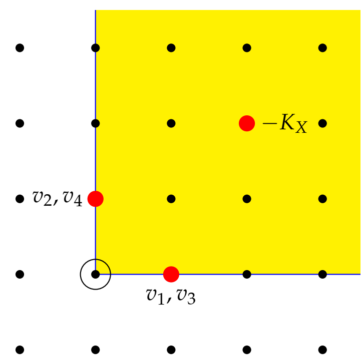

From here it is easy to read that the irrelevant ideal is given by:

$$I = \langle x_1x_2, x_1x_4, x_2x_3, x_3x_4 \rangle = \langle x_1, x_3 \rangle \cap \langle x_2, x_4 \rangle.$$

Recall the general definition of Plücker coordinates which can be studied from [59]. Given an algebraically closed field k, consider a $d \times n$ matrix M whose entries lie in k.

Definition 6.5.11. Given a subset $S \subset [n]$ where $|S| = d$, denote M_S as the $d \times d$ submatrix obtained by only considering the columns indexed by S. The maximal $d \times d$ minors of M form a list $(\det(M_S) : S \subset [n], |S| = d)$ called the *Plücker coordinates* of M.

Proposition 6.5.12 ([59, Proposition 14.2])**.** The list $(\det(M_S) : S \subset [n], |S| = d)$ considered up to scale, identifies the row span of M uniquely. More precisely a matrix M' has the same row span as M if and only if there exists $\lambda \in k$ such that:

$$\det(M_S) = \lambda \det(M'_S), \qquad \forall S \subset [n] \text{ with } |S| = d.$$

Given a toric variety X_P, we can associate Plücker coordinates through the GIT matrix M.

Definition 6.5.13. Suppose X_P has Picard rank 2, that is $|\mathcal{V}(P)| = 4$. The *Plücker coordinates* of X_P are given by the four maximal 2×2 minors of M such that the corresponding rays to the two chosen columns give variables whose product does not belong to the irrelevant ideal. In this case we say that the maximal minor *crosses* the irrelevant ideal. Furthermore there are two minors that do not cross the irrelevant ideal giving *forbidden* Plücker coordinates. Since Plücker coordinates are considered up to a scalar, assume that the greatest common divisor of the coordinates is zero.

Example 6.5.14. Consider $\mathbb{P}^1 \times \mathbb{P}^1$. The GIT matrix is given by:

$$\begin{array}{cc:cc} v_1 & v_3 & v_2 & v_4 \\ \hline 1 & 1 & 0 & 0 \\ 0 & 0 & 1 & 1 \end{array}$$

Here the columns of M have been reordered according to the anti-clockwise ordering of the secondary fan. It follows that the Plücker coordinates from Definition 6.5.13 of $\mathbb{P}^1 \times \mathbb{P}^1$ are given by $(1, 1, 1, 1)$. The *extended Plücker coordinates*, that is the usual Plücker coordinates with the two forbidden Plücker coordinates attached, are given by $({\color{red}0}, 1, 1, 1, 1, {\color{red}0})$ where the forbidden coordinates are in red.

This construction can be generalised to when the Picard rank of X_P is $k > 2$. It follows that P has $k + 2$ vertices and there will be k relations among them. As before we have the GIT matrix M, which will now have dimensions $k \times (k+2)$. The Plücker coordinates are the maximal $k \times k$ minors. The minors that give the usual Plücker coordinates are those where the two omitted columns of M correspond to two vertices that define an edge of P. The remaining maximal minors are the forbidden ones.

We calculate the GIT data and Plücker coordinates of the entries of the $\mathbb{P}^1 \times \mathbb{P}^1$ mutation graph, and this is shown in Figures 23 and 24.

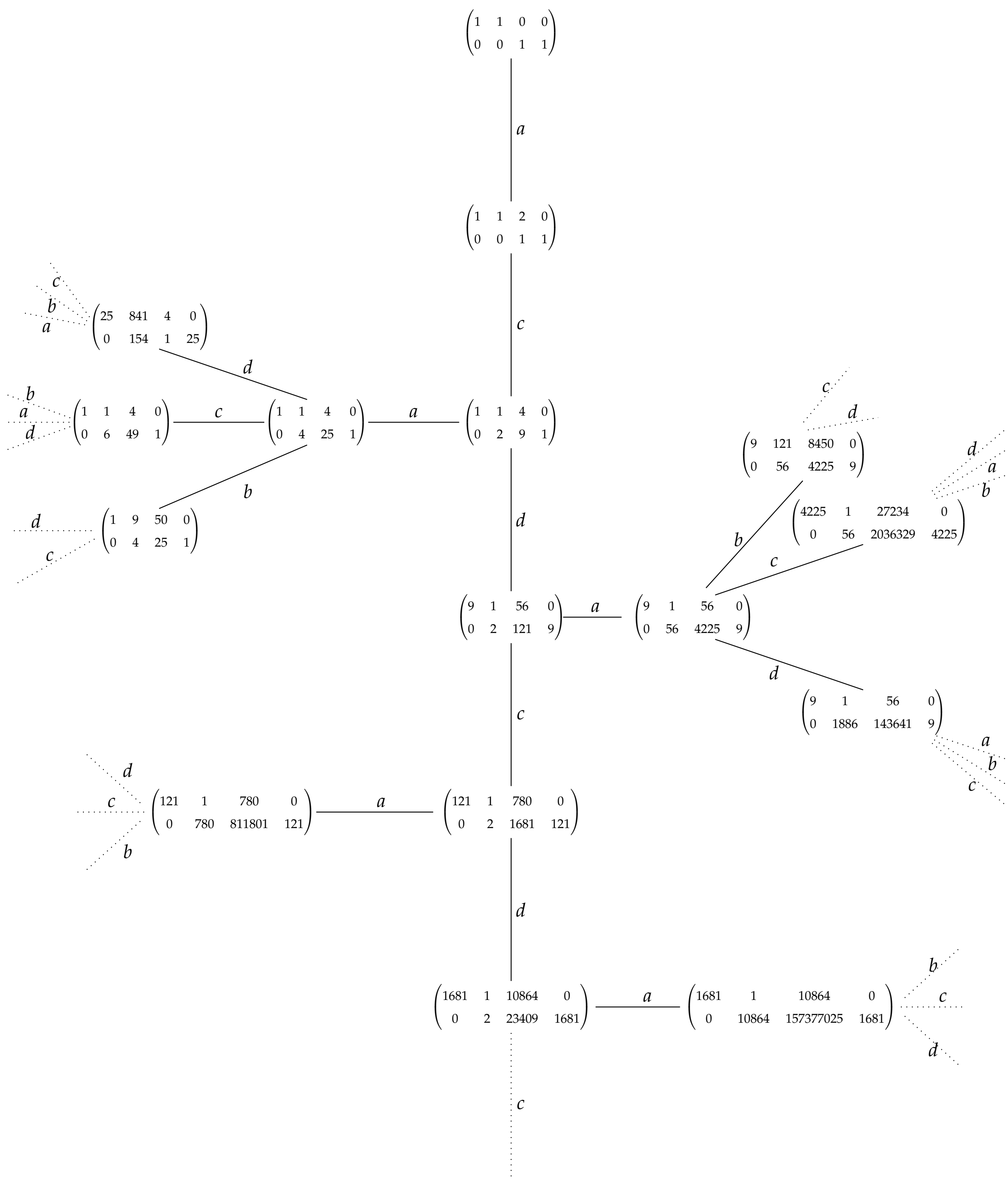

Figure 23: GIT matrix of mutation graph of $\mathbb{P}^1 \times \mathbb{P}^1$

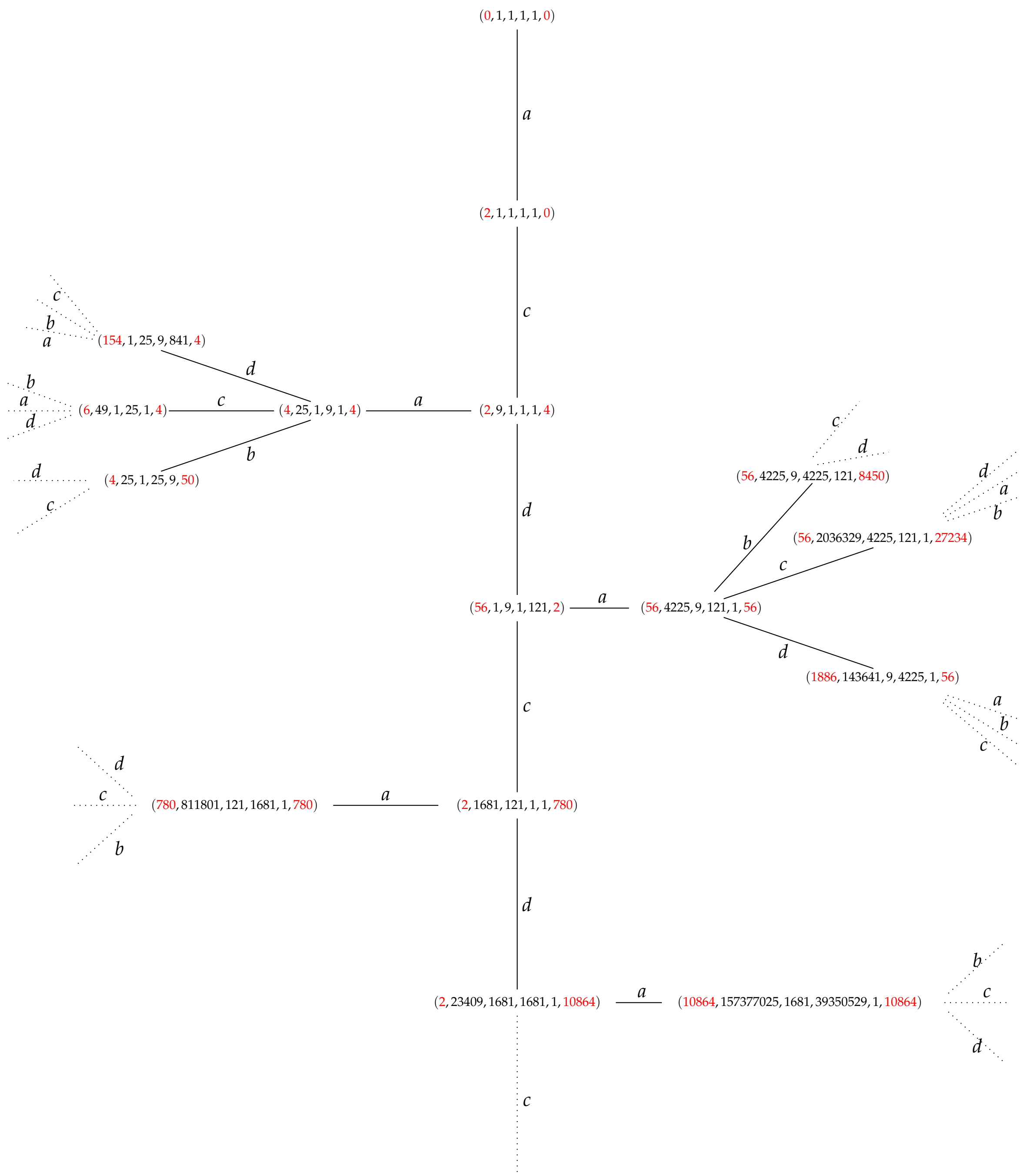

Figure 24: Plücker coordinates of mutation graph of $\mathbb{P}^1 \times \mathbb{P}^1$

6.6 EXTENDED QUIVER AND PLÜCKER COORDINATES

Ideally we would like to be able to answer the question 'When do six integers (a, b, c, d, e, f) describe the Plücker coordinates of an entry of the $\mathbb{P}^1 \times \mathbb{P}^1$ mutation graph'?

It is a known result that given a Fano polygon P such that $\mathrm{SC}(P) = (n, \varnothing)$ for some $n \in \mathbb{Z}_{>0}$, and corresponding balanced quiver $\mathcal{Q}_P^{(b)}$, that the balancing condition on a vertex $v \in \mathcal{V}\left(\mathcal{Q}_P^{(b)}\right)$ is the square root of one of the maximal minors of the GIT matrix. We generalise this statement:

Lemma 6.6.1. Let P be a Fano polygon and $v, w \in \mathcal{V}(P)$. Define E as the line segment from v to w. Let p_E be the maximal minor obtained by removing the two columns corresponding to v and w. Then:

$$p_E = l(E) \times h(E).$$

Combining Lemma 6.4.4 and Lemma 6.6.1 proves the following corollary which is a stronger version of the above statement.

Corollary 6.6.2. Let P be a Fano polygon, and $\mathcal{Q}_P^{(b)}$ be the corresponding balanced quiver. Let $v \in \mathcal{V}\left(\mathcal{Q}_P^{(b)}\right)$ correspond to the cone C of P. Then the Plücker coordinate p_C is equal to the balancing condition on v multiplied by $h(C)$.

When v and w are chosen in Lemma 6.6.1 to define a facet of P, then p_E is a usual Plücker coordinate. Alternatively in the case of p_E being a forbidden Plücker coordinate, E is a *forbidden edge* of P. However the statement of Corollary 6.6.2 still holds for these forbidden edges, that is, p_E is equal to $l(E) \times h(E)$.

Example 6.6.3. Consider the polygon $P_{\mathbb{P}^1 \times \mathbb{P}^1}$ shown below:

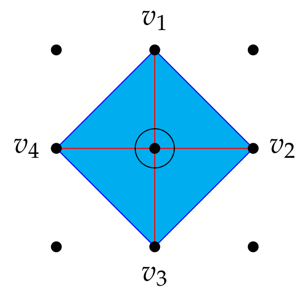

Note $\mathbb{P}^1 \times \mathbb{P}^1$ has four non-forbidden edges, that is the standard facets, and two forbidden edges: the line segment from v_1 to v_3 and the line segment from v_2 to v_4. These are marked in red. From Example 6.5.14 the Plücker coordinates of $\mathbb{P}^1 \times \mathbb{P}^1$ are given by $(0, 1, 1, 1, 1, 0)$. It is easy to verify Corollary 6.6.2 here.

Conjecture 6.6.4. The lattice length of a forbidden edge of a Fano polygon P belonging to the mutation graph of $\mathbb{P}^1 \times \mathbb{P}^1$ is two.

Note we do not go as far as to claim that the lattice length of forbidden edges is a mutation invariant. Indeed consider the counter-example to this statement given by a mutation of $P_{\mathbb{F}_1}$:

$P_{\mathbb{F}_1} =$ 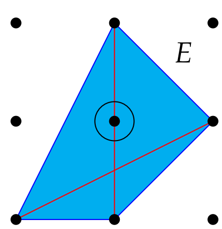

$\mathrm{mut}_E\left(P_{\mathbb{F}_1}\right) =$ 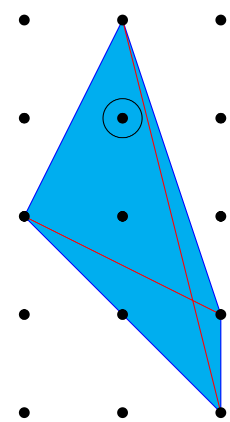

The forbidden lines of $P_{\mathbb{F}_1}$ have lattice lengths two and one, while both forbidden edges of $\mathrm{mut}_E\left(P_{\mathbb{F}_1}\right)$ have lattice length one. Therefore the lattice length of forbidden edges is not a mutation invariant in general.

Corollary 6.6.2 and Conjecture 6.6.4 can be used to provide restrictions on the Plücker coordinates of an entry P of the $\mathbb{P}^1 \times \mathbb{P}^1$ mutation graph. Specifically each facet E (a non-forbidden edge) of P describes a primitive T-singularity. Therefore $l(E) = h(E)$ and so the Plücker coordinate p_E must be square. Alternatively if E is a forbidden edge then $l(E) = 2$, and so p_E must be even. Therefore the Plücker coordinates of P take the form $(2a, b^2, c^2, d^2, e^2, 2f)$. Additionally the coordinates must satisfy the standard Plücker relation:

$$4af + c^2d^2 = b^2e^2.$$

Example 6.6.5. Consider the Fano polygon $acaP_{\mathbb{P}^1\times\mathbb{P}^1}$ of the mutation graph of $\mathbb{P}^1 \times \mathbb{P}^1$, see Figure 19, which has vertices:

$$\mathcal{V}(acaP_{\mathbb{P}^1\times\mathbb{P}^1}) = \{(-1,0), (4,1), (25,4), (0,-1)\}.$$

The Plücker coordinates can be calculated to be $(4, 25, 1, 9, 1, 4)$. This satisfies all the required conditions. Indeed starting with these coordinates it is possible to recover the Fano polygon $acaP_{\mathbb{P}^1\times\mathbb{P}^1}$, either by calculating the correspond GIT matrix, or by finding four vertices that satisfy the necessary length and height conditions.

Unfortunately these conditions are not a sufficient condition for the corresponding Fano polygon to belong to the mutation graph of $\mathbb{P}^1 \times \mathbb{P}^1$, as illustrated by the next example.

Example 6.6.6. Consider the Plücker coordinates $(2, 25, 1, 9, 1, 8)$, that describe a Fano polygon P. Note that the coordinates satisfy the desired even and square conditions. The corresponding GIT data is given by:

$$\begin{array}{cc:cc} 1 & 1 & 8 & 0 \\ 0 & 2 & 25 & 1 \end{array}.$$

Writing this as a matrix, dualizing, and taking the kernal gives us the matrix:

$$\begin{pmatrix} -1 & 1 & 0 & -2 \\ -8 & 0 & 1 & -25 \end{pmatrix},$$

whose columns represent the vertices of P, that is:

$$\mathcal{V}(P) = \{(0,1),(1,0),(-2,-25),(-1,-8)\}.$$

However $SC(P) = \left(2, \left\{\frac{1}{9}(1,4), \frac{1}{25}(1,2)\right\}\right)$, and so this cannot be any entry of the mutation graph of $\mathbb{P}^1 \times \mathbb{P}^1$.

BIBLIOGRAPHY

[1] Peter Abramenko and Kenneth S. Brown. *Buildings*, volume 248 of *Graduate Texts in Mathematics*. Springer, New York, 2008. Theory and applications.

[2] Hamid Ahmadinezhad. On pliability of del Pezzo fibrations and Cox rings. *J. Reine Angew. Math.*, 723:101–125, 2017.

[3] Mohammad Akhtar, Tom Coates, Alessio Corti, Liana Heuberger, Alexander Kasprzyk, Alessandro Oneto, Andrea Petracci, Thomas Prince, and Ketil Tveiten. Mirror symmetry and the classification of orbifold del Pezzo surfaces. *Proc. Amer. Math. Soc.*, 144(2):513–527, 2016.

[4] Mohammad Akhtar, Tom Coates, Sergey Galkin, and Alexander M. Kasprzyk. Minkowski polynomials and mutations. *SIGMA Symmetry Integrability Geom. Methods Appl.*, 8:Paper 094, 17, 2012.

[5] Mohammad Akhtar and Alexander Kasprzyk. Singularity content. `https://arxiv.org/abs/1401.5458`, 2014.

[6] Mohammad E. Akhtar and Alexander M. Kasprzyk. Mutations of fake weighted projective planes. *Proc. Edinb. Math. Soc. (2)*, 59(2):271–285, 2016.

[7] Valery Alexeev and Viacheslav V. Nikulin. *Del Pezzo and $K3$ surfaces*, volume 15 of *MSJ Memoirs*. Mathematical Society of Japan, Tokyo, 2006.

[8] Selma Altinok. *Graded Rings corresponding to Polarised K3 Surfaces and $\mathbb{Q}$-Fano 3 folds*. PhD thesis, University of Warwick, 1998.

[9] Klaus Altmann. Computation of the vector space T^1 for affine toric varieties. *J. Pure Appl. Algebra*, 95(3):239–259, 1994.

[10] Klaus Altmann. Minkowski sums and homogeneous deformations of toric varieties. *Tohoku Math. J. (2)*, 47(2):151–184, 1995.

[11] Klaus Altmann. Infinitesimal deformations and obstructions for toric singularities. *J. Pure Appl. Algebra*, 119(3):211–235, 1997.

[12] Klaus Altmann. The versal deformation of an isolated toric Gorenstein singularity. *Invent. Math.*, 128(3):443–479, 1997.

[13] Klaus Altmann. One parameter families containing three-dimensional toric-Gorenstein singularities. In *Explicit birational geometry of 3-folds*, volume 281 of *London Math. Soc. Lecture Note Ser.*, pages 21–50. Cambridge Univ. Press, Cambridge, 2000.

[14] Arnaud Beauville. *Complex algebraic surfaces*, volume 34 of *London Mathematical Society Student Texts*. Cambridge University Press, Cambridge, second edition, 1996. Translated from the 1978 French original by R. Barlow, with assistance from N. I. Shepherd-Barron and M. Reid.

[15] I. N. Bernšteĭn, I. M. Gel′fand, and V. A. Ponomarev. Coxeter functors, and Gabriel's theorem. *Uspehi Mat. Nauk*, 28(2(170)):19–33, 1973.

[16] A. A. Borisov and L. A. Borisov. Singular toric Fano three-folds. *Mat. Sb.*, 183(2):134–141, 1992.

[17] Gavin Brown, Miles Reid, and Jan Stevens. Tutorial on Tom and Jerry: the two smoothings of the anticanonical cone over $\mathbb{P}(1,2,3)$. `https://homepages.warwick.ac.uk/~masda/3folds/TJ_tutorial.pdf`.

[18] Daniel Cavey. Restrictions on the singularity content of a Fano polygon. `https://arxiv.org/abs/1808.06476`, 2018.

[19] Daniel Cavey and Akihiro Higashitani. Winding number of r-modular sequences and applications to the singularity content of a Fano polygon. https://arxiv.org/abs/1901.10929, 2019.

[20] Daniel Cavey and Edwin Kutas. Classification of minimal polygons with specified singularity content. *arXiv:1703.05266*, 2017.

[21] Daniel Cavey and Thomas Prince. Del Pezzo surfaces with a single $1/k(1,1)$ singularity. https://arxiv.org/abs/1707.09213, July 2018.

[22] Tom Coates, Alessio Corti, Sergey Galkin, Vasily Golyshev, and Alexander Kasprzyk. Mirror symmetry and Fano manifolds. In *European Congress of Mathematics*, pages 285–300. Eur. Math. Soc., Zürich, 2013.

[23] Tom Coates, Alessio Corti, Sergey Galkin, and Alexander Kasprzyk. Quantum periods for 3-dimensional Fano manifolds. *Geom. Topol.*, 20(1):103–256, 2016.

[24] Tom Coates and Alexander Givental. Quantum Riemann-Roch, Lefschetz and Serre. *Ann. of Math. (2)*, 165(1):15–53, 2007.

[25] Tom Coates, Alexander Kasprzyk, and Thomas Prince. Laurent inversion. *arXiv:1505.01855*, 2017.

[26] Keith Conrad. $SL_2(\mathbb{Z})$. http://www.math.uconn.edu/∼kconrad/blurbs/....

[27] Alessio Corti and Liana Heuberger. Del Pezzo surfaces with $\frac{1}{3}(1,1)$ points. *Manuscripta Math.*, 153(1-2):71–118, 2017.

[28] Alessio Corti, Aleksandr Pukhlikov, and Miles Reid. Fano 3-fold hypersurfaces. In *Explicit birational geometry of 3-folds*, volume 281 of *London Math. Soc. Lecture Note Ser.*, pages 175–258. Cambridge Univ. Press, Cambridge, 2000.

[29] David A. Cox. The homogeneous coordinate ring of a toric variety. *J. Algebraic Geom.*, 4(1):17–50, 1995.

[30] David A. Cox, John B. Little, and Henry K. Schenck. *Toric varieties*, volume 124 of *Graduate Studies in Mathematics*. American Mathematical Society, Providence, RI, 2011.

[31] Dimitrios Dais. Toric log del Pezzo surfaces with one singularity. `arXiv:1705.06359 [math.AG]`, 2017.

[32] Dimitrios I. Dais and Benjamin Nill. A boundedness result for toric log del Pezzo surfaces. *Arch. Math. (Basel)*, 91(6):526–535, 2008.

[33] Günter Ewald. *Combinatorial convexity and algebraic geometry*, volume 168 of *Graduate Texts in Mathematics*. Springer-Verlag, New York, 1996.

[34] Sergey Fomin and Andrei Zelevinsky. Cluster algebras. I. Foundations. *J. Amer. Math. Soc.*, 15(2):497–529, 2002.

[35] Kento Fujita and Kazunori Yasutake. Classification of log del Pezzo surfaces of index three. *J. Math. Soc. Japan*, 69(1):163–225, 2017.

[36] William Fulton. *Introduction to toric varieties*, volume 131 of *Annals of Mathematics Studies*. Princeton University Press, Princeton, NJ, 1993. The William H. Roever Lectures in Geometry.

[37] Alexander Givental. A mirror theorem for toric complete intersections. In *Topological field theory, primitive forms and related topics (Kyoto, 1996)*, volume 160 of *Progr. Math.*, pages 141–175. Birkhäuser Boston, Boston, MA, 1998.

[38] Paul Hacking and Yuri Prokhorov. Smoothable del Pezzo surfaces with quotient singularities. *Compos. Math.*, 146(1):169–192, 2010.

[39] Robin Hartshorne. *Algebraic geometry*. Springer-Verlag, New York-Heidelberg, 1977. Graduate Texts in Mathematics, No. 52.

[40] Robin Hartshorne. *Deformation theory*, volume 257 of *Graduate Texts in Mathematics*. Springer, New York, 2010.

[41] Akihiro Higashitani and Mikiya Masuda. Lattice multipolygons. *Kyoto J. Math.*, 57(4):807–828, 2017.

[42] Kentaro Hori, Sheldon Katz, Albrecht Klemm, Rahul Pandharipande, Richard Thomas, Cumrun Vafa, Ravi Vakil, and Eric Zaslow. *Mirror symmetry*, volume 1 of *Clay Mathematics Monographs*. American Mathematical Society, Providence, RI; Clay Mathematics Institute, Cambridge, MA, 2003. With a preface by Vafa.

[43] A.R. Iano-Fletcher. Working with weighted complete intersections. In *Explicit birational geometry of 3-folds*, volume 281 of *London Math. Soc. Lecture Note Ser.*, pages 101–173. Cambridge Univ. Press, Cambridge, 2000.

[44] Nathan Owen Ilten. Mutations of Laurent polynomials and flat families with toric fibers. *SIGMA Symmetry Integrability Geom. Methods Appl.*, 8:Paper 047, 7, 2012.

[45] The OEIS Foundation Inc. The online encyclopedia of integer sequences. `https://oeis.org`.

[46] Oleg Karpenkov. *Geometry of continued fractions*, volume 26 of *Algorithms and Computation in Mathematics*. Springer, Heidelberg, 2013.

[47] Alexander Kasprzyk, Ludmil Katzarkov, Victor Przyjalkowski, and Dmitrijs Sakovics. Projecting fanos in the mirror. *arXiv:1904.02194*, 2019.

[48] Alexander Kasprzyk, Benjamin Nill, and Thomas Prince. Minimality and mutation-equivalence of polygons. *Forum Math. Sigma*, 5:e18, 48, 2017.

[49] Alexander Kasprzyk, Thomas Prince, and Ketil Tveiten. Mutations of balanced quivers and affine polygons. In Progress.

[50] Alexander M. Kasprzyk, Maximilian Kreuzer, and Benjamin Nill. On the combinatorial classification of toric log del Pezzo surfaces. *LMS J. Comput. Math.*, 13:33–46, 2010.

[51] Alexander M. Kasprzyk and Benjamin Nill. Reflexive polytopes of higher index and the number 12. *Electron. J. Combin.*, 19(3):Paper 9, 18, 2012.

[52] J. Kollár and N. I. Shepherd-Barron. Threefolds and deformations of surface singularities. *Invent. Math.*, 91(2):299–338, 1988.

[53] János Kollár. Flips, flops, minimal models, etc. In *Surveys in differential geometry (Cambridge, MA, 1990)*, pages 113–199. Lehigh Univ., Bethlehem, PA, 1991.

[54] Yu. I. Manin. *Cubic forms*, volume 4 of *North-Holland Mathematical Library*. North-Holland Publishing Co., Amsterdam, second edition, 1986. Algebra, geometry, arithmetic, Translated from the Russian by M. Hazewinkel.

[55] Robert J. Marsh. *Lecture notes on cluster algebras*. Zurich Lectures in Advanced Mathematics. European Mathematical Society (EMS), Zürich, 2013.

[56] Anvar Mavlyutov. Deformations of toric varieties via minkowski sum decompositions of polyhedral complexes. *arXiv:0902:0967*, 2011.

[57] Obro Mikkel. An algorithm for the classification of smooth fano polytopes. *arXiv:0704.0049*, 2007.

[58] Valcho Milchev and Tsvetelina Karamfilova. Domino tiling in grid - new dependence. `https://arxiv.org/abs/1707.09741`.

[59] Ezra Miller and Bernd Sturmfels. *Combinatorial commutative algebra*, volume 227 of *Graduate Texts in Mathematics*. Springer-Verlag, New York, 2005.

[60] Stavros Papadakis. *Gorenstein rings and Kustin-Miller unprojection*. PhD thesis, University of Warwick, 2001.

[61] Bjorn Poonen and Fernando Rodriguez-Villegas. Lattice polygons and the number 12. *Amer. Math. Monthly*, 107(3):238–250, 2000.

[62] Miles Reid. Surface cyclic quotient singularities and Hirzeburch-Jung resolutions. Following URL last checked January 2020. https://homepages.warwick.ac.uk/ masda/surf/more/cyclic.pdf.

[63] Miles Reid. Young person's guide to canonical singularities. In *Algebraic geometry, Bowdoin, 1985 (Brunswick, Maine, 1985)*, volume 46 of *Proc. Sympos. Pure Math.*, pages 345–414. Amer. Math. Soc., Providence, RI, 1987.

[64] Miles Reid. Graded rings and birational geometry. In K. Ohno, editor, *Proceedings of Algebraic Geometry Symposium*, Kinosaki, October 2000.

[65] Miles Reid and Kaori Suzuki. Cascades of projections from log del Pezzo surfaces. In *Number theory and algebraic geometry*, volume 303 of *London Math. Soc. Lecture Note Ser.*, pages 227–249. Cambridge Univ. Press, Cambridge, 2003.

[66] Jacques Tits. *Buildings of spherical type and finite BN-pairs*. Lecture Notes in Mathematics, Vol. 386. Springer-Verlag, Berlin-New York, 1974.

[67] Ben Wormleighton. Reconstruction of orbifold del Pezzo surfaces from Hilbert series. *(In progress)*, 2014.